universität wien

MASTERARBEIT / MASTER'S THESIS

Titel der Masterarbeit / Title of the Master's Thesis

„The northwestern continuation of the Mentawai Fault in western Sumatra“

verfasst von / submitted by

Christian Steinbauer, BSc

angestrebter akademischer Grad / in partial fulfilment of the requirements for the degree of

Master of Science (MSc)

Wien, 2018 / Vienna 2018

Studienkennzahl lt. Studienblatt / degree programme code as it appears on the student record sheet:	A 066 815
Studienrichtung lt. Studienblatt / degree programme as it appears on the student record sheet:	Masterstudium Erdwissenschaften
Betreut von / Supervisor:	Univ.-Prof. Mag. Dr. Bernhard Grasemann

Table of contents:

1. Abstract

The convergence between the Australian and Asian tectonic plates is accommodated by a huge subduction zone, a so called megathrust SW of Sumatra resulting in numerous hazardous earthquakes. The oblique convergence is partitioned into a number of large scale faults with varying kinematics. The Mentawai fault is located between the Mentawai archipelago and mainland Sumatra crossing the equator, but mainly identified south of the equator and continuing into the Sunda Strait. It represents one of the faults which potentially uptake a certain amount of the oblique convergence between the big scale tectonic plates, but its kinematics is poorly understood. Therefore, a reason lies in the fact that it is mostly imaged on seismic profiles below sea level. Nias is one of the few islands where the Mentawai fault is exposed above sea level in contrast. This master thesis investigated in structural fieldwork to broaden the knowledge concerning the location and kinematics of the Mentawai fault exposed in Nias.

Die Konvergenz zwischen der Australischen- und Asiatischen Tektonischen Platte wird entlang einer überdimensionalen Subduktionszone, auch als Megathrust bezeichnet, im Südwesten von Sumatra kompensiert. Dadurch werden laufend zerstörerische Erdbeben verursacht. Die schiefe Konvergenz der tektonischen Platten wird in verschiedenen Störungen von größerer Magnitude mit unterschiedlicher Kinematik aufgeteilt. Die Mentawai Störung befindet sich zwischen dem Mentawai Archipel und dem Festland von Sumatra und streckt sich quer über den Äquator. Identifiziert wurde die Störung allerdings hauptsächlich südlich des Äquators, wo sie sich bis in die Sundastraße erstreckt. Vermutet wird, dass diese Störung einen Teil der schiefen Konvergenz der tektonischen Platten kompensiert, allerdings versteht man ihre Kinematik nur dürftig. Das liegt zum Teil daran, dass man sie bisher nur in seismischen Profilen unter dem Meeresspiegel ausfindig machen konnte. Auf der Insel Nias hat man die Mentawai Störung über dem Meeresspiegel entdeckt. Diese Masterarbeit beschäftigt sich mit strukturgeologischer Feldarbeit, um das Wissen rund um die Mentawai Störung, derer geographischen Lage und Kinematik zu erweitern.

2. Geological overview:

2.1. Introduction and aims

Nias Island, or rather my special field of interest is one of several islands offshore Sumatra Indonesia following a line of several islands parallel to the Sunda Subduction Zone. This is overall summarized as the Sunda Arc between the Indo-Australian and the south-eastern part of the Eurasian plate, stretching from northwest to southeast from the eastern Himalayan syntaxis to western Myanmar (Burma), the western Andaman Sea, Sumatra, Java and finishes in the Banda arc of east Indonesia. It stretches about 6000 km from the Himalayans to east Indonesia. The island is located approximately 100 km north of the equator and about 120 km offshore the west coast of Sumatra and depicting the largest of the forearc islands covering 4772 km^2, stretching about 120 km parallel and about 40 km normal to the subduction zone (Curray, 1989).

The reason for the research on Nias Island is partly the fact that it is a very active area when it comes to seismicity, earthquakes and natural hazards such as tsunamis. The last dramatic incidents occurred in 2004 as the great Sumatran – Andaman earthquake, which caused a devastating tsunami (Subarya et al., 2006) and in 2005, only few months later, as the Simeulue - Nias earthquake (Briggs et al., 2008). A similar event happened in 1861 (Newcomb and McCann, 1987) and both had a magnitude around 8.6 according to Briggs et al. (2006). So this is a perfect area to study seismicity, earthquakes and other natural hazards.

Another reason for the investigation of Nias Island is the very classic morphology of a trench. It consists of an accretionary prism, an outer arc-ridge, a forearc basin and a volcanic chain (Karig et al., 1979). Additionally we have direct access to the trench forming due to the Eurasian plate thrusting over the Indio-Australian plate and accumulating material as the accretionary prism. According to Samuel et al. (1997) it is a type example of an uplifted accretionary complex. The Sunda Arc is perfect to study and understand accretionary complex formation, terrane accretion, obducted ophioliths and the tectonic mechanisms involved in it. This knowledge is important to interpret and extrapolate to other arc formations in the context of tectonics and accretion (Curray, 1989). Beyond that I focused on evidence for the potential northwestern continuation of the Mentawai fault identified further to the southwest by Diament et al. (1990).

Generally speaking subduction occurs when the rigid lithosphere, or rather two tectonic plates collide while moving on the asthenosphere which is the ductile, upper part of Earth's mantle. In reality there is a density or rather bouncy difference of colliding plates, which is correlated with the exact age and temperature of a tectonic plate. The older the lithosphere, the colder it gets and therefore colder lithosphere has less bouncy in respect to the less cold, young lithosphere. The older and colder plate tends to be subducted.

In terms of plate boundary situation, subduction means converging plate boundaries. In the Wilson Cycle, which describes the live cycle of rocks or rather tectonic plates including all its lithological units, subduction marks the last stage where lithosphere gets recycled. While sliding into the upper mantle underneath the relatively younger lithosphere, the rocks and minerals with the lowest melting point start to melt after they reached a certain depth and tend to rise and form volcanic arcs, which are characteristic for subduction zones. The hotter it gets with increasing depth of the subducted plate, the more minerals with higher and increasing melting points get melted and rise up to the surface. Therefore, partial melting and mineral differentiation occur while the subducted lithosphere gets continuously molten. Moreover magmatic melts can be influenced by fluids in the rocks and in fractures. The fluids mostly consist of H_2O, CO_2 or as a mixture of both chemicals which can influence the melting point of the rock and the characteristics of the melting process dramatically. The chemical composition of the erupted, volcanic melt in the volcanic chain is characteristic for the type of rocks and minerals which were melted while being subducted (Frisch and Meschede, 2011).

Hamilton (1979) describes the tectonic situation in the Indonesian and Melanesian region as very complex. He presented an oversimplified model of three major tectonic plates obliquely converging, which are characterized by several dynamic clusters of small tectonic plates with changing directions of motion, several oroclines, migrating arcs, transform faults and several young and old subduction zones. The Sundaland which incorporates Sumatra, Malaysia, Java and Borneo is an aggregate of past continental fragments. These fragments derive from several changing subduction patterns which can be dated and verified back to the late Palaeozoic. Hamilton deduces subduction zones by the encountering of characteristic ophiolites, melange, olistostroms, high-pressure metamorphic rocks, such as blueschist, intermediate and silicic calc-alkaline igneous volcanism, that forms above the Benioff zones and assumes that a truncation of an orogenic belt is caused by rifting processes (Hamilton, 1979).

2.2. Tectonic overview of Indonesia

Warren Hamilton was one of the first scientists who tried to explain the tectonics of Indonesia. He engaged in subduction zones which there are many in Indonesia. The one which recently got very much attention due to the hazardous seismic activity is the subduction zone in the southwest offshore of Sumatra. Hamilton (1979) characterizes a subduction zone by the presents of ophiolites, melange, wildflysch and blueschist; intermediate and silicic calc-alkaline igneous rocks, which form above the Benioff zone and truncations of orogenic belts which occur due to rifting processes.

In Southeast Asia, also called Sundaland the crust is an aggregate of small continental fragments. Hamilton identifies several former subduction zones e.g. dating back to the late Paleozoic in Malaya and Thailand indicated by granites in eastern Malaya and several melange zones in western Laos and Cambodia. According to Hamilton (1979) the subduction ended when the collision of the continental crust with Indochina started. Another subduction event occurred in the early and middle Triassic eastwards beneath the west side of the Sundaland aggregate. Around 30 Ga later, in the late Triassic and Jurassic subduction from the north was responsible for the collision of the Sundaland aggregate with China. Early Cretaceous subduction from the west was followed by late Cretaceous subduction beneath the east side of the aggregate and additionally indicates continental rifting processes. In the Cenozoic we have another subduction event eastward which ended at least in the northern part when the aggregate collided with India. In the southern part we still have subduction. In the early Tertiary Australia and New Guinea had a stable, continuing shelf and a consistent northern margin which was moving northwards until the collision with a former island arc which was the front of the Caroline oceanic plate took place. In the late Cenozoic southward subduction of the Caroline oceanic plate beneath Australia and New Guinea occurred. Sinistral strike-slip faulting led to the separation of the Sula Islands, a former part of Northwest New Guinea and the transportation closer to Sulawesi.

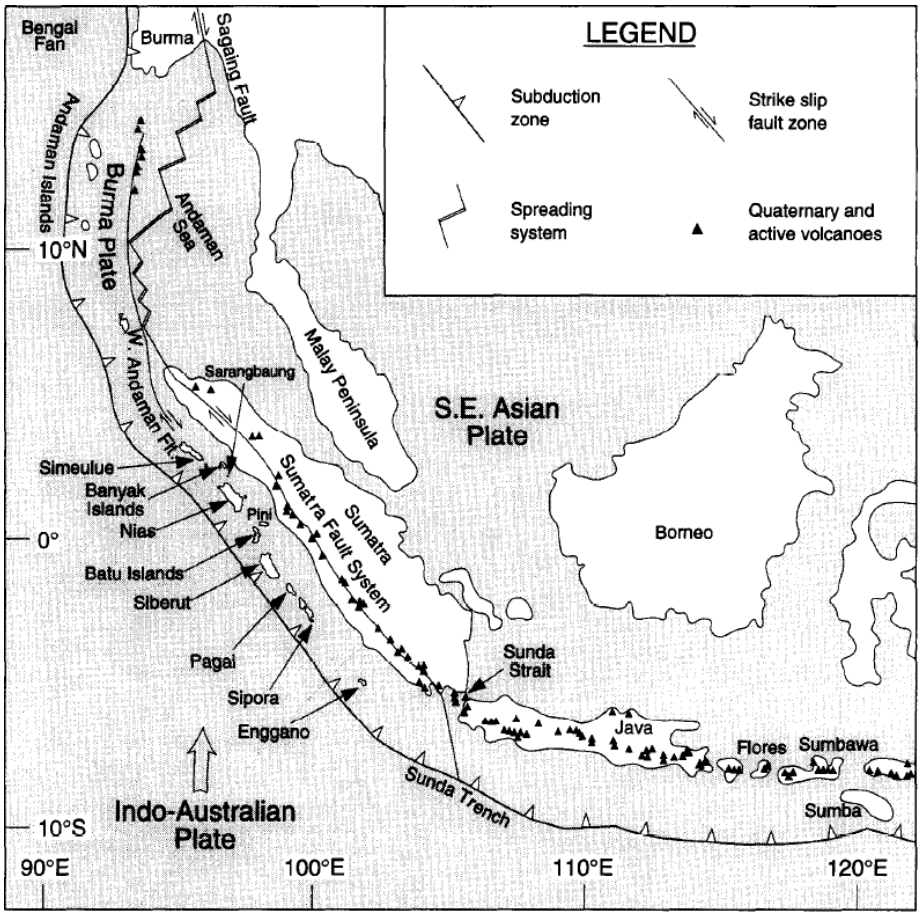

Figure 1: Map of the Sunda Arc (From Samuel et al. 1997)

To summarize there are several still identifiable subduction zones dating back to the late Paleozoic. Especially in the southeast of Indonesia there is a very complicated mosaic-like pattern of subduction zones trending in all directions in different time periods leaving several Paleozoic, Mesozoic and Cenozoic remnants of island arcs and magmatic complexes in the Philippines, Sulawesi, Borneo and Halmahera. This results in a very complicated tectonic situation especially in the southeast of Indonesia (Hamilton, 1979).

Hamilton was one of the first scientists who investigated in the very complex tectonic situation of Southeast Asia. Although he was correct in some points, he made several errors, which were corrected or complemented later on based on more sophisticated research.

2.3. The Sunda Arc

2.3.1. Definition

The Sunda Arc is the continental margin stretching from the eastern Himalayan syntaxis, through western Burma, the western Andaman Sea, Sumatra, including my special field of interest, namely Nias Island and Java. It connects with the Banda Arc of eastern Indonesia. It is characterized as a classical subduction margin. The Indo-Australian plate is underthrusting the Southeast Asian plate towards the northeast.

The Sunda Arc is further subdivided into several distinct morphological zones normal to the striking direction. It comprises the outer arc rise outside of the trench, the trench itself, which is the physical border between the two distinct tectonic plates, a landward trench slope, including slope basins that are ponded behind ridges in the underlying accretionary prism, the outer arc ridge, which coincides with the trench slope break, between the trench slope break and the mainland is the forearc basin and it finishes with the mainland of Sumatra which comprises the mostly andesitic volcanic arc and various backarc environments, some of which are important hydrocarbon basins (Curray, 1989).

2.3.2. Variations along strike of the megathrust

2.3.2.1. Oblique convergence and terrane transport

Curray et al. (1979), Karig (1980) and Karig et al. (1986) beside many others have indicated that in subduction zones with oblique convergence, the lateral component of movement is accounted by a strike slip fault with appropriate sense of motion and located behind the subduction zone. In the case of the Sunda Arc the Sumatran Fault System takes up the transform motion compensating the opening of the Andaman Sea and the relative motion of a microplate, or rather the Burma microplate in respect to the Southeast Asian plate having a dextral sense of shearing. It bisects the island of Sumatra and approximately follows the alignment of the volcanic arc.

Although an oversimplified two plate model of the movement of the Indo-Australian- in respect to the Southeast Asian plate would suggest mainly transform motion in the Andaman-Nicobar region and even some parts of divergence. In reality geological evidence shows compression and convergence indicated by folding and thrusting is dominant in that particular region. That is explained with the lateral northward motion of the Burma microplate causing transform faulting in Sumatra and in Burma and extension in the Andaman Sea. In fact, the evolution of the Andaman Sea region is an extreme effect of oblique convergence. Curray (1989) describes the situation as follows. At first a proto-Andaman Sea started to open in approximately east-west direction as a typical backarc extensional basin during the Oligocene. The results were the formation of the

Mergui Basin, which is interpreted as a northward continuation of the North Sumatra Basin. This Mergui Basin structure consists of several horst, graben and half-graben structures originating from Oligocene to early Miocene, indicating an extensional regime opening in NNE-SSW direction. It is cut by a younger divergent wrench fault system with a trend approximately NNW-SSE, which is suspected of taking up some of the early post middle Miocene opening of the modern Andaman Sea. Robert Kieckhefer, (1980) found a long reversed seismic refraction line leading down the axis of one of the grabens. There they could see several kilometers of sediments on top of the continental crust as well as mantel arrivals in approximately 20 km depth. Curray (1989) interprets these findings as indicators for a thinning of continental crust, which was stretched during the Oligocene rifting stage. The stretching stopped at the time of rapid subsidence of the basin in early Miocene. So as the Mergui Basin opening phase aborted, the present phase of opening started with formation of oceanic sea floor around middle Miocene, about 13 Ma, in NW-SE direction. The approximate 460 km opening of the modern Andaman Sea have mostly been compensated by the Sagaing fault and the parallel Kabaw fault of Myanmar (Burma) which are two parallel major land transform faults (Curray et al., 1979).

In Java there is no strike-slip faulting parallel to the arc. The Burma microplate seems to extend from the Himalayan syntaxis down to the Sunda Strait where its plate margin probably crosses the forearc (Curray, 1989). Huchon and LePichon (1984) have suggested an extensional regime at the Sunda Strait due to the northward movement of the microplate causing the stretching and thinning of the accretionary prism and potentially leading to the hazardous volcanism at Krakatoa.

2.3.2.2. Sediment volume within the accretionary prism

The sediment volume of the accretionary prism increases drastically from Java to the Andaman Sea region. While offshore of Java the outer arc ridge is narrow and deeply submerged, offshore Sumatra the ridge emerges intermittently above sea level as an island chain and further north in the Andaman Sea region the accretionary prism forms an entire mountain chain and continues up north into the Indoburman Ranges. Curray et al. (1981) calculated several estimates of the sediment volume of different parts of the accretionary prism including parameters like sediment thickness on the lower plate and rate, speed and duration of convergence. The different sediment budgets obtained by the calculations suggest that most of the sediments incorporated into the subduction zone since early Cretaceous can still be accounted for along the accretionary prism (Curray et al., 1981).

2.3.2.3. Benioff zone

A good visible Benioff zone can be seen all around the Sunda Arc, although it changes drastically in depth and pattern. Beneath Java deep focus earthquakes to depth of almost 700 km dominate, but

end abruptly near the Sunda Strait at the southern end of the Burma microplate. Further to the northwest, off the coast of Sumatra the deepest earthquakes don't exceed 150 km in depth. The cutoff lies beneath the Sumatran Fault System and the magmatic arc. Shallow subduction beneath the Burma microplate is seismic, whereas the deeper subduction to the northeast of the Sumatra Fault System, beneath the Southeast Asian Plate is aseismic (Curray, 1989).
The situation to the north of Sumatra beneath the Andaman Sea and Myanmar (Burma) gets very controversial and complicated. Shallow seismicity can be accounted following the plate edge in the Andaman Sea and Sagaing fault with a ragged Benioff zone with earthquakes not exceeding 180 km in depth and continuing northward to the Himalayan syntaxis. Controversial is whether the Benioff zone beneath the northern Indoburman Ranges still marks active subduction or rather only a strike-slip regime for today (Curray, 1989).

2.3.2.4. Convergence speed

The rate of subduction perpendicular to the Sunda Arc lies around 70 to 72 mm/yr south of Java, decreases from around 74 to 46 mm/yr off the coast of Sumatra, rises slightly near the southern part of the Andaman Sea and further decreases to the west of the Andaman and Nicobar Islands, while it increases again off the coast of Myanmar (Burma). Measuring the mostly convergent plate motions in the Sunda Arc region is complicated due to the fact that there are several different plates involved, which are not well-defined. Movements can only be measured relatively to each other. Due to the fact that it is not that clear how many tectonic plates and micro-plates are involved and how they move independently in respect to each other, errors must be accepted (Curray, 1989).

2.3.3. Plate kinematics

In a broad sense the plate kinematics in the Sunda Arc are based on the movement of the Indo-Australian and the Eurasian plate. It gets more complicated contemplating the two separated plates of the Indo-Australian plate as in each case independent, but bounded by a broad, slowly deforming region (DeMets et al. 1994), the Sunda plate independent of the Eurasian plate moving relative to Eurasia at a few millimeter to centimeters per year relatively eastward (Bock et al., 2003) and the independent motion of the forearc microplate. This forerarc microplate further complicates the plate kinematics due to the fact that it is not rigid, but exposed to extensive internal deformation. Subarya et al. (2006) suggests two independent motions along the forearc microplate, based on a change in earthquake slip directions with a break near 6° to 7°N close to the Nicobar Islands. Therefore, an Andaman section and a Sumatran section of the microplate each moves independently.
Additionally, along-strike forearc extension is indicated due to variations in the slip directions of earthquakes on the thrust fault. The rate of extension is little in the southeastern part of the microplate, near the Sunda Strait and increases further northwest (McCaffrey, 1991). Genrich et al.

(2000) and McCaffrey (2000) stated that southwest of central Sumatra slip vectors and GPS velocities indicate that the Sumatran oblique slip system is partitioned with ~2/3 of the shear component on the Sumatran fault and ~1/3 of the shear on the subduction fault.
The rate of convergence offshore Sumatra is about 40 to 50 mm/yr. Further up north, in the Andaman and Nicobar region the orientation of the trench is nearly parallel to the direction of relative plate motion, therefore convergence was thought to be around < 20 mm/yr or less, causing the not contemplating of great earthquakes in the northern regions prior to the 2004 megathrust rupture (McCaffrey, 2000).

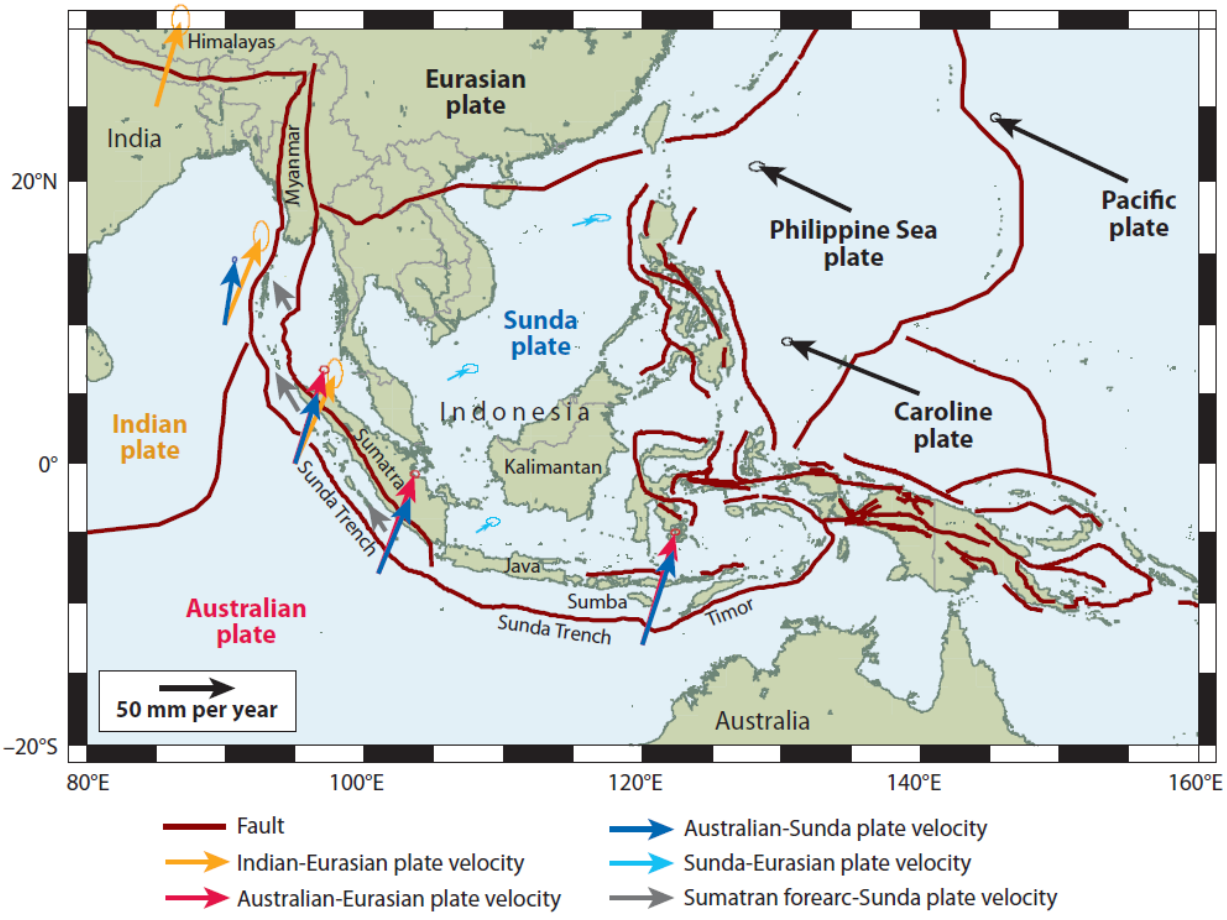

Figure 2: Plate tectonic setting of Sumatra with relative velocities of plate pairs (From McCaffrey 2009)

2.4. The Sumatran Fault and generalities of the subduction zone

The Sumatran Fault Zone is an approximately 1900 km long dextral strike-slip fault, which compensates the lateral portion of the oblique subduction movement between the Indo-Australian and Southeast-Asian tectonic plate. It roughly follows the active Sumatran volcanic arc, which is no coincidence. According to Beck (1983) a fault e.g. a strike-slip fault tends to develop along a preexisting zone of weakness, such as a volcanic arc as given in our case. The Sumatran fault separates the Southeast Asian plate to its northeastern side, which is separated from the Eurasian plate only by the slow slipping Red River fault of Vietnam and southern China (Allen et al., 1984). On its southwestern side is the Sumatran Burma microplate, which is a 300 km wide strip of lithosphere between the Sumatran fault and the Sumatran deformation front (Natawidjaja and Sieh, 2000). Further to the northwest the fault continues into the Andaman Sea spreading centers which according to Curray et al., (1979) result from an extreme effect of oblique convergence. Southeast of Sumatra or in the Sunda Strait the fault curves southward towards the deformation front (Diament et al., 1992). Fitch (1972) suggested that the right-lateral component of the oblique convergence offshore Sumatra is the cause for the dextral Sumatran fault. McCaffrey (1991, 1992) added more certainty to these claims with the presentation of slip vectors of moderate earthquakes along the Sumatran portion of the subduction zone that are nearly perpendicular to the strike of the plate boundary. He noted that if these vector directions are representative of long-term slip trajectories along the subduction interface, then subduction itself is only slightly oblique and most of the dextral component of plate motion must be accommodated elsewhere. The Sumatran Fault Zone therefore is the most obvious candidate, but the discovery of the Mentawai fault by Diament et al. (1992) complicates this slightly. Huchon and LePichon, (1984) and McCaffrey, (1991) proofed that the rate of dextral slip along the Sumatran fault increases from southeast to northwest.

2.4.1. Fault geometry

The Sumatran fault has an overall sinusoidal shape in the major scale. The northern half is gently concave to the southwest and the southern half is concave to the northeast. Sub-aerially exposed it is over 1650 km in length and has an amplitude of about 55 km. A great irregularity between the equator and around 1,8°N latitude is the Equatorial Bifurcation. In this region the Sumatran fault gets split into two separated active strands. Interestingly, the two strands are already distinct from each other at their northern point of bifurcation. Additionally, the western branch does not rejoin the eastern branch further south, but dies out geomorphically. Superimposed on the overall sinusoidal geometry of the fault are several discontinuities characterized as second order geometric irregularities ranging in length from 35 to 220 km in length. These can show major local changes in strike and are mostly right stepping in the fault trace, therefore represent dilatational step overs. These right stepping faults coupled with the dextral movement are predestined to produce graben

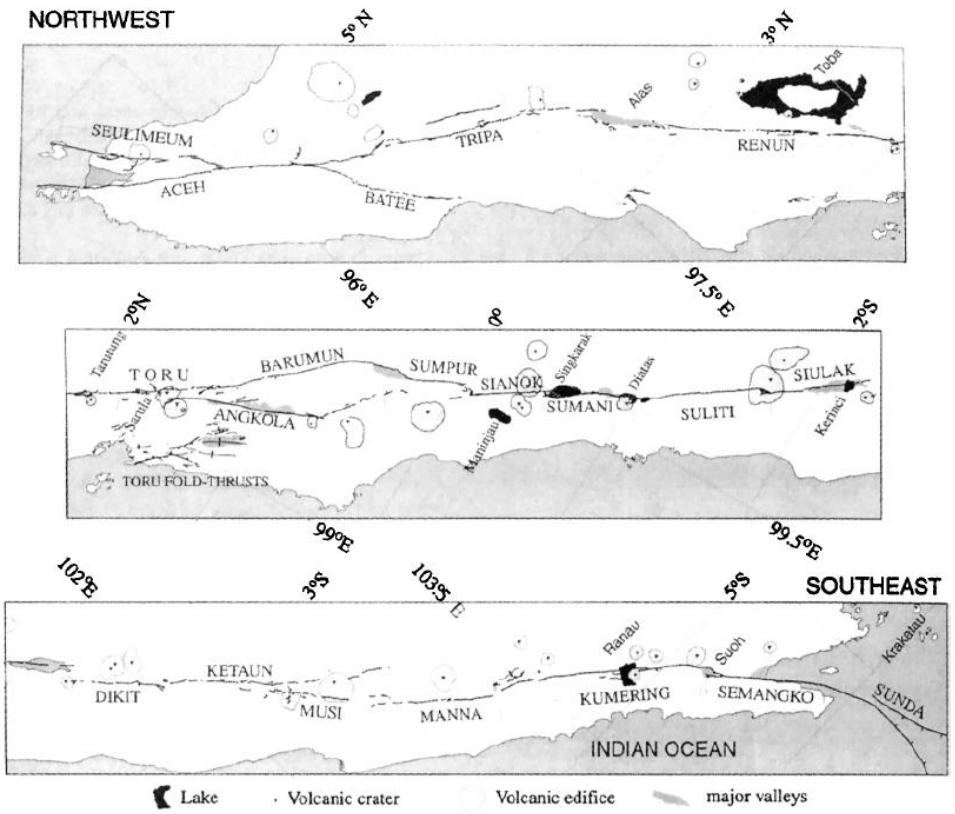

Figure 3: The twenty segments of the Sumatran fault (From Natawidjaja and Sieh, 2000*)*

structures in intra-montane valleys or pull-apart basins (Natawidjaja and Sieh, 2000). Natawidjaja and Sieh, (2000) divide the Sumatran fault into 20 major segments for easier investigation and research in more detail. They present only strong estimates of how seismicity along the Sumatran fault behaved and will behave in the future. Nevertheless, what is obvious for them is that the geometric segmentation has a strong influence on the seismic rupture. Therefore, the fault produces earthquakes correlating to rupture lengths no greater than approximately 100 km, although the overall length is far greater.

2.4.2 The Mentawai fault

The purpose of the oceanographic expedition on the Indonesian ship R/V Baruna Jaya III was to further study the accretionary wedge and the forearc region offshore Sumatra. The result of several seismic refraction profiles done in the Mentawai archipelago region was the discovery of a long linear structure, parallel to the Sumatran Fault Zone, located on the western flank of the forearc basin which was called the Mentawai fault. It can be identified from the southernmost part of Sumatra to the north of Siberut Island, although its structure is highly variable along strike. It manifests as faulted anticlines, faulted blocks, horst and graben systems and flexures. Diament et al. (1992) claim the Mentawai fault to be a strike-slip fault parallel to the Sumatra Fault Zone which is further compensating the change of frontal (offshore Java) to oblique subduction (offshore Sumatra) between the Indo-Australian and Southeast Asian tectonic plates. The basis for their claims firstly is

the seismic refractory profiles which commonly show a positive flower structure, secondly the linearity and continuity of the structure for more than 600 km, and thirdly a pronounced difference generally found in the acoustic basement depth on both sides of the zone. These indicators suggest a N300°-N310° trending strike-slip fault located on the western side of the forearc basin along the Mentawai archipelago, which is responsible for the observed features according to Diament et al. (1990). Karig et al. (1980) identified a similar flexure zone on Nias Island as well, which potentially could be the northwestern continuation of the Mentawai fault. Diament et al. (1990) and Huchon and Le Pichon (1984) see a correlation of this large strike-slip fault and the widening of the southward extensional domain of the Sunda Strait and the limited role of the Sumatran Fault Zone in the southern part of Sumatra in terms of dextral movement. Beaudrey and Moore (1985) suppose the displacement of the Mentawai fault to be totally or partially relayed to the Batee fault or structures alike, which would explain the growing dominance of the Sumatran fault to the north of Sumatra. So far the link between the Mentawai fault and the Batee fault has not been clearly discovered (Diament et al. 1992). A proposal from Karig et al. (1980) stated that oblique subduction is accommodated by several arc-parallel strike-slip faults, which speaks for the results of Diament et al. (1992). Therefore the Mentawai fault acts as a dextral strike-slip fault, which leads to the assumption that the Burma microplate consists of several strips or platelets moving toward the northwest (Diament et al. 1992). The formation of a strike-slip fault as a result of oblique subduction occurs mainly along a preexisting zone of weakness in the overriding plate (Beck,

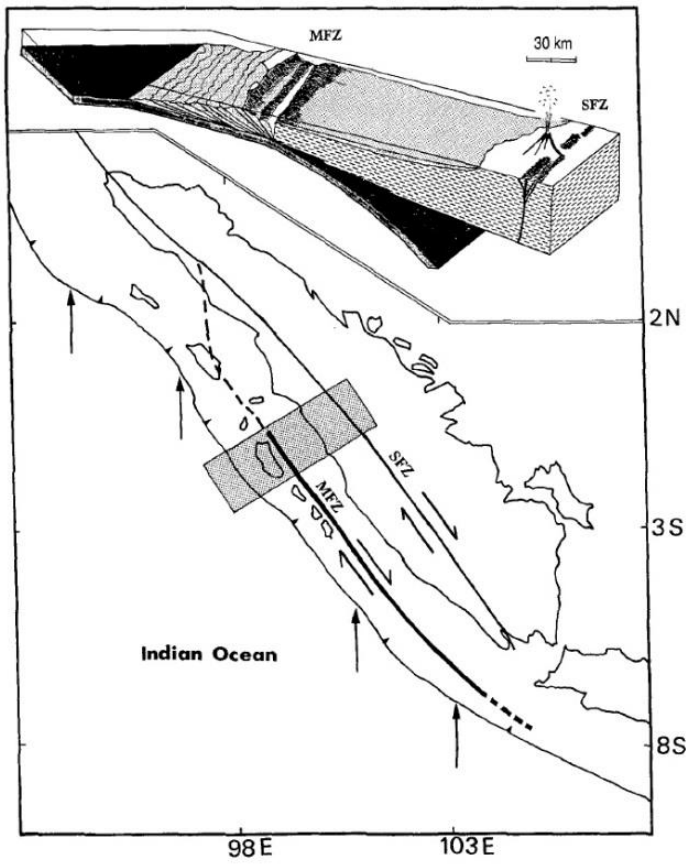

Figure 4: The proposed dextral Mentawai Fault Zone (MFZ) (From Diament et al. 1992)

1983). In case of the Sumatran Fault Zone the volcanic arc served as the zone of weakness along which a strike-slip fault could be formed most easily. The Mentawai fault is located between the forearc ridge and western flank of the forearc basin. The forearc ridge is interpreted as part of the accretionary wedge and the forearc basin as part of the continental domain. Therefore the zone of weakness required for a fault zone to occur is given in the boundary between deformed, mainly oceanic sediments or rather the accretionary prism and the forearc basin belonging to the continental plate (Diament et al. 1992). Samuel and Harbury (1996) agree with Karig et al. (1980) with the suggestion that the flexure on Nias Island and the Mentawai fault in general marks the arc-ward limit of accretionary prism deformation. Therefore it is a deformation front. But they don't agree with the occurrence of deformation of the Mentawai fault in the accretionary prism and don't see it as a backthrust either, but rather as a manifestation of subduction-driven deformation resulting from an inversion of sedimentary basins which originally formed during Oligocene to early Miocene at the outer edge of the Sumatran forearc. Its straightness and position parallel to the trench suggests that its location is controlled by the angle and rate of the subducting Indio-Australian Plate (Samuel and Harbury1996).

Still different authors have different opinions about the Mentawai fault. According to Schlüter et al. (2002) transpression could be the main force for its development. They identify several successive, transpressional phases along the Mentawai Fault Zone, indicating differences in the strength of the deformation interpreted by the differences in the grade of up-doming and steepening of the sedimentary sequences next to the fault along the zone.

I will go into more detail concerning the Mentawai fault and its characteristics in Chapter 2.5.1. *Extensional, arc-parallel deformation (arc-parallel vs. arc-crossing strike-slip faults).*

2.4.3. The Batee fault

The Batee fault is a major dextral strike-slip fault that diverges from the Sumatran fault at about 4,65°N. It traverses the northwestern end of the Barisan Mountains, continues onto the continental shelf and is responsible for major dextral offsets of up to 150 km along the edge of the continental shelf and around 100 km along the eastern edge of the outer arc ridge (Karig et al., 1980). On the mainland of Sumatra the Batee fault does not appear to be active, except for small local exceptions. Natawidjaja and Sieh (2000) suspect the deflection of several large river channels of up to 10 km to be dextral, but the lack of offsets in smaller ridge lines and channels suggests that either there was no activity in the past few tens of thousands of years or the rate of activity is about an order of magnitude lower than along the Sumatran fault.

2.4.4. Produced offsets along the Sumatran fault

Proof for offsets in the lower scale speaking in global geological terms can be found all along the Sumatran fault in different magmatic features, such as tuff, in riverbeds or ridges. The greatest geomorphic offsets found in Sumatra are no greater than 20 km. It is difficult to answer the question if this resembles the total offset of the Sumatran fault, focusing on the magnitude of the overall fault. Natawidjaja and Sieh (2000) state that total offset as great as around 100 km cannot be ruled out. Nevertheless, evidence in the young volcanic cover, mostly much younger in age than half a million years, which traverses over roughly a quarter of the Sumatran fault shows that no more than around 15 km of offset could have accumulated since their deposition. According to Natawidjaja and Sieh (2000) there is reason to favor the hypothesis that the largest geomorphic offsets are the total offset across the fault. Offsets of 20 to 21 km of deeply incised channels in northern Sumatra are very likely to have recorded the total offset since the initiation of uplift of the Barisan Mountain range, which started about 10 Ma (late to mid Miocene) ago (Karig et al., 1979). Different publications present variable results, but many come to the same conclusion. Katili and Hehuwat (1967) infer a total dextral offset of 20 to 25 km on the basis of regular-scale maps of late Paleozoic to early Cenozoic rocks. Cameron et al. (1983) matches the former publication with an estimate of 20 km of dextral offset in an Oligocene sedimentary unit, which would indicate a total offset of 20 km since the Oligocene.

2.4.5. The arc-parallel extension in the Sunda Strait

In the region of the Sunda Strait between Sumatra and Java the forearc basin and the outer-arc ridge are attenuated. These features nearly disappear in this region and additionally the deformation front bows landwards. Following Huchon and LePichon (1984), Natawidjaja and Sieh (2000) interpret this as indicators for fault-parallel stretching and fault-normal necking of the forearc region. Samuel et al. (1997) and Samuel and Harbury (1996) proofed that the forearc basin and the outer-arc ridge developed throughout the Miocene. Therefore, it can be inferred that the deformation of these features in the region of the Sunda Strait has occurred in the past few million years. According to Natawidjaja and Sieh (2000) the extension of the Sunda graben and the filled graben farther east is consistent with dextral slip of the order of 10 km along the Sumatran fault. For calculating a maximum limit of stretching in the last few million years they used geometrical observations of Huchon and LePichon (1984) and calculated a simple volumetric balancing of the forearc wedge and arrived at a sum of approximately 100 km of maximum stretching of the forearc parallel to the Sumatran fault. Nonetheless, Natawidjaja and Sieh (2000) add authority to the fact that more analysis and calculations are needed to get better results and that previous work of e.g. Lassal et al. (1989) or Le Pichon and Sibuet (1981) lacks precision and detail due to several important parameters for their calculations which were simply assumed (Natawidjaja and Sieh, 2000). How

much exact extension occurred in the Sunda strait is still unclear, but the reality is very likely to lie within the calculated borders of Natawidjaja and Sieh (2000). The next interesting and difficult question is how much of this extension was accommodated along the Sumatran fault. Diament et al. (1992) presented data which clearly demonstrate an additional discontinuity located between the forearc basin and the outer-arc ridge titled the Mentawai fault. This fault is a potential candidate for additional accommodation of the extensional movement in the Sunda Strait. In Chapter *2.5. The Burma microplate* I summarized different research concerning the Mentawai fault and deformation in the Burma microplate.

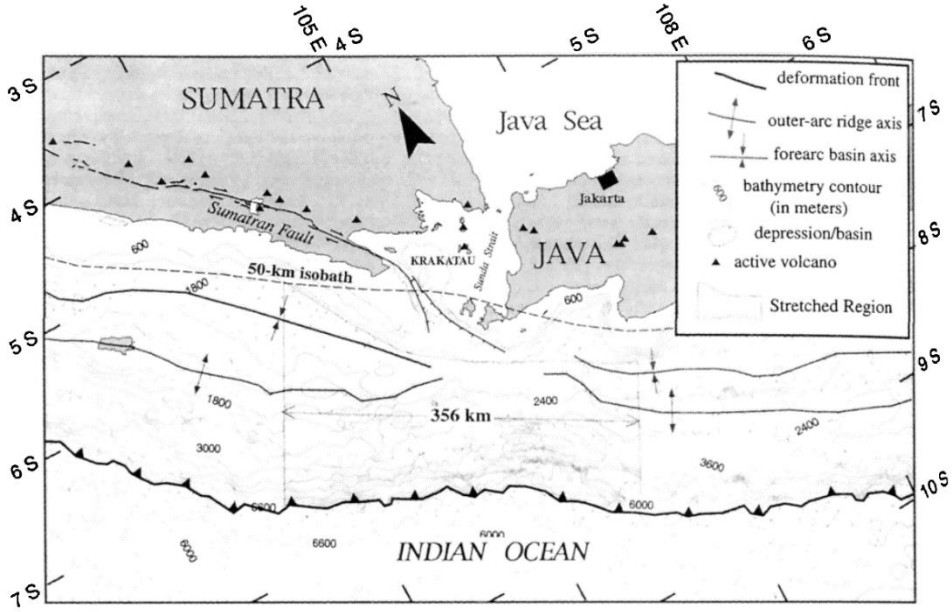

Figure 5: Stretching of the forearc region near the Sunda strait. By volumetric balancing Natawidjaja and Sieh (2000) calculated a maximum stretch amount of 100 km perpendicular to the deformation front since the formation of the outer-arc ridge and the forearc basin. (From Natawidjaja and Sieh, 2000)

2.4.6. Evolution of dextral slip

Although the existing knowledge about the Sumatran fault and its geology is incomplete, enough data exists to attempt a reconstruction of the deformational history of the system over the last few million years. The model must include the magnitude and timing of the discrepancy between spreading in the Andaman Sea and stretching near the Sunda strait; a range of plausible total offsets for the Sumatran fault; the timing, style and magnitude of deformation in the Sumatran forearc region; and a northwestward increase in the current rates of slip along the Sumatran fault. These constraints highly suggest that the fault system evolved significantly since the Miocene and that current configuration of deformation is not necessarily representative for pre-Quaternary deformation (Natawidjaja and Sieh, 2000).

Curray et al. (1979) suggested an overall opening of the Andaman Sea spreading centers of around 460 km. At first view that contrasts significantly the maximum opening calculated by Natawidjaja

and Sieh (2000) for the compensation of the opening along the Sumatran fault via dextral movement of the landmasses. The contrast vanishes when both events are set in their right time context. In the past 3 Ma approximately 118 km of Andaman Sea extension may have accumulated (Curray, 2005). According to Natawidjaja and Sieh (2000), that amount is close enough to the maximum offset already calculated for the Sumatran fault in the same time frames.

There are two options for the calculations of approximately 100 km of fault-parallel stretching of the forearc near the Sunda strait. Either the total offset of the Sumatran fault is much larger than 20 km or another structure in the Sumatran Fault System has accommodated around 80 km of stretching. The only other plausible candidate for dextral slip would be the Mentawai fault, well defined by seismic reflection data by Diament et al. (1992). According to Natawidjaja and Sieh (2000) the arguments that the Mentawai fault zone acted as a strike-slip fault in the last few millions of years is not very convincing, because in their point of view it is missing the typical flower structure characteristic. It is more likely that the Mentawai fault is a backthrust, along which the outer-arc ridge has risen due to the faults location to the northeast of the outer-arc ridge. Karig et al. (1980) identified a large homocline in a similar position relative to the outer-arc ridge further north of the equator on Nias, which supports the former argument. Therefore, Natawidjaja and Sieh (2000) do not accord with seeing the Mentawai Fault Zone as a strike-slip fault.

To reconstruct the history and development of the dextral slip along the Sumatran fault is pretty tricky, complicated and vague, but a plausible evolution is depicted in figure 5. This model is consistent with several available geologic, geodetic and seismographic data, but variations in the history are still plausible. The main intention is to show that the fault system evolved drastically in the past few million years. The main characteristics are the young age of the approximately 15 mm/yr difference in Sumatran fault slip rate to the north and south of the equator (maybe younger than 100 000 years) and the active normal- and dextral slip or transtensional faulting in the forearc and outer-arc slightly north and south of the equator are an ancient and maybe still occurring analogue to the stretching at the southern end of the Sumatran fault.

In figure 5A, we can see a potential geometry for the Sumatran subduction zone at around 4 Ma ago. Shortly prior to that time, according to Karig et al., (1980), Samuel et al., (1997) and Samuel and Harbury (1996) the relief between the forearc basin and the outer-arc ridge increased greatly across the homoclinal fold between it. Speculations of Natawidjaja and Sieh (2000) state that as the outer-arc ridge grew, the subduction deformation front jumped southwestward to its present location, from a deformation front still visible in the bathymetry, closer to the outer-arc ridge. From 4 to 2 Ma before present, dextral slip in the region of the Aceh segment of mainland Sumatra along the Batee fault occurred at a rate of 37 mm/yr, therefore the homocline, the outer-arc ridge and the inner trench slope experienced around 37 km of offset by a curved southern extension of the Batee fault, off the north coast of Nias Island and additionally around 37 km across the Pini basin.

According to Natawidjaja and Sieh (2000), this is consistent with the stratigraphy of Matson and Moore (1992). Samuel and Harbury (1996) present evidence for several kilometers of arc-parallel elongation of Nias Island along the north striking dextral-slip and conjugated sinistral-slip faults that played a role during this period. At this time subduction south of the equator was parallel to the relative plate motion vector and highly oblique to the deformation front. Subduction north of the equator was partly or completely dip-slip because most or the entire dextral component of plate motion was occurring along the Batee fault.

Figure 5B resembles the potential situation about 2 Ma before present. This was when the Sumatran and the Mentawai fault formed. According to Natawidjaja and Sieh (2000) from 2 Ma to 100 ka these two faults carried around 40 mm/yr of dextral component of oblique convergence further south beyond the equator, while the subduction interface accommodated only the dip-slip component. To the north of the equator the Sumatran fault accommodated around 10 mm/yr of dextral slip and the Batee fault approximately 30 mm/yr which represents the overall 40 mm/yr of dextral slip when added.

In figure 6C, these are the suggestions for the current neotectonic partitioning of deformation from Natawidjaja and Sieh (2000). The Aceh-Batee fault is no longer or only minimally active. The Sumatran fault is slipping at a rate of 15 mm/yr faster north than south of the equator. The evolving mass balance problem caused by the discrepancy in slip is taken up by a potential belt of deformation crossing the outer-arc ridge near the equator. This belt of deformation could resemble the findings of Fauzi et al. (1996) who indicated high seismic activity in the down going oceanic slap in this area. Furthermore the active Toru folds of the mainland cost, two young faults on and south of Nias and a north-south graben suggested by bathymetric measurements on the inner trench slope compliment these equatorial area. Figure 6C is consistent with recent measurements of geologically measured Sumatran fault slip rates but is inconsistent with the rates of geodetic strain measured by GPS south of the equator (Natawidjaja and Sieh, 2000).

The model seen in figure 6A, B and C is consistent with the timing of activity on faults both offshore and onshore Nias (Karig et al., 1980; Matson and Moore, 1992; Samuel and Harbury, 1996). Additionally, it matches the present state of activity of the Batee fault, which is inactive at the moment, although retaining clear evidence for approximately 5 km dextral offsets of some of the largest channels crossing it. The concavity of the deformation front to the west of Nias resembles the concavity to the southwest of the Sunda Strait. They are potential features inherited from Plio-Pleistocene dextral strike-slip motion in the forearc region (Natawidjaja and Sieh, 2000).

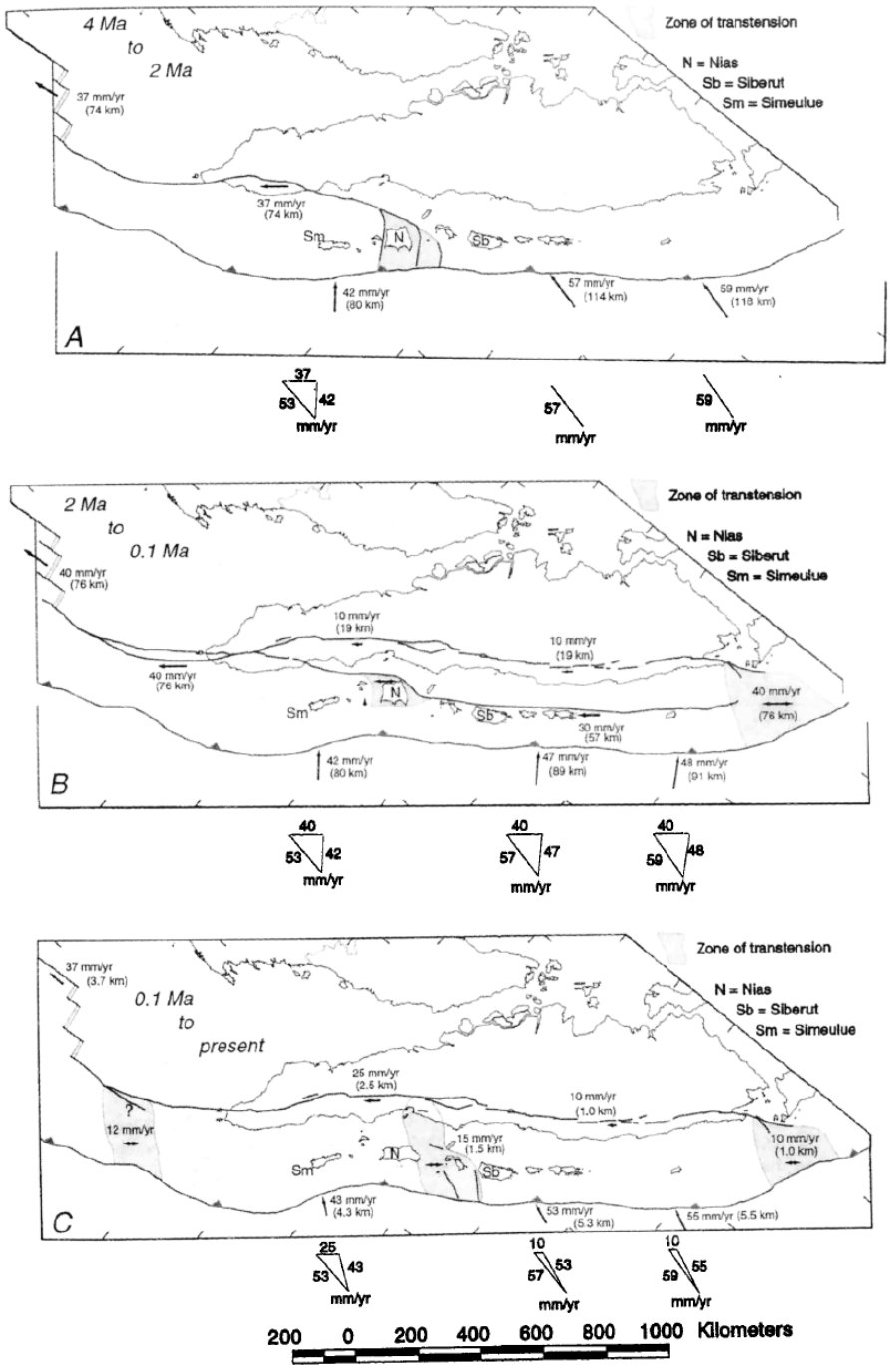

Figure 6: A potential history of deformation in the last 4 Ma along the obliquely convergent Sumatran plate margin. (From Natawidjaja and Sieh, 2000)

2.4.7. A tectonic model of the Sumatran plate margin

Natawidjaja and Sieh (2000) divide the Sumatran plate boundary into three tectonic domains, based upon their relationship to the Plio-Pleistocene transtension process in the equatorial portion of the margin. The southern domain has only been part of the forearc microplate since the last 2 Ma and is most simple in geometrical and structural terms. The central domain is the most complex, because it comprises all the transtensionally fragmented pieces.

The characteristics of the southern domain starting in the east are the right-stepping en echelon

pattern of the Sumatran fault above the 100-135 km isobaths of the subduction interface; the volcanic arc is predominantly located to the northeast of the fault; the forearc basin is remarkably simple and uniform; the outer-arc ridge is relatively narrow, forms a single antiformal high and is geometrically simple; the Mentawai fault and homocline, separating the basin and ridge, are unbroken and relatively straight; and the inner trench slope is relatively uniform and possesses a prominent plateau about half way between the active deformation front and the outer-arc ridge. The giant subduction earthquake of 1833 Mw = 9.0 had its source on the subduction interface beneath this domain (Newcomb and McCann, 1987). Prawirodirdjo et al. (1997) showed via strains measured by GPS in the early to mid-1990s that the outer-arc islands are moving parallel to the relative plate motion vector and that the subduction interface beneath the southern domain is currently fully locked. According to Sieh et al. (1991) the Sumatran fault appears to be slipping at a rate of around 10 mm/yr in the southern domain.

The characteristics of the northern domain from east to west are as follows: A geometrically irregular Sumatran fault, with releasing and restraining bends, residing above the 125 to 140 km subduction isobaths; a volcanic arc on and to the north of the fault; a 1 to 2 km deep forearc basin; a very broad structurally and bathymetrically complex outer-arc ridge; a homocline along its southernmost few hundred kilometers that is similar to the Mentawai structure of the southern domain; and a very narrow inner trench slope.

The complex central domain can be distinguished by the following features: From east to west we start with a 350 km long section of the Sumatran fault that is markedly discordant with the subduction isobaths; a volcanic arc that cuts across the fault; a topographically shallow forearc basin, fragmented into several blocks during oblique-normal faulting; a fragmented outer-arc; a fragmented homocline between the outer-arc ridge and forearc basin; and a fragmented inner trench slope (Narawidjaja and Sieh, 2000). According to Newcomb and McCann (1987) the giant earthquake of 1861 and many other large historic subduction earthquakes originated in this domain. Strain measurements via GPS in the early 1990s indicate that the hanging wall block across the central domain is currently moving parallel to the subduction deformation front (Prawirodirdjo et al., 1997).

Narawidjaja and Sieh (2000) suspect the reason for the fragmentation of the central domain to be the subduction of the Investigator fracture zone on the underthrusting, oceanic plate for the past million years. Its locus of impingement on the deformation front migrated from north to south arriving at the central domain during the past 5 Ma. Furthermore, this could be the reason for the restriction of fault activity in the hanging wall block of the forearc region during this period to the central domain. In this area orientations of faults are predominantly north-south, which is more or less parallel to the topographic and structural grain of the underlying Investigator fracture zone. The topographic heterogeneity would be a potential reason for the disruption of the forearc and the

outer-arc regions. Additionally, Fauzi et al. (1996) expects this scenario to be associated with a band of intense seismicity within the downgoing slab.

2.4.8. Volcanism in the Barsian Mountains

The Barisan Mountains are synonymous with the backbone of Sumatra. It is a 100 km wide mountain range approximately parallel to the subduction front consisting of pre-Tertiary rocks covered by Cenozoic volcanic rocks. The active volcanoes of Sumatra are found within this mountain range and above the 100 to 150 km depth contours of the subducted plate (Sieh and Natawidjaja, 2000). According to Hamilton (1979) the pattern of subduction-related volcanism has persisted since at least Oligocene time (~30 Ma). The modern volcanic arc consists of andesitic, dacitic, and rhyodacitic to rhyolitic rocks, with variable amounts of crustal contribution resulting from measurements of the strontium ratios. The continuation of the volcanic arc up north forms the small islands of Barren and Narcondam, approximately 100 km east of the Andaman Islands (McCaffrey, 2009). According to Curray (2005) inactive volcanoes in Myanmar could be part of the same volcanic chain even further to the north.

Speaking of volcanism in Indonesia you cannot skip mentioning the Toba caldera. 74 000 years prior to present more than 2800 km³ of dacitic and rhyolithic material were ejected from the Toba caldera complex (Chesner et al., 1991), resulting in a 100 by 30 km topographic depression in the volcanic arc (McCaffrey, 2009). According to Masturyono et al. (2001) the Toba depression overlies two magma reservoirs in the shallow crust (<10 km), one of which appears to be at least 40 by 60 km across. These reservoirs were partly responsible for caldera-forming, ash-flow eruptions at 0.5 and 0.84 Ma. Rampino and Ambrose (2000) and others claim that the eruption 74 000 years before present had an enormous impact, given that it caused a near extinction of the human population.

2.4.9.The forearc region of the Sunda Subduction Zone

2.4.9.1. The morphology of an accretionary wedge in general

The inner trench slope of an active arc system describes the slope from the trench up to the frontal arc. Karig (1974) divides two morphotectonic sections. An upper section which is relatively smooth with little-deformed sediments lying on top and a steeper, less regular lower section with deformed and acoustically unresolvable or absent sediments. The border between these two sections is a ridge, a bench or a simple break in slope. Dickinson (1979) defined this boundary as the so-called trench slope break. It is equivalent to the outer-arc ridge which is a continuous feature throughout western Indonesia from north of the Andaman Islands to southwest Java (Hamilton, 1973).

On Nias Island, my special field of interest the trench slope break of the Sunda arc system, as well as the seaward edge of the forearc basin is accessible.

2.4.9.2. The deformational history of the forearc region

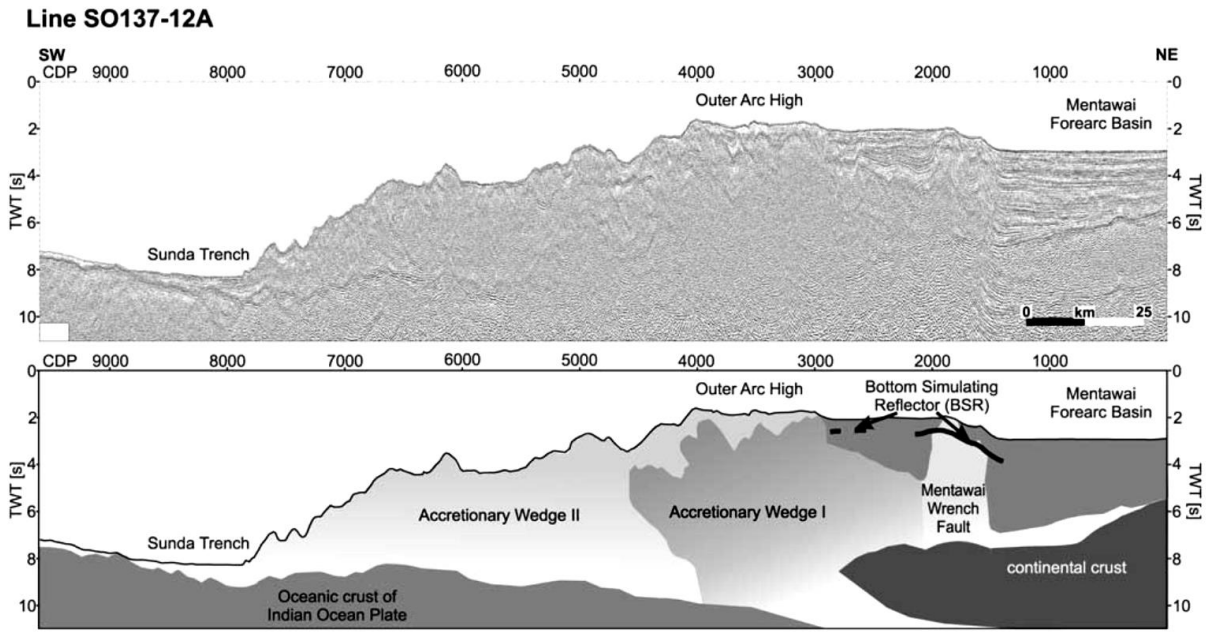

Figure 7: Interpretation of a geoseismic section in the southwest of mainland Sumatra by Schlüter et al. 2002 considering the deformational history of the forearc region (From Schlüter et al. 2002)

According to Schlüter et al. (2002) the forearc region of the Sunda Trench is more complex than previously thought. They divide two different sections of the forearc wedge. An accretionary wedge I, which originates from the Paleogene and an accretionary wedge II which started to form since the Neogene (Figure 7). They distinguish four different stages in the evolution of the forearc (Figure 7). Stage 1 starts in the early Cenozoic and marks the point on which the Indian and the Australian plate become one plate. This was when subduction began, but according to Hall (1998) may have changed the direction and the rate of convergence over time. Accretionary wedge I originated in the early Paleogene along the paleo-Sunda Arc. The paleo-forearc-basin subsided and was filled with prograding slope sediments from the adjacent continental margin. Parts of this first accretionary wedge can be found on Nias Island. The accretionary wedge I and the forearc basin were altered by erosion due to continuous convergence, tectonic uplift and eustatic sea level lowering (about 100-150 m). This discontinuity can be recognized in the seismic profiles of Schlüter et al. (2002).
Stage 2 spans from upper Oligocene to early Miocene. A subsidence of the forearc region may be related to changes of the movement and direction of the Indo-Australian Plate approximately 32 ma ago (Glebovsky et al., 1995). That change led to a slow down or even cessation of convergence in the upper Oligocene to early Miocene. Furthermore a simultaneous sea level rise or transgression with visible, sedimentary onlap structures on the Oligocene erosional surface is identified. This

sedimentation in the unconformity of the Oligocene started with shallow water limestone which merged downslope into deep water carbonates and mudstones and showed an upward increase of clastic material. At the end of stage 2 renewed convergence sets in, combined with increased seismicity and steepening of the paleo-slope, which may have caused submarine disruption and the sliding of the newly formed sediments, causing synsedimetary overturned and strip-thrust folds.
Stage 3 is reached in the early to middle Miocene. The Burma microplate was partly coupled with the north moving Indo-Australian Plate. That caused stretching of the Sunda continental margin to the north of Sumatra and the subsequent formation of new oceanic crust in the Andaman Sea since the Pliocene. According to McCarthy and Elders (1997) the setting at the time led to the inversion of older rift basins and following Longley (1997) marine sediments were deposited due to an additional eustatic sea level rise. Furthermore Nishimure et al. (1986) states that paleomagnetic studies suggest a clockwise rotation of Sumatra in respect to the Indo-Australian Plate, which can be reassured by Zen (1983) due to volcano-tectonic analysis. Based on their studies there was an increase of obliquity and rate of convergence, which was compensated by increased subduction (Hall 1998). This caused the formation of the accretionary wedge II in front of accretionary wedge I in the middle Miocene. The boundary between these complexes is interpreted to be the pronounced thrust-related step of the seafloor, resulting in different water depths. The Paleogene accretionary wedge I acted as a backstop for younger trench-fill sediments. A potential detachment between younger downgoing sediments and the accretionary wedge I may have caused the initial uplift, the northeast tilting, duplexing at depth and the rotation of the letter. The accreted and consolidated mass of wedge I more and more started to form the outer arc ridge. Simultaneously subsidence of the forearc basin on top of the seaward thinned continental crust began. Since the lower Miocene deposition of carbonate-rich sediments was followed by prograding clastic and shale-prone sediments coming from the volcanic arc terrains of the upper plate.
Stage 4 marks the last stage and occurred during the Plio- to Pleistocene. The outer arc ridge acted as a buttress against incoming sediments in a time of steady subduction, forming the accretionary wedge II. Therefore this accretionary wedge became severely deformed and chaotic already at its front of the paleo-trench. That is pretty uncommon compared to other convergent plate margins. Usually the internal stratification of the first outer thrust slices of the respective wedges remain intact, but not so in the Sumatran forearc region. The high deformation of accretionary wedge II is therefore thought to be the result of an extreme strain-slip cleavage caused by the high compression on accretionary wedge I and by the obliquity of convergence. This was suggested to even cause the backthrust of accretionary wedge II to the northeast along the border between the forearc ridge and the forearc basin. This transpression could be the main force for the development of the Mentawai fault. In fact several successive, transpressional phases can be identified along the Mentawai Fault Zone indicated by differences in the strength of the deformation interpreted by the differences in the

grade of updoming and steepening of the sedimentary sequences next to the fault. What is still unclear is the subsidence of the forearc basin since the Plio- to Pleistocene. It cannot be explained in terms of deformation and a loading effect of the sedimentary cover. A potential answer could be found in subcrustal erosion and microing processes (Schlüter et al. 2002).

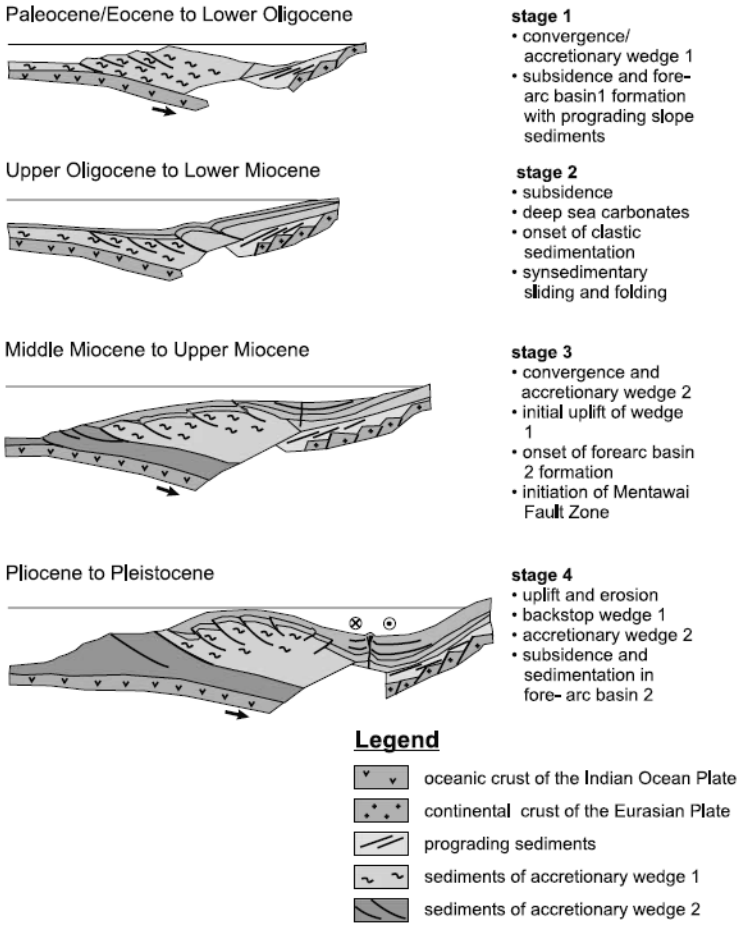

Figure 8: Model for the evolution of the forearc region of the Sunda trench in four stages (From Schlüter et al. 2002)

2.5. The Burma microplate

Curray (1989) in general described the idea of a microplate in between two converging tectonic plates as a consequence of oblique subduction, for which the oblique, underthrusting motion of the downgoing plate gets compensated along two separated faults. It gets described as a decoupling of motion by McCaffrey (1991). The reason for these globally visible results at zones of oblique subduction is that it requires smaller overall shear forces when the shearing (trench-parallel) and the underthrusting (trench-normal) component of the relative plate motion are partitioned between two separated faults instead of compensating the relative motion on one fault (McCaffrey, 2009). These two distinct fault planes isolate a platelet or rather a small independent microplate between the converging tectonic plates of greater scale, which can show separated characteristics in terms of movement, deformation, seismicity, rigidity and so on (Curray, 1989).
In the mid-90s two contrasting models to explain the decoupling, the increasing slip-rate along the Sumatran fault and deformation of the Burma microplate were formulated. Diament et al. (1992) found evidence for an additional, potential major strike-slip fault, within the Burma microplate, namely the Mentawai fault and therefore thought it responsible for the arc-parallel, extensional feature of the forearc region and the increasing slip-rate along the Sumatran fault, while McCaffrey (1991) has evidence for more or less north-south and east-west trending strike-slip faults which cause extension of the microplate and the accommodated increase of slip along the Sumatran fault (Samuel and Harbury, 1996). In the following chapter I tried to summarize both models in detail.

2.5.1. Extensional, arc-parallel deformation (arc-parallel vs. arc-crossing strike-slip faults)

Dextral strike-slip earthquakes, along the Sumatra fault and subduction earthquakes, below the forearc region, which show nearly perpendicular underthrusting in respect to the arc, despite the oblique plate convergence offshore Sumatra are strong evidence for the decoupling of motion along the Sumatran subduction zone, according to McCaffrey (1991). He states that the forearc ranging from Java to NW Sumatra experiences varying degrees of arc-parallel extension, therefore rigid plate behavior of the Burma microplate can be ruled out. The rate of northwestward motion of the Burma microplate or rather the forearc relative to the Southeast Asian plate increases from south of Java to northwest Sumatra from nearly zero to 45-60 mm/yr. Although the deformation process which is responsible for the stretching of the forearc is not completely understood, according to Samuel and Harbury (1996) certain evidence speaks for the greater dominance of strike-slip faults which are crossing the margin at least offshore Sumatra, instead of arc-perpendicular normal faults proposed by Diament et al. (1992). Huchon and Le Pichon (1984) present evidence for the basin producing extension with normal faulting near the Sunda strait, which plays a less significant role

for the arc-parallel extension in the Nias area according to McCaffrey (1991). Karig et al. (1980) claims that two sets of strike-slip faults cut the forearc in approximately north-south and east-west direction and produce tens of kilometers of displacement. The nodal planes of shallow strike-slip earthquakes in the forearc region speak in favor for that claim due to the fact that they strike more or less north-south and east-west, rather than parallel and perpendicular to the arc. The arc-parallel extension and the accumulated strain leads to a thinning of the forearc in a pure-shear manner of around 1-2 mm/yr and could possibly result in a greater frequency of ascending mantle material, which is the case in the Sunda strait. The slip vector data speaks in favor for increasing decoupling of the Burma microplate towards the northwest, but not for complete decoupling (McCaffrey, 1991).

Although the Mentawai Fault Zone is clearly visible in seismic refraction profiles there is not enough evidence for a significant amount of strike-slip motion at least on Nias Island, according to Samuel and Harbury (1996). That does not automatically exclude the assumption that there is substantial, dextral strike-slip movement further to the southeast. However, it is very unlikely, because of two characteristics of the Mentawai fault which are highly atypical for a strike-slip fault. Number one is the fact that the zones in close proximity northeast and southwest next to the Mentawai fault are mainly downthrown in respect to the central portion of the fault. Whereas Underhill et al. (1988) stated that a characteristic of strike-slip fault zones is the change of magnitude and sense of displacement along the length of the fault system. Number two is the atypical narrowness and straightness for a major strike-slip system of the Mentawai fault, which is about 25 km.

Samuel and Harbury (1996) were able to identify strike-slip faults with small amounts of movement (less than 5 km) on Nias Island, which cut across the strike of the island. The movements on these structures resulted in arc-parallel stretching and a northwestward extension of the island (Figure 9). Additionally, a network of arc-perpendicular extensional faults is responsible for further arc-parallel extension. The strike-slip faults found on Nias Island can be matched in terms of orientation and sense of movement to the larger-scale strike-slip faults like the Batee and Singkel faults to the north and northeast of Nias Island. Therefore, according to Samuel and Harbury (1996) the forearc, or rather the Burma microplate is not behaving as a rigid plate and at least in the Nias area is clearly subject to arc-parallel stretching in a way postulated by McCaffrey (1991). Additionally, they interpret the Mentawai fault as the surface expression of an originally arc-parallel extensional fault which has been mildly reactivated in a contractional sense. The features identified by Diament et al. (1992) don’t necessarily need strike-slip motion to be explained. Samuel and Harbury (1996) state that the sea floor topography in the area of the proposed dextral Mentawai Fault Zone can also be explained by mud diapirism and the inversion of an originally extensional structure.

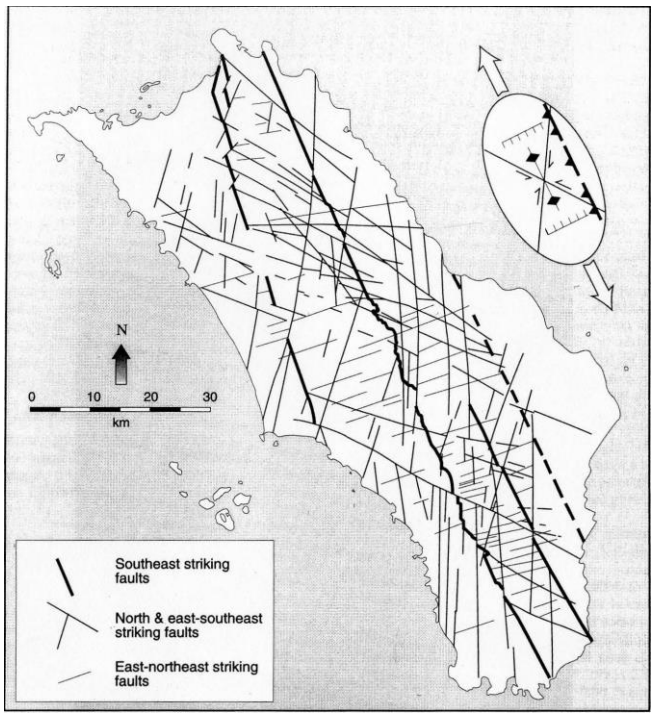

Figure 9: Map of the fracture network on Nias Island indicating arc-parallel extension since Pliocene (From Samuel and Harbury, 1996)

2.5.2. The Mentawai and the Aceh microplate

Malod & Kemal (1996) interpret the Mentawai fault to be a positive flower structure originating from a transpressional regime. Therefore it should experience strike-slip and compressional motion, although recent transcurrent motion cannot be detected along the Mentawai fault. Some authors claim there was strike-slip motion along the fault in Neogene times which ceased (Diament et al., 1992).

Malod & Kemal (1996) identify two additional, potential microplates along the forearc region of west Sumatra which move separately to each other, the mainland and the accretionary complex. First, there is the Mentawai microplate which extends from the south of Sumatra to the south of Nias. It is bound by the Mentawai, the Sumatran and the Batee fault. The southern limit is where the subduction changes from normal to oblique. The northern limit is said to be a large discontinuity interrupting the subducting slab to the north of Nias. There is weak to no evidence for extensional deformation within the Mentawai microplate. According to Matson & Moore (1992) the NNW-SSE striking Batee fault connects the Mentawai with the Sumatran fault. Following Malod & Kemal (1996) the existence of the Mentawai microplate shows that the accretionary prism moved relative to the forearc domain.

Second, the Aceh microplate is bound by the Batee, Sumatran and the west Andaman fault. The last is interpreted as the equivalent further north of the Mentawai fault. In this area there is still no evidence for an active strike-slip movement along the Mentawai fault, but there is evidence for backthrusting of the accretionary prism over the forearc basin. A flexural bending of the forearc

basin under the accretionary prism would explain the deepening of the forearc basin towards the west (Malod et al., 1993).

Malod & Kemal (1996) present a model which tries to explain a potential movement of the accretionary complex in respect to the forearc basin region. This accretionary complex experiences a higher degree of coupling due to the frontal setting and the loading of the downgoing oceanic plate which increases the coupling effect. Additionally the deeper part of the accretionary complex was better consolidated in the Eocene and Oligocene when the subduction was more perpendicular. Moreover large structures on the oceanic seafloor entering the subduction zone e.g. the Investigator Ridge or the Wharton Spreading Ridge should increase the coupling effect on the accretionary complex compared to the forearc region. Respectively the Mentawai and the Sumatran fault must be decoupled.

Three different zones along the accretionary prism off Sumatra get described. In the south or rather the Sunda strait there we can see extension and material ablation (Figure 10). The northwest movement of the Mentawai microplate as a single block is related to the extension in the Sunda strait. Additionally oceanic sediments get accreted to deeper parts of the margin. These two mechanisms are said to cause the concave shape of the margin south of the Sunda strait.

In the central portion of Sumatra both the Mentawai microplate and the accretionary complex are displaced to the northwest, marked in figure 10 as "*Transfert*". Relative movement between the first and the letter is said to occur along the Mentawai fault. The amount and the timing of relative motion cannot be established in detail.

In the north the movement was mainly concentrated along the Sumatran fault, while in the accretionary complex subduction occurred as being frontal (Figure 10 "*Accumulation*"). The Mentawai fault is having a horsetail shape in the region around Simeulue Island, which further visualizes its reduced role in transcurrent motion (Malod & Kemal, 1996).

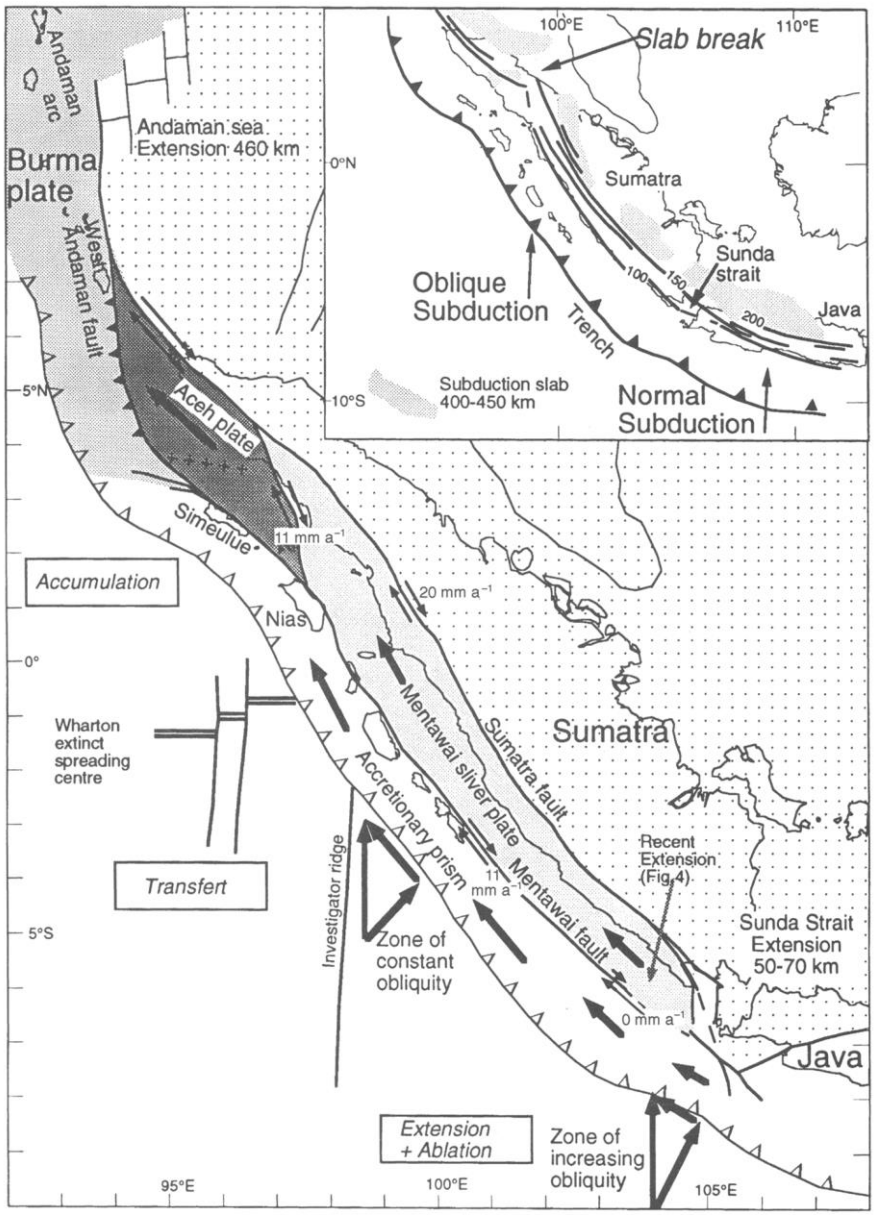

Figure 10: Sepparated microplates moving independently in respect to the mainland and the accretionary complex (Malod & Kemal, 1996).

2.6. The tectono-stratigraphic units on Nias Island

In my special field of interest there is a tectono-stratigraphic differentiation of two sorts of units. Linear belts of chaotically deformed rocks are seen as the lower most unit and classified as melange or Oyo Complex. On top are the so called Nias Beds, comprising the Lelematua and the Gomo Formation (Figure 11), which are less deformed, structurally coherent sedimentary rocks. The distinction of the two different stratigraphic units happens in the field via the analysis of structural style, physical properties and the lithology (Moore and Karig 1980). Tjia and Boentaran (1969) recognized a major structural trend in Nias which is parallel to the longitudinal axis of the island and to the Sunda trench itself with a direction of approximately 330° (NW). The relative proportions and width of the outcropped terrains of melange increase towards the west of the island, whereas the Nias Beds have increasing proportions and width towards the east.

Only very little gradation of the following characteristics for differentiation at contacts between the two stratigraphic units support the interpretation that the Oyo Complex is not made of deformed Nias Beds, but that they originated and evolved separately (Moore and Karig 1980).

The original contact between the Oyo Complex and the Nias Beds is supposed to be depositional. The consistent age distribution at the lowermost base of the top unit speaks in favor for this assumption. The western margin (seaward) of the Nias Beds is thought to be originally deposited on the underlying melange, but due to shearing parallel to the contact it is difficult to interpret the results found in the outcrops. The Nias Beds show steep dips to the east, nearly parallel to the contact between the stratigraphic units. While the melange zone is pervasively sheared in this stratigraphic contact zones, the Nias Beds are well bedded and highly fractured.

The eastern boundaries of the Nias Beds seem to be basically tectonic. Adjacent east dipping thrust faults are responsible for overturning, folding and shearing the topmost unit. In these areas the Nias Beds are sheared and folded into tight synclines with eastern limbs dipping steeply to the west, if they are not overturned and dipping to the east. In contrast to the western margin of the Nias Beds, the eastern margin shows significant change in ages of the strata along strike indicating a tectonic boundary (Moore and Karig (1980).

I will now further describe the characteristics of each tectono-stratigraphic unit in detail.

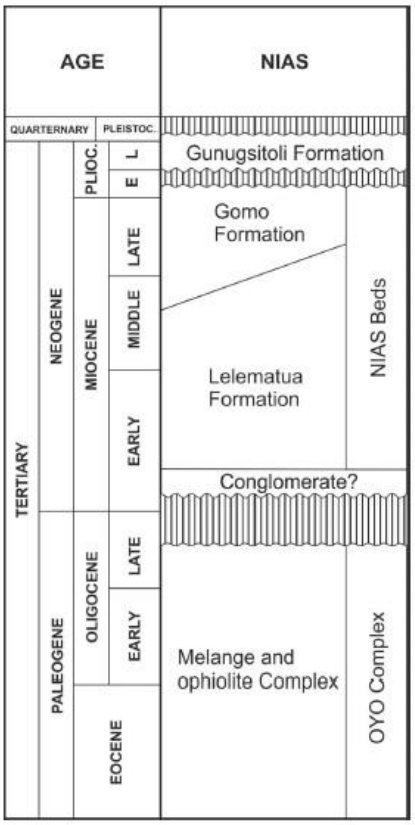

Figure 11: Stratigraphic table of the units found on Nias Island resembling its geochronological time context (From Barber et al., 2006)

2.6.1. The Melange Zone:

The term melange in the case of the stratigraphic lowest unit exposed on Nias Island is used in a descriptive and nongenetic way. It consists of mappable bodies with a characteristic internal fabric dominated by penetrative mesoscopic shear fractures and all sizes of inclusions. Attempts to subdivide single melange terrains failed by Moore and Karig (1980), for the reason that the quality of outcrops is poor and frequent landslides occur throughout the island. The same difficulties emerged in the fieldwork for this master thesis. Reworked foraminifera suggest an age not older than Eocene for the Melange Zone (Douville, 1912). Due to the fact that the Oyo Complex is overlain by lower Miocene strata, in central Nias it cannot be younger than early Miocene.
The melange matrix consists of pervasively sheared and fine-grained sedimentary rock debris and is described as being a cohesive gray paste when weathered, but can be friable in some outcrops. About 60-70% of the matrix consists of silt- to clay-sized fragments of quartz, feldspar and sedimentary rock. About 30-40% consists of clay minerals.
The Oyo Complex shows a certain amount of oceanic crustal rocks, such as basalt, chert and ultramafics, although comprising a high amount of sedimentary rocks. The sediments of the Oyo Complex are on average more coarse-grained than the lower most few hundred meters of the Nias Beds and have a gray and brown color.
Structurally speaking the Melange Zone shows a weekly developed foliation which is thought to have evolved due to multiple shear planes dispersed through the matrix. This foliation strikes approximately parallel to the Melange Zone trend and is steeply dipping to the east (Moore and Karig, 1980). According to Moore (1979) the Oyo Complex shows a higher grade of diagenetic and metamorphic alteration, indicated by growth of phyllosilicates in grain interstices of the sandstones. These phyllosilicates dominate the style of cementation for the Melange sandstones. In general it is carbonate-poor and lacks porosities which can be correlated with a higher grade of compaction.
In terms of structural style pervasive shearing, a chaotic dismemberment of bedding and the absence of large scale folds can be observed throughout the Melange Zone (Moore and Karig, 1980).

A great difference in the lithic fragments composition exclude the assumption that the Oyo Complex sandstones are simply deformed Nias Beds sandstones (Moore and Karig, 1980).

2.6.2. The Nias Beds

On top of the Oyo Complex, or rather the Melange Zone sits the neogene strata or the so called Nias Beds. These are linear belts of sedimentary rocks, which trend is subparallel to the Sumatran trench and were deposited in the lower Miocene to Pliocene. The Nias Beds consist exclusively of sedimentary rocks which appear to be green-gray, fossiliferous and carbonate-rich. These

sediements have a higher amount of porosities and are cemented by carbonate. Nias Beds sandstones have a higher amount of K-felspar and glauconite, which lacks in the underlying Oyo Complex. In the close surrounding several uplifted coral terrace complexes and beach deposits reside. In structural terms the Nias Beds are folded and not strongly sheared.
The thickness spans from 3 to 5 km and they show a coarsening upward sequence. From bottom to top a cross section of the Nias Beds exhibits a series of thin-bedded, carbonate-poor siltstones and shales, which are overlain by a deep-water sequence (lower bathyal to abyssal) of foraminifera-rich calcilutite turbidites including thin interbeds of terrigenous turbidites and occasionally tuff beds. This sequence shows a grading upward trend resulting in sandstone, conglomerate and shales consisting of shallow-water carbonate debris mixed with terrigenous detritus (Moore and Karig, 1980). Moore (1979) detects the origin of the Nias Beds sandstones to be mainland Sumatra via petrographic analysis of their mineral and lithic fragment compositions. Along the east coast of Nias the upper Pliocene and younger strata contains large, reworked Oyo Complex clasts. These appear partly as being derived from a Nias source.
The structural style of the Nias Beds further away from the Melange Zone is dominated by chevron-type folding showing asymmetric and tight folds, due to the different dips of the fold limbs. The east dipping limbs are dimensionally longer and less steep, while the west dipping limbs are steeper. The common direction of fold asymmetry points to the southwest, indicating a shear couple directed east over west. In the central part of the Nias Beds, further away from the Melange Zone coherent outcrops with no significant disruption are observed (Moore and Karig, 1980).

2.6.3.The history of deposition and deformation

The Oyo Complex is interpreted as a tectonically disrupted sequence of oceanic crust and mantle, oceanic plate strata and trench deposits. Clearly speaking for this interpretation are the occurrence of pillow basalt, gabbro, ultramafic rocks, chert, pelagic limestone from the subducting oceanic plate and coarse sedimentary rocks originating from mainland Sumatra, and the structural position which is underneath fine grained, hemipelagic, deep water deposits known as the Nias Beds. The sandstones and conglomerates are interpreted to be deformed trench deposits.
Subduction of the Indo-Australian oceanic plate started in early Miocene. Karig and Sharman (1975) suggested that the subducted plate had only a thin sedimentary cover. That is the reason why we can find many mafic and ultramafic rock inclusions derived from the previous subducted plate in the Oyo Complex. Parts of the oceanic crust have been sliced off and accreted to the inner trench slope. A potential analog for this subduction scenario of the Oligo-Miocene Sunda trench in the area of Nias can be seen nowadays southwest of Java. Only a thin cover of oceanic sediments is present on the underthrusting oceanic crust (Curray et al. 1977). Beck and Lehner (1974) believe oceanic crust to have already been incorporated into the accretionary wedge offshore Java, potentially

resembling the situation during the origination of the Oyo Complex.

Analysis of the Nias Beds via comparison of structural style, lithology, and structural position and several core samples, and seismic reflection profiles in the area of the lower trench slope indicates that the Nias Beds represent uplifted and deformed trench-slope deposits. Generally speaking many seismic profiles of lower trench slopes show that slope sediments are very likely to be ponded in basins behind ridges of structurally complex material (Moore and Karig, 1976). Typically these deposits get progressively more deformed with depth in the basins. In the late Cenozoic the accretion of the Nicobar Fan led to the uplifting of the deep water slope strata of Nias above sea level. This process can be seen in the coarsening- and shallowing upward sequence of the Nias Beds.

On Nias Island we can observe steep east, or rather landward dips of the contacts between the stratigraphic units and several other structures. This is explainable with rotating thrust packets on the inner trench slope due to accretion of material to the base of the lower trench slope (Seely, Vail and Walton, 1972; Karig and Sharman, 1975). Several published seismic reflection profiles across trench slopes all over the world, as well as profiles of the trench slope seaward from Nias show progressively increasing landward dips with depth of sediments in slope basins (Moore and Karig, 1976).

Samuel et al. (1995) stated that it is difficult to put the fragments of the Ophiolitic Complex found in the Melange Zone back into an original paleogeographic setting, but suggest that lineated bastite serpentinites experienced ductile deformation, therefore a potential point of origination could possibly be an oceanic transform zone. Diorite incorporated into the Melange Zone could resemble the plutonic portion of oceanic island arcs, while plagiogranite could originate from differentiated intrusions at a prior mid-ocean ridge. According to Fisher and Schmincke (1984) pillow fragment breccias, which are most frequently found in the ophiolithic rocks on Nias evolved on the steep slopes of pillow volcanoes and large seamounts or accumulated at the foot of submarine fault scarps which can be found in faulted mid-ocean ridges. Kallagher (1989) proofed that the basalts and gabbros commonly found on Nias show geochemical characteristics of MORB type crust. Therefore the spectrum of ophiolithic material found on Nias Island stems from oceanic crust, oceanic islands, seamounts and from oceanic fractures zones.

Samuel et al. (1995) interprets the evolution of the Sumatran forearc ridge differently than previous authors. They interpret the rocks found on Nias as sediments deposited in extensional basins despite their proximity to the Sunda Trench and subduction zone. Matson and Moore (1992) describe the orientation of the original extensional and oblique slip faults as similar to faults bounding actually present sub-basins. Daly et al. (1991) relate the extensional basin formation of SE Asia in the Eocene to first order changes in global plate motions, or rather the collision between India and Eurasia which happened in the same geological time causing a rapid decrease in plate motion or

convergence. Daly (1989) stated that forearc areas are particularly sensitive in response to changes in subduction parameters. Samuel et al. (1995) see the effect of the collision of the Australian plate and the Sunda Arc on the Sumatran forearc as the Early Miocene inversion. In the late Miocene and Pliocene an increase in subduction rate coupled with the accretion of thick Bengal fan sediments in the northern part of the Sunda trench as stated by Karig et al. (1979) led to an increase in compressional stress along the outer margin of the Sumatran forearc causing a second basin inversion and reactivation of faults on Nias. The formation of the Melange Zone occurred mainly during the Pliocene inversion. It formed in accord with diapiric mobilization of thick Oligocene and Lower Miocene mudrock dominated sedimentary successions (Samuel et al. 1995). Barber et al. (1986) and others have already documented diapiric melange formation around convergent plate boundaries, especially in accretionary wedges, but so far had no connection to basin inversion.

2.6.4. A representation of subduction zone tectonics

On Nias we get a clear impression of how deformation is distributed in the inner slopes of trenches. The highest shearing and folding is observed at the landward, or rather eastern margin of the Nias Beds. That indicates the cause for the deformation of the slope strata to be the movement of the thrust faults that bound the basins to the east. In some outcrops and in many seismic profiles (Karig et al., 1980) it is possible to see the decrease in deformation from oldest to youngest strata of the Nias Beds. This observation together with the sharp contrast in deformational intensity between the two different stratigraphic units suggest that tectonism was strongest at the base of the lower trench slope and continuously decreases up to the trench slope break. Due to continued accretion of trench sediments and the present, horizontal, compressive stress field the thrust slices get rotated and uplifted, same as the overlying slope sediments.

Many scientists tried to explain the evolution of melange zones not only for the Sunda trench, but all around the world. Some people tried to explain it via gravity sliding processes and olistostromes, but they failed to give a sound explanation. Moore and Karig (1980) claim thrust-related shearing on the lower trench slope to be responsible for the formation of melange zones such as the Oyo Complex. The spatial-temporal relationship of the Melange Zone and the occurrence as structural highs in linear belts parallel to the trench and regional fold trends is seen as strong evidence for their model.

The fact that the Oyo Complex is not strongly sheared is a clear structural style contrast to other subduction zones around the world, such as Barbados (Baadsgaard, 1960) or in the Aleutian Islands (Moore and Wheeler, 1978). Normally we can observe folding rather than pervasive shearing and disruption as we do in the Sunda accretionary wedge. It appears that folding is the dominant style of deformation in subduction zones where subduction rates are low and sediment thickness high. A modern analogue to that scenario is the Shikoku Trench (Moore and Karig, 1976).

Moore and Karig (1980) suggest that subduction of an oceanic plate with thin sediment covers and with moderate to high convergence rates, leads to a rapid dewatering of the sediments and deformation dominated by shearing and total disruption of the sediments.

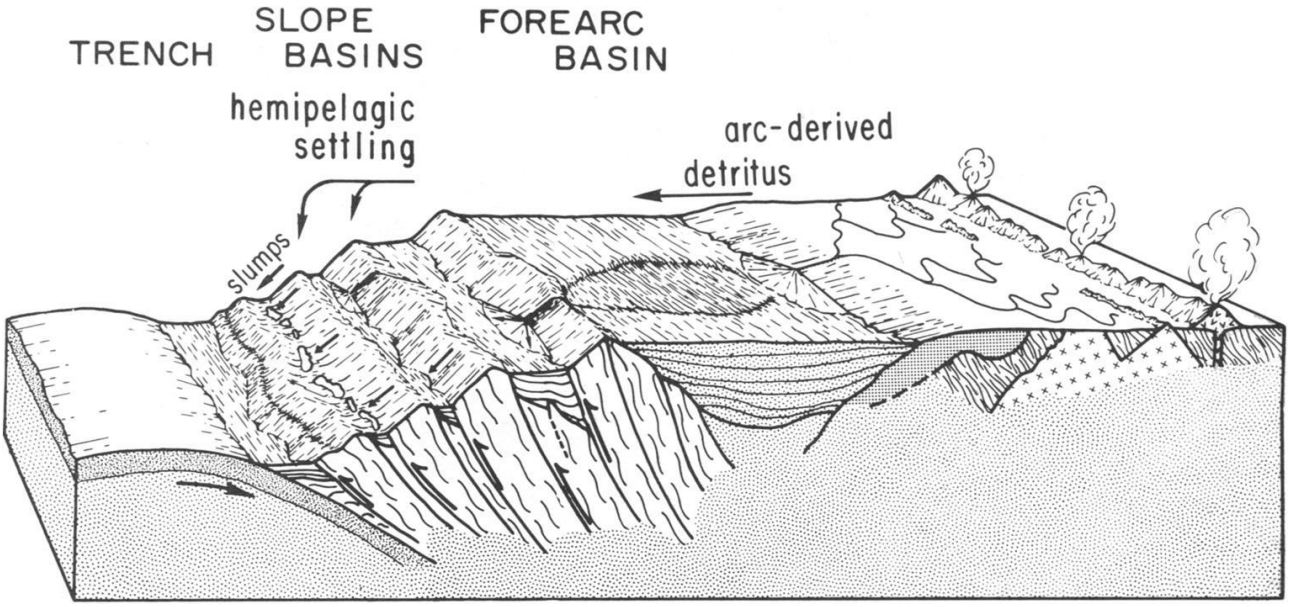

Figure 12: A model for trench slope sedimentation in the Nias Beds. Sedimentation near the base of the slope happens via slumping and hemipelagic settling. Further landward some thrust faults potentially become inactive allowing basins to combine. They are filled with terrigenous detritus from the arc via canyoning of the forearc basin, showing a coarsening upwards sedimentary sequence. (From Moore et al. 1980)

2.6.5. The inversion of extensional sub-basins

According to Samuel et al. (1995) and others the basement beneath most of Nias Island consists of amalgamated, ophiolithic fragments, which originate from different tectonic settings and has collected a deep marine sedimentary cover. The extension of this basement began in Mid-Eocene to Mid-Oligocene times. Several sub-basins developed under transtension which were filled with a thick sedimentary succession. The vertical movement along several faults transecting the sub-basins is responsible for topographic highs along strike on which carbonate and deep marine sediments were deposited. A localized Early-Miocene inversion of the extensionally formed basins was followed by regional subsidence during the Middle to Early Pliocene. A second inversion of extensionally formed basins caused the uplift of all the sub-basins during the Pliocene. Both phases of basin inversion caused the deformation of sediments on Nias. The contractional reactivation of originally extensional and oblique faults controlled the deformation of the basinal, sedimentary successions. This model of Samuel et al. (1995) does not necessarily need accretionary prism processes to account for the exposed Paleogene and Neogene rocks found on Nias Island. But still they claim that the formation of an accretionary wedge to the southwest of Nias contributed to the observed fault reactivation during inversion.

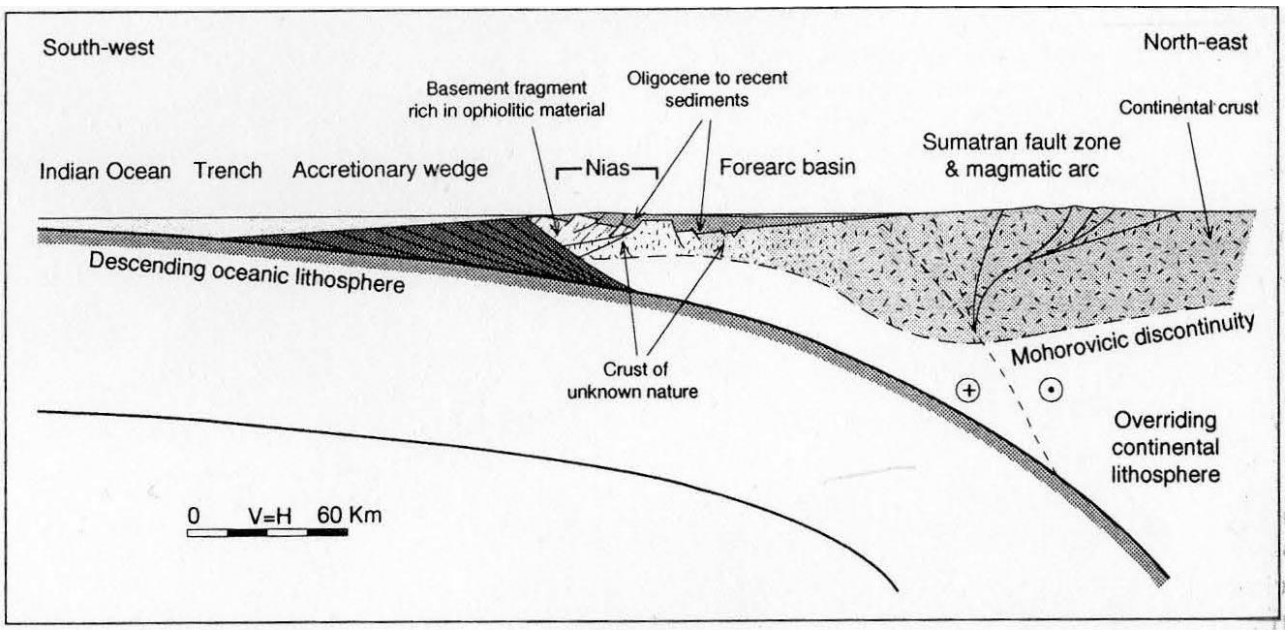

Figure 13: Cross-section of the Sumatran forearc according to the model of Samuel et al. (1995) (From Samuel et al., 1995)

2.7. Slip partitioning of megathrust ruptures

2.7.1. Heterogeneous strain accumulation, locked patches and coupling

Slip along a subduction megathrust can either be aseismic or seismic. While seismic slip has a duration of seconds to minutes, slip velocities of about a meter per second and rupture velocities of a few kilometer per second (Ruff & Kanamori, 1983), aseismic slip dominates at depths greater than 40 km, but can also occur in shallower depths (Pacheco et al., 1993; Sieh et al., 1999). Heterogeneous strain accumulation and stress building up around locked patches in the interseismic period are the results which tend to fail during megathrust earthquakes, such as e.g. in the 2004 Andaman-Nicobar, the 2005 Nias-Simeulue, the 2007 Mentawai events besides many more (Konca et al., 2008). Konca et al. (2008) modeled geodetic and paleogeodetic measurements of interseismic strain and showed that the Sunda megathrust especially offshore Sumatra is a patchwork of aseismic and seismic areas. He suggests a correlation between megathrust earthquakes and coupling. While comparing recent rupture events with historical accounts (Rosen et al., 2004) and paleoseismic data (Ji et al., 2002) of geographically and seismically similar events in the past, he made clear that certain areas along the Sunda megathrust tend to slip on a regular basis speaking in geological terms. One example is the Nias-Simeulue earthquake in 2005, when a 350 km section ruptured resulting in Mw = 8.6 (Briggs et al., 2006). The same patch produced a similar earthquake in 1861. To the south of Nias, close to the equator, coupling is low and consistent with only moderate seismic activity in the past few centuries (Chen et al., 2002). Beneath the Mentawai Islands, further to the south, coupling has been high for the past 40 years, therefore great earthquakes have happened repeatedly (Ji et al., 2002). In figure 14 the slip distribution of the 2005, Mw = 8.6 Nias - Simeulue earthquake is shown with 5 m contour lines in green (Bürgmann et al., 2005), grey and black polygons are estimates for the rupture events in 1797 and 1833 (Perfettini et al., 2008) and dark and pale blue lines show the 1 and 5 m slip contour lines of the seismic ruptures in 2007. Stars mark the respective epicenters. 1935 a smaller earthquake occurred near the Batu Island which is a region with weak coupling (Natawidjaja et al., 2004). The earthquake of 2000 to the north of Bengkulu is predominantly an intraslab strike-slip event, but still falls in an area of low

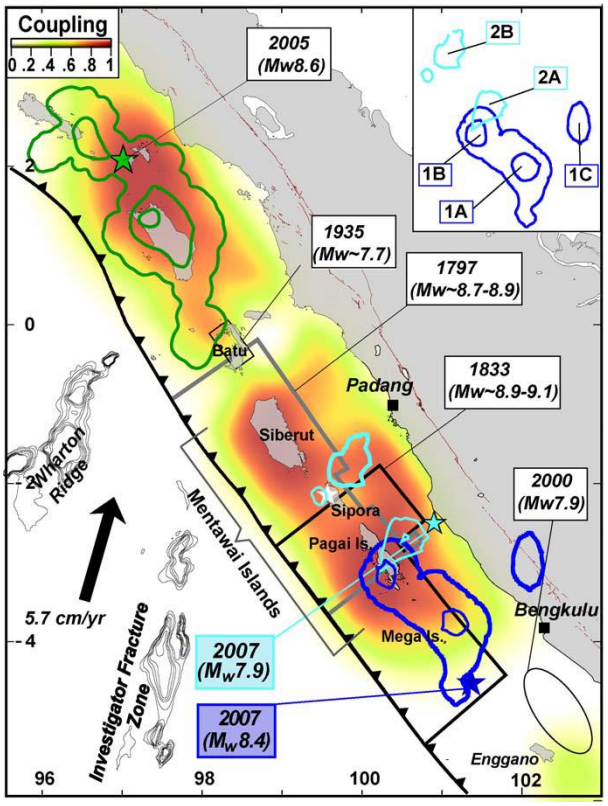

Figure 14: Patches with strong interseismic coupling on the Sunda megathrust, offshore Sumatra, coincide with large seismic ruptures (Figure from Konca et al., 2008)

coupling (Abercrombie et al., 2003).

2.7.2. Varying spatiotemporal patterns of strain accumulation and release

According to Konca et al. (2008) the pattern of interseismic strain accumulation has a profound influence on the characteristics of large megathrust earthquakes. Nonetheless, successive seismic ruptures in the same geographical locations differ significantly in extent and magnitude (Lay et al., 1982; Thatcher, 1990). Konca et al. (2008) shows such variations for the 2007 earthquakes in the southern part of the Mentawai Islands. In fact, the 2007 sequence of large seismic ruptures in the strongly coupled Mentawai patch differs significantly from historical events in this area in 1833 and 1797. The slip and extent in 2007 summed are far smaller than during the previous historical events and far less moment was released than the deficit of moment that has accumulated since the previous great events. The estimates for the released moment for each event come from measurements of coseismic uplift (Konca et al., 2008).

South of Siberut Island, the moment deficit accumulated since the last great event in 1833 is less than the moment released during the 1797 and 1833 events. Below Siberut Island the moment deficit is far greater than the moment released during both historical events. Therefore, the next megathrust rupture could have been expected to occur to the north of 2°S or underneath Siberut. Instead the earthquakes of 2007 occurred south of Siberut and the released moment was far less than the one of the great previous events in this area and far less to compensate the entire accumulated moment deficit. Konca et al. (2008) clearly demonstrates that the Mentawai patch is behaving in neither a slip- nor a time-predictable manner. If time-predictability would be given, slip would have occurred below Siberut and if slip-predictability would be given, the 2007 event south of Siberut would have been a unified major event (Konca et al., 2008).

But why didn't the 2007 event duplicate the 1833 event? Konca et al. (2008) sees the reason for this in the not effective cooperation of several spatially and temporally separate asperities. If two neighboring asperities on the same fault plane rupture jointly, they are expected to release more moment than if they had ruptured independently (Rundle et al., 1987). The static stress change induced by one asperity increases the stress on the other and therefore the elastic stress which is released during the rupture. In the 2007 events, analyzing the spatiotemporal evolution proofed that this kind of cooperation was not effective, because the slip on the second (2B in figure 14) asperity started slightly after the slip on the first asperity (2A in figure 14) was over. The reloading of asperity 2A due to rupture of 2B did not lead to any additional slip. One potential reason therefore could be the intervening area between the two asperities acted as a barrier to rupture propagation. This intervening area, which lies beneath north Pagai Island experienced little coseismic slip in the 2007 event, but cannot count as a permanent barrier due to the fact that it experienced the largest cumulative slip (around 17 m) if the slip models from the 1797 and 1833 event are summed up

(Natawidjaja et al., 2007). A locally lower stress level in this area before the 2007 earthquake, resulting from previous earthquakes in the surrounding region could have been the reason for the barrier function of the area beneath Pagai Island in the 2007 event. Minimal cooperation between the ruptures of asperities 1B and 2A in figure 14 is evident from the 12 hour time lag between the two ruptures. Although the two rupture locations (1B and 2A in figure 14) are in very close proximity to each other, one explanation for the lack of cooperation could be a narrow zone with low pre-stress due to the slip distribution related to the 1833 and 1797 events, which could have acted as a barrier. Another explanation could be a zone of aseismic creep, which is too narrow to show up in the pattern of interseismic strain (Konca et al., 2008). Konca et al. (2008) summarizes the case that the static stress increase in asperity 2A due to the Mw = 8,4 event was enough to trigger a delayed rupture of this asperity, whereas the dynamic stresses induced by the earthquake failed to trigger the rupture of asperity 2A immediately. The megathrust beneath the Mentawai area is described as subset of a locked portion which is surrounded by creep during the interseismic period. This complex spatiotemporal pattern of the 2007 rupture probably emerged due to the fact that it produced only around 25 % of slip in respect to the historical earthquakes. The sequence essentially ruptured a set of asperities, which triggered each other through static and dynamic interactions, but did not cooperate effectively because of several intervening barriers, which are very likely no permanents and resulting from varying stress distribution of previous earthquakes (Konca et al., 2008).

2.7.3. Segmentation of megathrust ruptures in long-term behavior

Briggs et al.(2006) investigated in the pre-, co- and postseismic motions of the great Nias – Simeulue earthquake 2005 and the Sumatra – Andaman earthquake 2004 and tried to set the results in context with earlier occurring megathrust earthquakes along the Sunda Subduction Zone. They used geodetic measurements, Global Positioning System (GPS) data and massive amounts of corals of the genus Porites to investigate in the deformation, emergence and submergence of the areas of interest. The reason for the use of these corals is the fact that they are very sensitive natural recorders of lowest tide levels (Zachariasen et al., 2000), therefore ideal natural instruments for measuring emergence and submergence relative to a tidal datum. The coral can only survive at an elevation slightly above the lowest tidal level, but will grow radially upward and outward until it reached exactly that level of the lowest tide. The subaerial exposure kills the uppermost portion of the coral and further upward growth is restricted. During an earthquake submergence or emergence of certain regions can lead to an elevation of these microatolls of corals and therefore can cause the overall death of a corallite when it is completely emerged above the lowest tidal level or a partial death of the uppermost portion when it is partly emerged and the head is above the lowest tidal level but the bottom is still below, therefore the bottom part will still grow radially outward. Sometimes it

is even possible to distinguish two different uplifting events on only one coral head (Sieh et al., 1999; Natawidjaja et al., 2004).

Simeulue Island was uplifted about 1.45 m on the northwestern tip of the island. It is possible to identify the southeastern limit of megathrust rupture during the 2004 event as about 2.5°N which is the center of Simeulue (Meltzner et al., 2006; Subarya et al., 2006). The southeastern third of Simeulue Island subsided, but time was too short to investigate that portion in detail for the reason that three months later the next megathrust rupture occurred. In the March 2005 event the vertical deformation pattern brought arc-parallel uplift of Nias and Simeulue Island and a broad subsidence trough between these islands and mainland Sumatra. It comes to an asymmetric deformation with maximum uplift of 2.9 m and maximum subsidence of 1.15 m. This pattern of uplift and subsidence matches several other megathrust rupture events around the world (Plafker et al., 1970; Fitch et al., 1971). The contours of uplift and subsidence are predominantly arc-parallel, but have a pronounced misalignment near the Banyak Islands between Nias and Simeulue (Briggs et al., 2006).

The research of Briggs et al. (2006) further manifests the segmentation of the megathrust in its long-term behavior. The misalignment of the coseismic deformation contours near the Banyak Islands and Nias are marking a border between two principle rupture patches. It also coincides with a disruption in the bathymetry of the outer-arc ridge, which could possibly be the southwestward extension of the Batee fault. Karig (1980) presents 90 km of dextral offset along this fault. The segmentation and break in the megathrust could suggest different dips of the rupture patches between Simeulue and Nias Island. Therefore the dip of the subducted plate beneath Simeulue should be shallower than bellow Nias, for the reason that the uplift ridge on Simeulue is farther from the trench than the uplift ridge on Nias. Davis et al. (1983) suggest that the megathrust is segmented in portions of high friction, therefore resulting in steep slopes (beneath Nias) and portions of low friction (beneath Simeulue) resulting in more gentle slopes along the megathrust. A rapid up-dip decrease in slip further seaward from the islands and a broad band of aftershocks in this region suggest that stresses imposed by the coseismic rupture were high enough to induce several aftershocks surrounding the shallower part of the interface. The question is why the rupture did not progress further up-dip? One explanation would be that the shallower parts had been de-stressed by coseismic rupture in earlier large historical earthquakes in 1907 or 1861 and another that aseismic slip keeps the up-dip section de-stressed. Further research is necessary in these aspects (Briggs et al., 2006).

Another anomaly of the two megathrust ruptures 2004 and 2005 is the size of the triggered tsunami (Kerr, 2005). In 2004 a hazardous tsunami formed shortly after the megathrust rupture, while for the earthquake three months later the tsunami was negligible. The answer therefore can be found in the length of the rupture, the maximum uplift and the area of greatest vertical displacement of the earthquakes. In 2004 the rupture length was about 1600 km compared to only around 400 km

(Subarya et al., 2006), the maximum uplift was twice the size of 2005 and the area of greatest displacement occurred mostly under deep water, whereas in 2005 the greatest displacement occurred on land or shallow water (Briggs et al., 2006).

With the help of the microatolls on Nias and Simeulue it is noticeable that submergence associated with strain accumulation was dominant in the decades previous to the sudden megathrust rupture. This interseismic behavior, abruptly terminated by coseismic uplift is consistent with slow elastic strain accumulation and abrupt release. Nonetheless, the pattern of coseismic uplift matches the preexisting topography of the islands, which leads to the assumption that a portion of the coseismic uplift is not elastic and has contributed to building the outer-arc ridge (Briggs et al., 2006).

The two patterns of coseismic uplift resolve in an interesting feature on Simeulue. While the 2004 earthquake led to coseismic uplift of up to 1.45 m on the northwest of the island with a decrease to nearly zero further to the southeast, the 2005 earthquake led to up to 1.65 m uplift in the southeastern portion of the island with a decrease towards the northwest to nearly zero. These patterns reveal a 70 km long saddle shaped depression centered on Simeulue Island. Exactly at this center the relative uplift was at least 1 m less than to the northwest and southeast. Therefore the slip in the center of Simeulue was less than to the northwest or southeast (Briggs et al., 2006). DeShon et al. (2005) showed that during a previous event 2002 with a M_w = 7.3 the maximum uplift in the central portion of Simeulue was about 0.2 m which is not enough to fill the saddle. An interpretation for the Simeulue saddle is that the section slips preferable aseismically or fails in lesser earthquakes. It could act as an impediment for the propagation of large megathrust ruptures along strike due to the fact that it is largely unstressed at the times of these earthquakes occurring (Briggs et al,. 2006). The same behavior can be seen at the Batu Islands section of the Sunda megathrust. These islands have been flanked in the northwest by the giant ruptures of 1861 and 2005 and on the southeast by the giant earthquake of 1797. In 1935 a Mw = 7.7 event was the largest seismic rupture in the

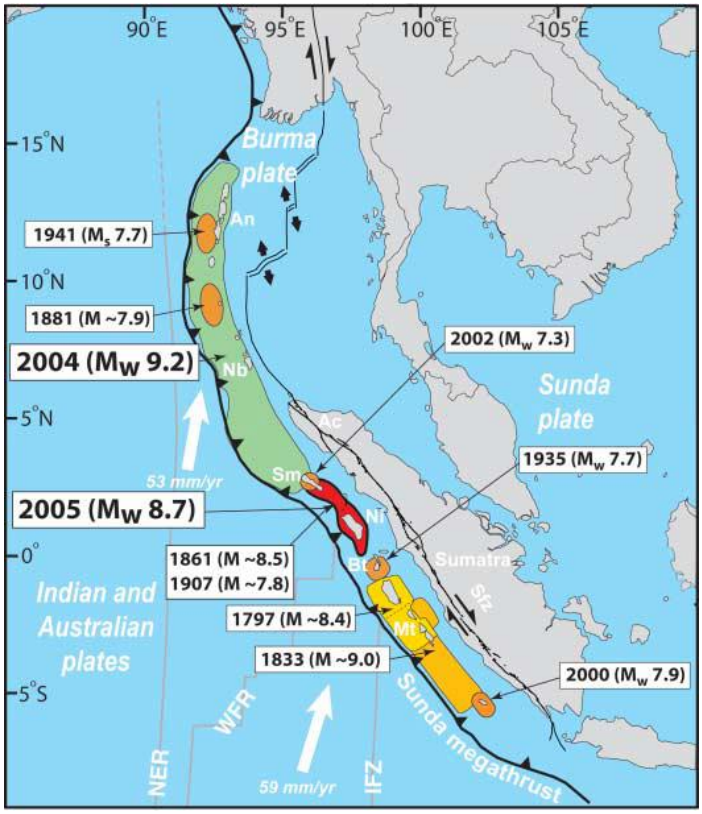

Figure 15: Regional map of the 28 March 2005 rupture and previous large ruptures of the Sunda megathrust. Previous earthquake locations and magnitudes are from (Subarya et al., 2006; Natawidjaja et al., 2004; DeShon et al., 2005; Sieh et al., 2005). Indian and Australian plate motions relative to Sunda are from (Prawirodirdjo et al., 2004) and faults are generalized from (Karig et al., 1980; Curray et al., 2005). (From Briggs et al., 2006)

last 250 years for the 70 km long Batu Islands patch (Natawidjaja et al., 2004). This leads to the assumption that slip along the megathrust beneath the Simeulue saddle and the Batu Islands is predominantly seismic (Briggs et al., 2006).

The reasons for the lateral variations in the mode of failure along strike of the Sunda Subduction Zone are unclear, although some theories bear great potential. Lithological and pore pressure variations may have an impact on the mode of slip along strike. Structural complexities on the downgoing plate could prohibit throughgoing rupture such as former mid-ocean ridges such as the Investigator Fracture Zone which gets subducted beneath the Batu Islands. Therefore further investigation is necessary (Briggs et al., 2006).

2.7.4. Assuming strike-slip events along the Sumatran fault, after megathrust events in 2004 and 2005

After the two dramatic thrust earthquakes from 2004 and 2005 on the Sunda Subduction Zone, McCloskey et al. (2005) besides others expected triggered earthquakes along the Sumatran fault. They argued that the normal slip on the subduction interface after the immense ruptures should decrease the normal stress on the Sumatran fault, therefore result in an increase of the shear stress to normal stress ratio along the fault what would bring it closer to failure. McCaffrey (2009) thinks that scenario rather unlikely to happen due to the following reasons. First, it takes a long time for the stress changes to act in the Earth caused by fluids that modify the stress field due to poro-elastic effects. Second, McCaffrey (1992) and Platt (1993) stated that both the normal and shear stress on a strike-slip fault are derived from the thrust interface, therefore, the apparent thrust earthquakes caused a stress drop which altered the normal and shear stress along the Sumatran fault proportionally bringing it not closer, nor farther to failure. Following McCaffrey (2009) this could explain the lack of seismicity along the Sumatran fault as expected by McCloskey et al. (2005).

3. Fieldwork

The geologic fieldwork stretched from 20.2.15 to 5.3.15 and resulted in approximately 14 days of actively collecting data on Nias Island. The project was commissioned and funded by Red Bull Media House GmbH, with duration of 01.07.2013-31.03.2019, the project leader Wolfgang Straka and bearing the title "Animal Perception of Seismic and Non-Seismic Earthquake Phenomena, Part 2" (Straka, 2013 - 2019).

3.1. Logistics

The two weeks of fieldwork were spatiotemporally splitted into the first week investigating in the south and the second week focusing on the west coast of Nias Island. Each weekly session started with an introductory discussion on what to concentrate on and where to find outcrops of specific potential, while coordinating an effective route with our local drivers.
The actual fieldwork comprised searching for qualitative outcrops and taking GPS Data in respect to lithology, stratigraphy, structural setting, and soil gas concentrations, while occasionally sketching and interpreting geological structures in the field. Due to the thick vegetation on the main portion of the island, the highest chance of discovering high quality outcrops was restricted to river beds, quarries, fault scarps or recent landslides. Each day the collected data was summarized, interpreted and further discussed, which occasionally lead to the readjusting of the route.

3.2. Field Data

The following report summarizes the data gained in the geological fieldwork from 20.2.15 to 5.3.15 on Nias Island. The overall project deals with animal perception of seismic phenomena (Straka, 2013 - 2019). This report, besides other work investigated in this area, are pioneers for further research in the direction of the overall project. The report is based on an outcrop description, which was used to prepare a geological map and get a geological overview of the island. Additionally, the selection of the outcrops and further assistance for the fieldwork was supervised by Wolfgang Straka (Institut für Angewandte Geologie, University of Natural Resources and Life Sciences, Vienna), head of the project, Bernhard Grasemann (Department of Geodynamics and Sedimentology, University of Vienna) and Robert Faber (www.terramath.com). For the regional geology and stratigraphy on Nias we refer to the publication of Barber et al. (2006).

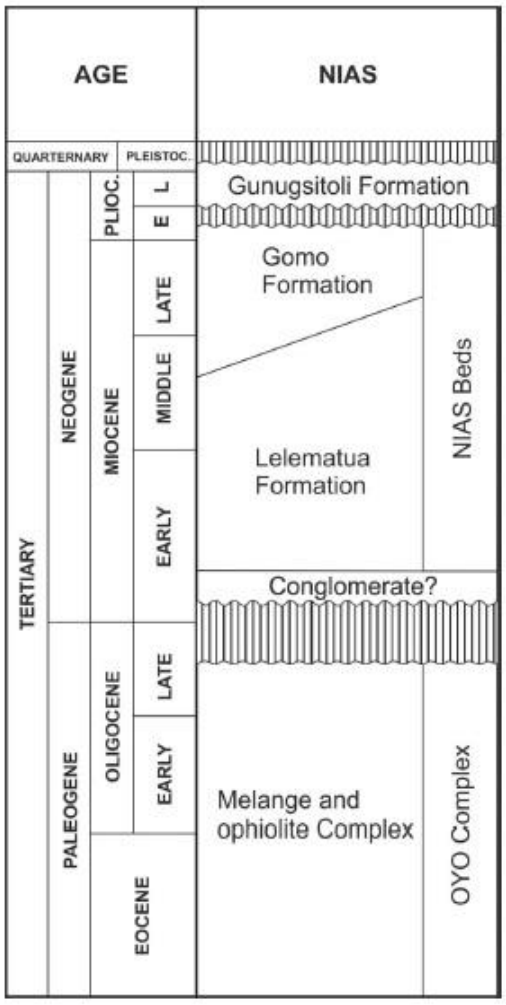

Figure 16: Stratigraphic table of Nias Island based on Barber et al. (2006)

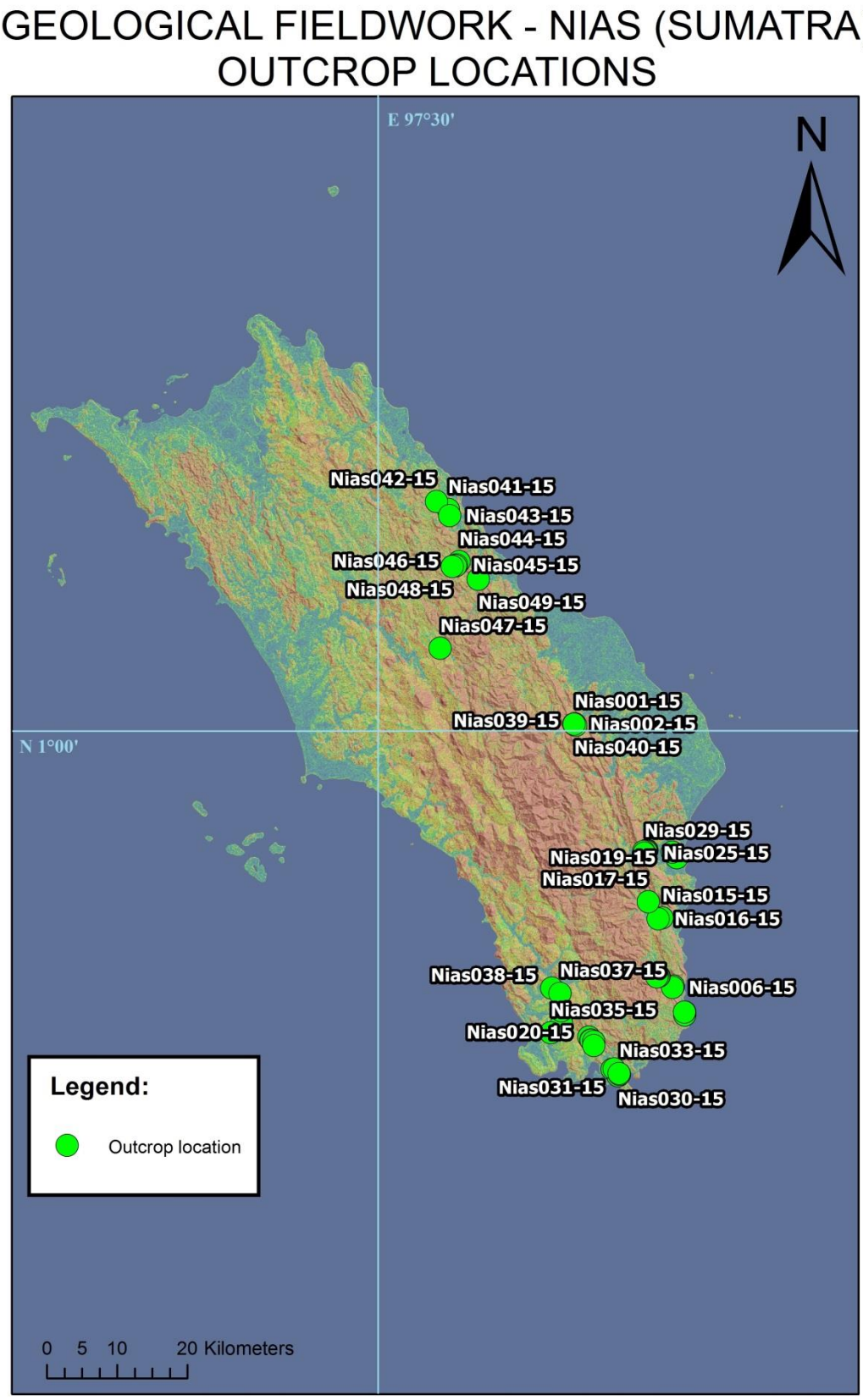

Figure 17: Map of outcrops on Nias (Sumatra) during the fieldwork from 20.2.2015 until 5.3.2015

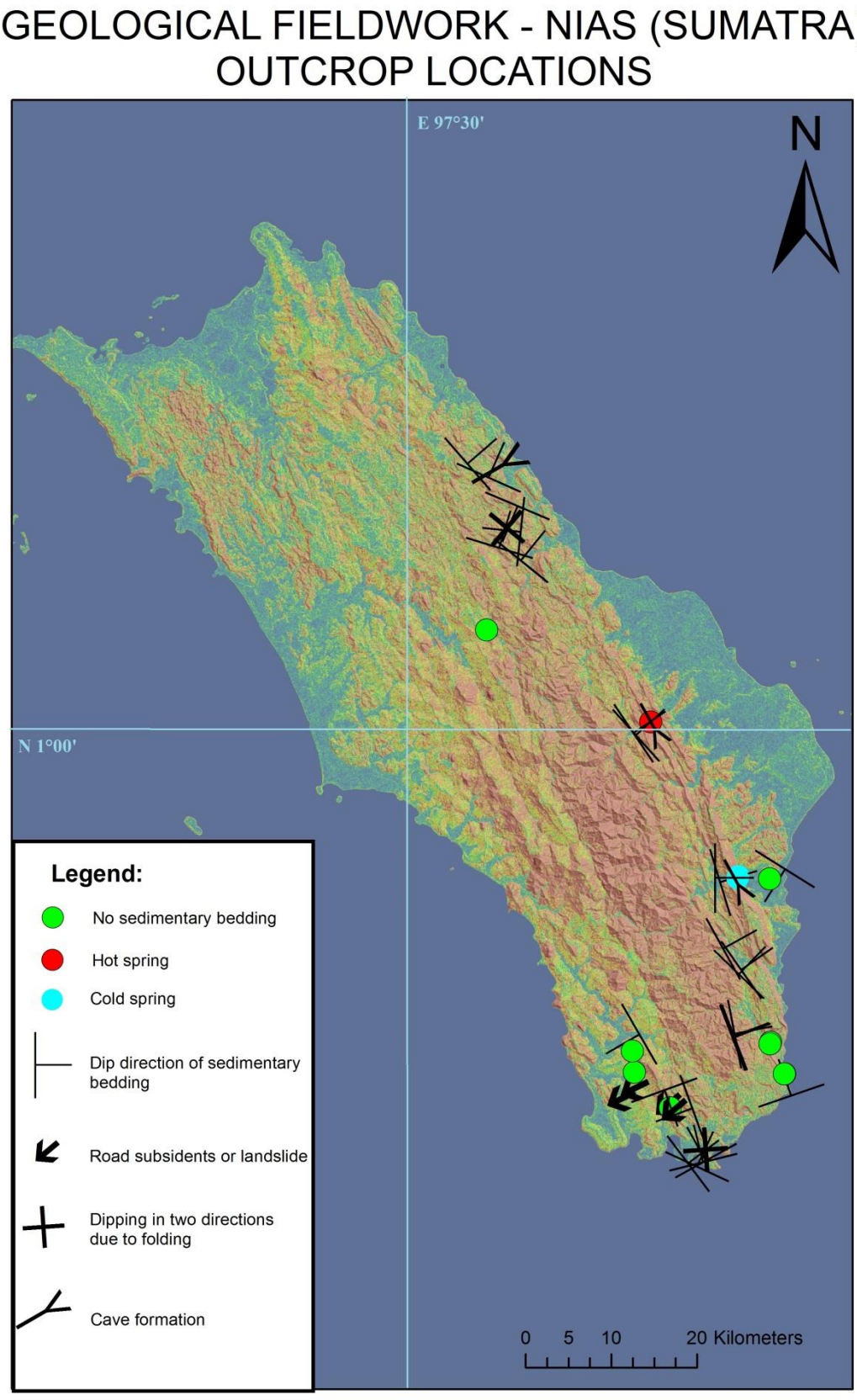

Figure 18: Symbolic outcrop description of Nias (Sumatra) during the fieldwork from 20.2.2015 until 5.3.2015

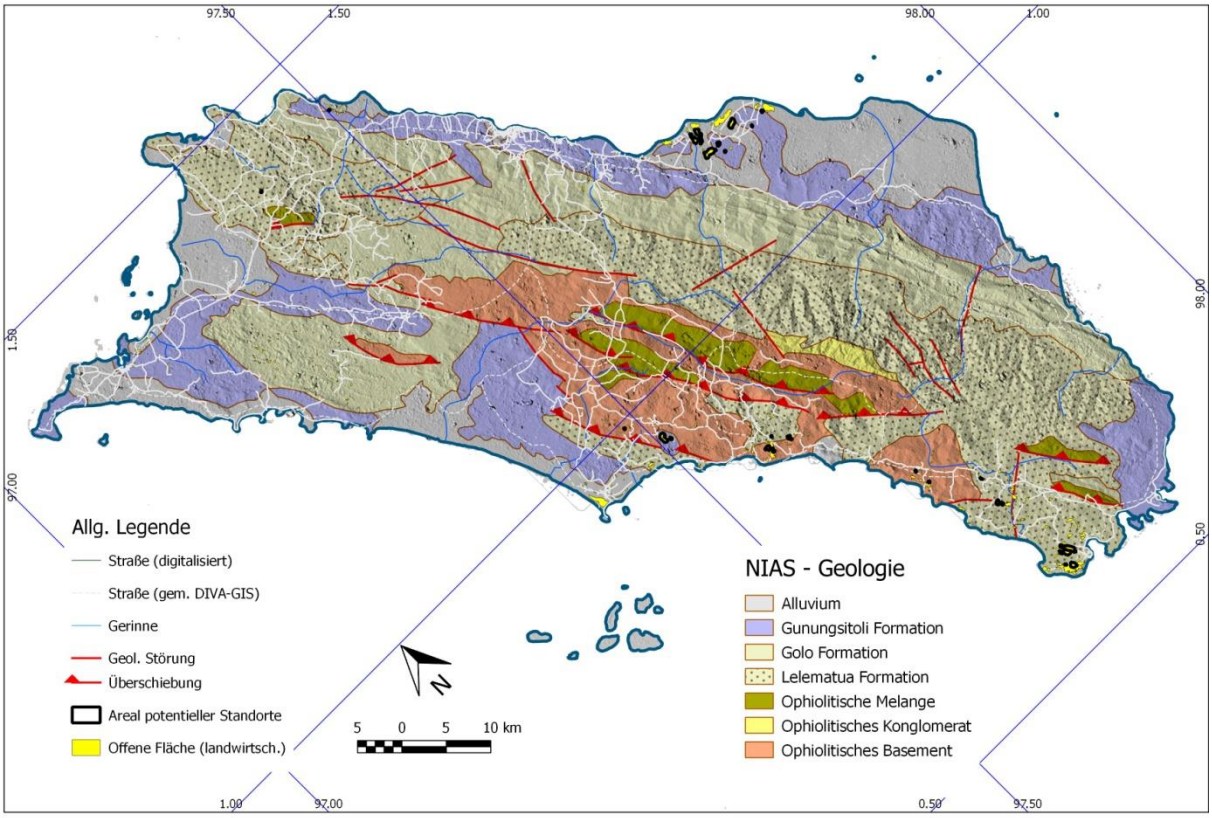

Figure 19: Geological map of Nias Island (Barber et al. (2006))

3.2.1. Outcrop description:

Nias001-15:

Date: 19.2.15

GPS (UTM 47): 112193.547 m N 361397.499 m E

Outcrop Location: 150 m distance to the village Air Panas, present location of the hot springs

Lithology: Limestone, Sandstone

Stratigraphy: Gomo Formation (Late Miocene)

Description:

The recently active hot springs are located approximately 300 m to the northwest of the village Air Panas (meaning hot water). The village is situated in approximately 35 km distance to the southeast of the Capital Gunungsitoli. Since the earthquake in 2005 the geographical location of the hot spring moved from southeast to northwest along a potential fault, striking ~310. It appears that the lateral movement of the geographical location of the hot spring gets triggered by seismic ruptures. Prior to the earthquake in 2005 the hot spring was located within the village (Outcrop Nias039-15). It was used to provide hot water for a local bath.

Figure 20: Hot spring, water temperature 47°C

Figure 21: Close up of the hot spring

Nias002-15:

Date: 19.2.15

GPS (UTM 47): 112152.262 m N 361261.810 m E

Outcrop location: Riverbed to the north of the village Air Panas, 300 m distance WNW to the local bath, approximately 100 m west of Nias001-15

Lithology: Limestone, Sandstone

Stratigraphy: Gomo Formation (Late Miocene)

Description:

On the northern side of the river the sedimentary bedding is subvertical and striking more or less north-south (Figure 22). On the southern side is a fault zone showing a synthetic Riedel shear indicating a top towards E directed extension (Figure 23). Both opposed outcrops were not directly approachable due to the river.

Figure 22: Subvertical bedding plains

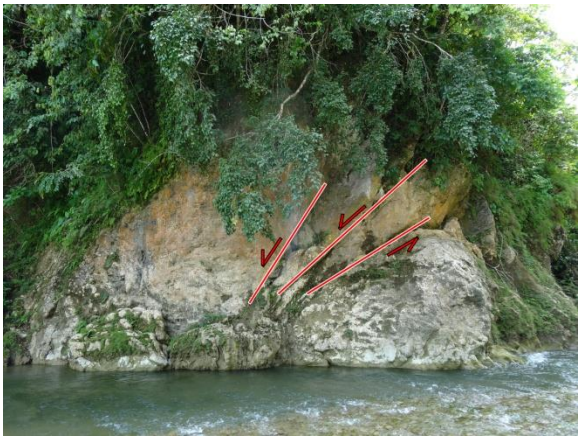

Figure 23: Synthetic Riedel shear, indicating top to the E normal faulting

Nias003-15:

Date: 19.2.15

GPS (UTM 47): 63038.604 m N 366751.011 m E

Outcrop Location: Quarry on the northern side of the road, 3 km to the east of Telukdalam

Lithology: Fossil-rich calcarenite

Stratigraphy: Gunungsitoli Formation (late Pliocene)

Description:

The quarry is located at the northern side of the road on the way to Telukdalam, around 3 km distance to the east of the village. Lithologically speaking the sediments consists of 10-20 cm thick fossil rich calcarenite, which is interbedded with 2-5 cm thin Fe-rich sandstone. There is a general dipping direction of approximately 305/33 which is consistent for the whole outcrop. On the top of the outcrop, some whitish layers are potential paleosols.

Figure 24 Image of the quarry

Figure 25: Sedimentary layers dip to the NNW

Nias004-15:

Date: 20.2.15

GPS (UTM 47): 76320.670 m N 374145.881 m E

Outcrop Location: Active quarry, 6 km distance NNW of Hilinamaniha

Lithology: Limestone, Conglomerate, Clay, Sandstone, Reef Debris

Stratigraphy: Gomo Formation (Late Miocene)

Description:

In this outcrop we see a cataclastic fault zone which could be an evidence for a dextral pull-apart basin along a potential fault. The outcrop shows several cataclastic shear zones. The rocks inside this cataclastic zones appear to be cohesionless and nearly pulverized due to the relatively low confining pressure they have been exposed to while being crushed along NNW-SSE striking strike slip faults. That characterizes it as a fault gauge.
Figure 27 shows mode I fractures with a σ 3 in approximately E-W direction and a σ 1 that is vertical. These sorts of fractures develop when the ratio of σ 1 to σ 3 passes a certain critical point, where σ 1 is the maximum- and σ 3 is the minimum stress direction. When the differential stress exceeds the rupture strength the fractures open. In this case the opening in E-W direction would speak in favor for the existence of a pull-apart basin. In terms of stratigraphy the river could follow the border between the Gomo and Lelematua Formation.
On the outcrop wall it seems that there are several lithological changes. Unfortunately only the one on the bottom are directly approachable. The other lithologies we analyzed through loose rocks in the scree in front of the outcrop (Figure 29).
Clearly distinguishable is the lithology at the bottom of the outcrop. (Lithology 1 in figure 29) Blue to grey clay is interbedded with dark blue/grey sandstone. Within localized zones the layers are tectonically deformed. (Figure 26) The boundary between lithology 1 and lithology 2 indicates a discordant, erosive lithological contact. Lithology 2 consists of conglomerate with decimeter thick components which consist of siltstone in a sandstone matrix and is rich in fossils. Moving upwards as far as we could indirectly analyze lithology 3 consists of brown sandstone and lithology 4 of reef debris. The upper most layers in figure 28 identified as lithology 5 is limestone.
Local villagers mine the rock powder or rather the fault gauge for producing concrete.

Figure 26: Panorama of the outcrop

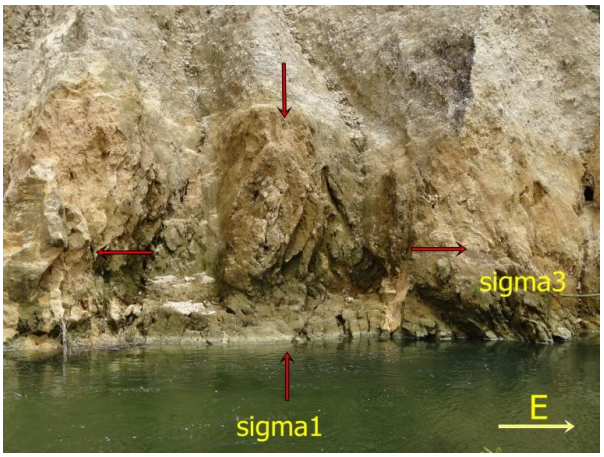

Figure 27: Mode I fractures

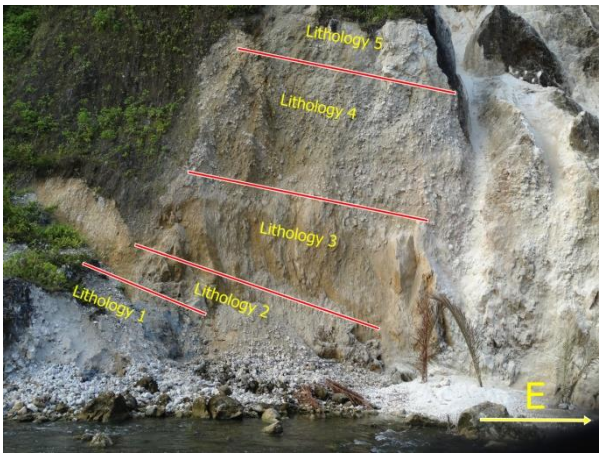

Figure 28: Lithological changes

Figure 29: Lithology 1: Blue clay and sandstone

Nias005-15:

Date: 20.2.15

GPS (UTM 47): 74873.399 m N 375413.243 m E

Outcrop Location: Inactive quarry beneath the road, 4 km distance NNW of Hilinamaniha

Lithology: Limestone

Stratigraphy: Gomo Formation (Late Miocene)

Description:

This outcrop was located approximately 200 m northeast of a big quarry (Nias06-15). A local sulfur smell was observed. The limestone seemed to be hydrothermally altered and a causal correlation with the sulfur exhalation is assumed.

Figure 30: Altered limestone outcrop with a recognizable sulfuric smell

Nias006-15:

Date: 20.2.15

GPS (UTM 47): 74670.116 m N 375331.374 m E

Outcrop Location: Active quarry beneath the road, 4 km distance NNW of Hilinamaniha

Lithology: Fossil-rich limestone

Stratigraphy: Gomo Formation (Late Miocene)

Description:

The limestone we found in this quarry consists of bryozoa, coral fragments, foraminifera and gastropoda. It can be described as framestone with the classification of Dunham. The grains are bigger than 2 mm and build a rigid framework.

Figure 31: Panorama picture of the whole active quarry

Nias007-15:

Date: 21.2.15

GPS (UTM 47): 65865.330 m N 369209.636 m E

Outcrop Location: 500m distance N of Hilinamaniha

Lithology: Limestone

Stratigraphy: Gunungsitoli Formation (late Pliocene)

Description:

As seen in plot 1, the bedding plains are subhorizontal and the fractures could be part of a conjugate fault system with E-W shortening direction. Unfortunately no shear sense indicators have been found.

Seawater is strongly altering the outcrop as well as rain water which penetrates the rock through a system of fractures on which we found lots of karst structures. Interesting is the abrupt stop of the fracture seen in figure 33 which penetrates the sedimentary layer on the bottom, but not the one on top.

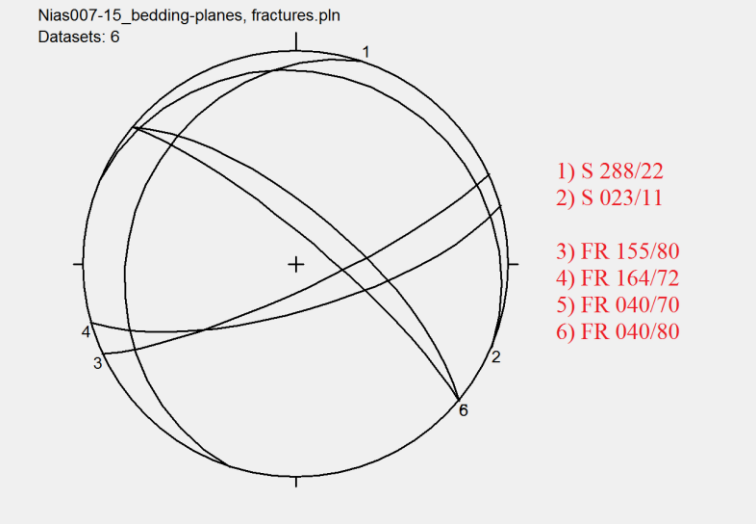

Plot1: Subhorizontal bedding plains, potential conjugate fault system indicating W-E shortening.

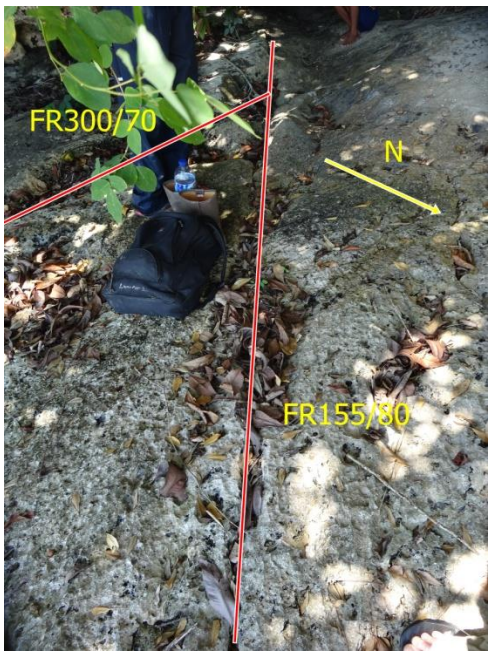

Figure 32: Marked fractures

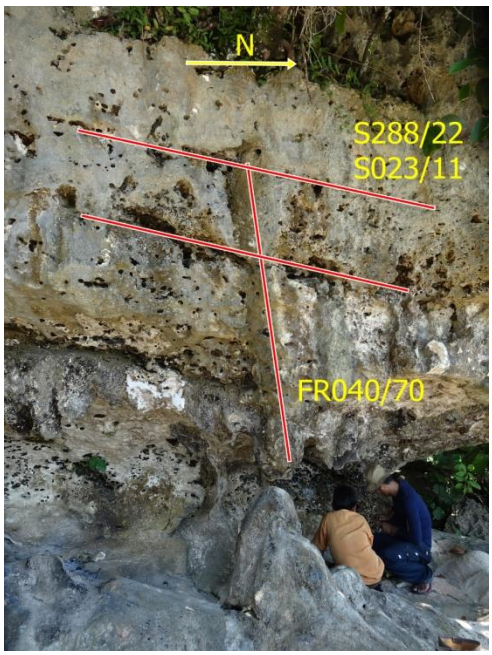

Figure 33: Marked bedding plains and karst structures along a fracture

Nias008-15:

Date: 21.2.15

GPS (UTM 47): 71169.90 m N 377038.93 m E

Outcrop Location: 1 km distance N of Hilinamaniha, near school

Lithology: Fossil-rich limestone

Stratigraphy: Gunungsitoli Formation (late Pliocene)

Description:

This outcrop was approximately 100 m afar from a small school. In lithological terms we found the typical reef limestone of the Gunungsitoli Formation, which is traceable all along the south east coast.

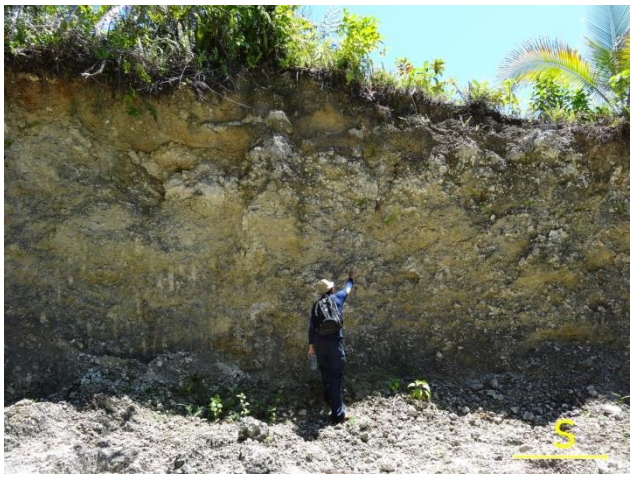

Figure 34: Fossil-rich reef limestone

Nias009-15:

Date: 21.2.15

GPS (UTM 47): 71186.868 m N 376998.472 m E

Outcrop Location: 1 km distance N of Hilinamaniha, behind school

Lithology: Limestone

Stratigraphy: Gunungsitoli Formation (late Pliocene)

Description:

Nias009-15 is located directly behind a school building. Indicators for hydrothermal activities along certain fractures had been observed. (Figure 35)

Figure 35: Hydrothermal alteration of the limestone along a fracture (FR 166/56), pencil points towards N

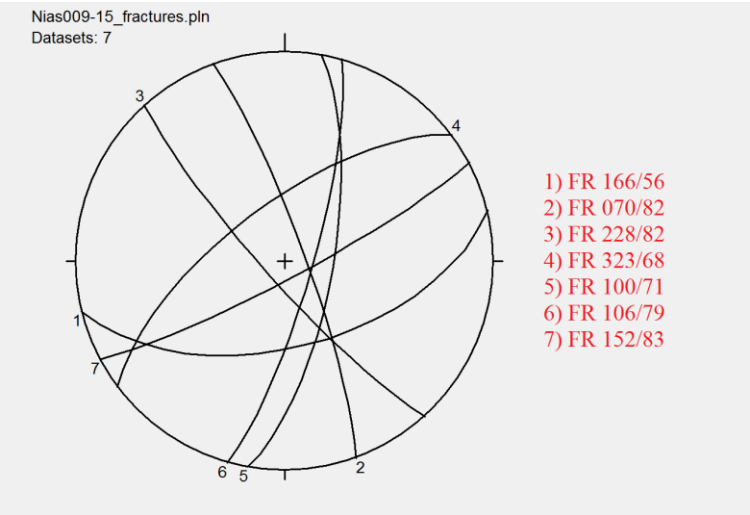

Plot 2: Irregular set of fractures

Nias010-15:

Date: 21.2.15

GPS (UTM 47): 76263.542 m N 373434.811 m E

Outcrop Location: Riverbed 1 km upstream of Nias004-15

Lithology: Sand-Siltstone, Claystone

Stratigraphy: Lelematua Formation

Description:

On the way to Nias010-15 erosive structures interpreted as fracture zones with incohesive cataclasites have been observed in an inaccessible rock cliff, which could indicate a NNW-SSE striking fault system. This could be part of the suggested pull-apart basin in this area. Additionally in the riverbed some brittle structures indicate a compression direction of NE-SW (Figure 37).

Figure 36: On the way to Nias010-15, distance observation of a potentially NNW-SSE striking fault

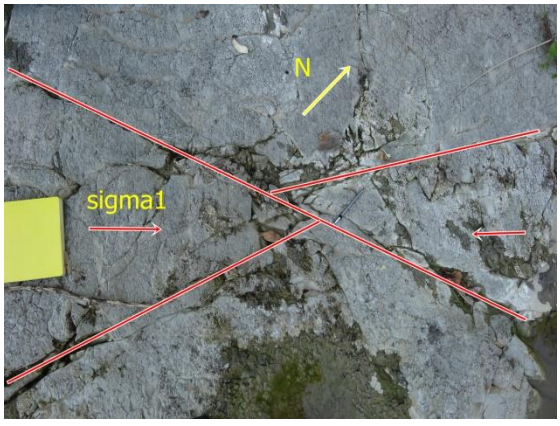

Figure 37: Conjugate fault-system direction of compression NE-SW

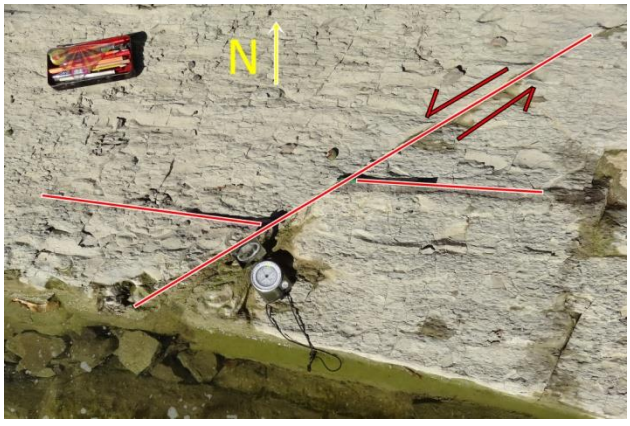

Figure 38: Sinistral strike-slip fault

Nias011-15:

Date: 22.2.15

GPS (UTM 47): 76240.179 m N 373313.613 m E

Outcrop Location: 300 m upstream of Nias010-15

Lithology: Sand-Siltstone, Claystone

Stratigraphy: Lelematua Formation

Description:

All along the riverbed from Nias010-15 to Nias014-15 the dip of the sedimentary bedding is identical. The dipping direction is ENE with approximately 45°. Lithologically speaking the layers of sandstone approximately 1-2 decimeters thick are interbedded with very weak claystone layers. The river flows from W to E in this outcrop, but changes its curse along the upcoming outcrops which can be seen in figure 43, outcrop Nias014-15.
A dextral fault zone cuts through the striking N-S. (Figure 40)

Figure 39: Consistent dip directions

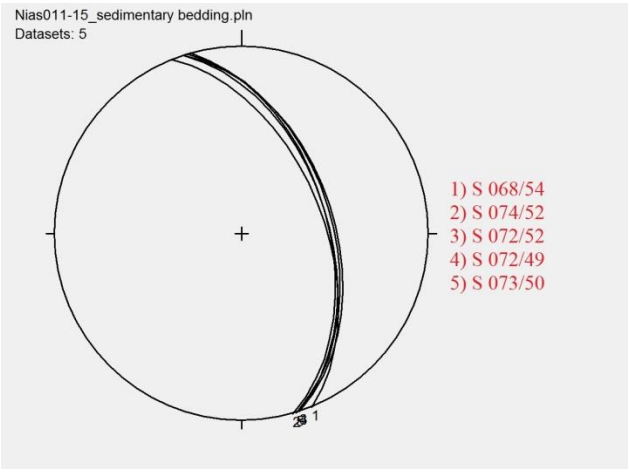

Plot 3: Consistent dip of the sedimentary bedding plains

Figure 40: Dextral slickenside, pencil is parallel to lineation

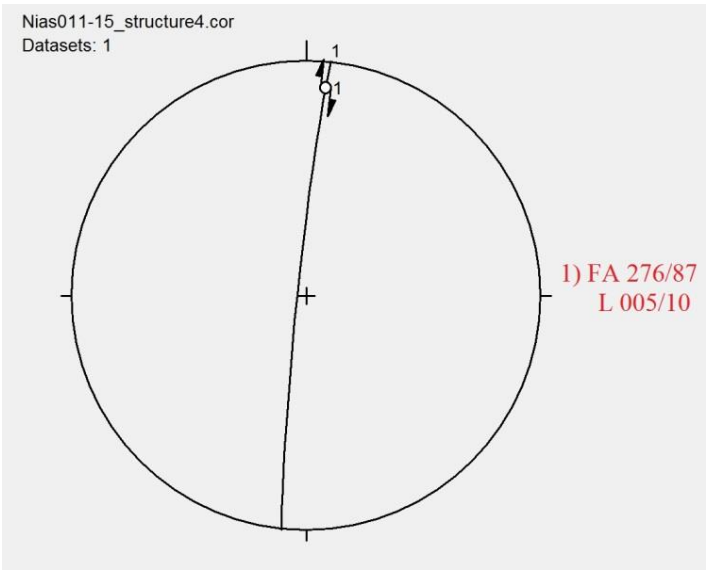

Plot 4: Dextral fault zone

Nias012-15:

Date: 22.2.15

GPS (UTM 47): 76299.362 m N 373131.455 m E

Outcrop Location: 500 m upstream of Nias011-15

Lithology: Sand-Siltstone, Claystone

Stratigraphy: Lelematua Formation

Description:

The dipping of the sedimentary layers is consistent with Nias011-15. The sand- siltstone layers are approximately 30 cm thick and interbedded with claystone layers 2-5 cm in thickness. We identified a very shallow thrust fault indicated by drag folding on the hanging wall of the fault with a dip direction of 150/10 (Figure 41). Unfortunately we could not identify a detailed shear sense via lineations or other indicators.

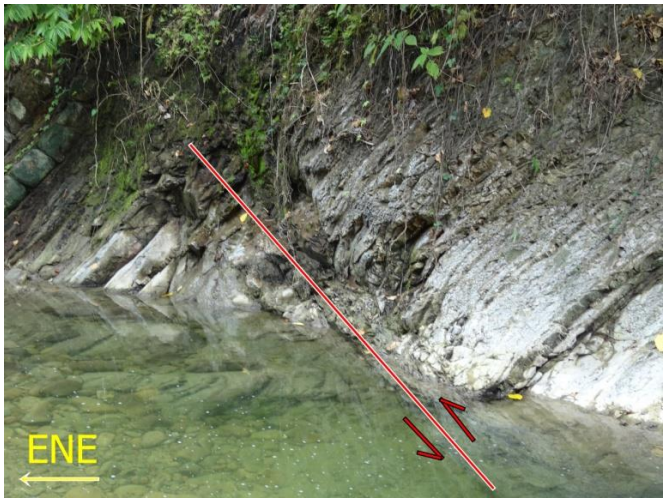

Figure 41: Thrust fault with fault drag on hanging wall

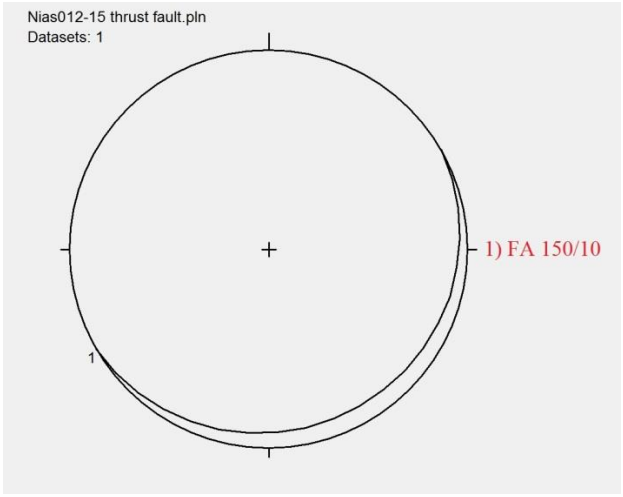

Plot 5: Thrust fault

Nias013-15:

Date: 22.2.15

GPS (UTM 47): 76274.983 m N 373083.346 m E

Outcrop Location: 300 m upstream of Nias012-15

Lithology: Sand-Siltstone, Claystone

Stratigraphy: Lelematua Formation

Description:

The flow direction of the river is slightly changing from W-E to NNE-SSE. The river course can be seen in figure 43, outcrop Nias014-15. The river is cutting the sedimentary layers nearly parallel to its strike direction and therefore the topmost layers have a preferred sliding plane downdip into the river. Catastrophic sliding may have been triggered by an earthquake.

Figure 42: Sedimentary layers slid into the riverbed

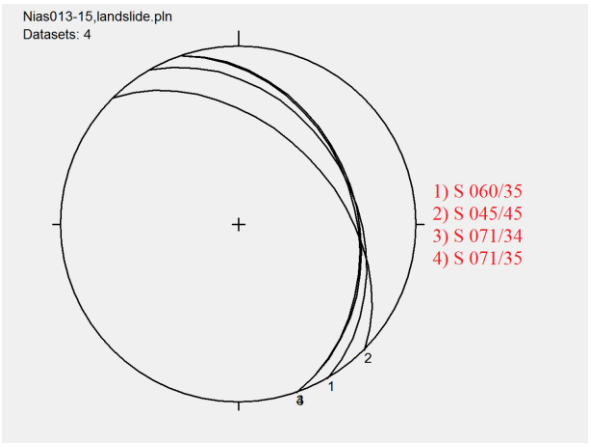

Plot 6: Sedimentary bedding plains

Nias014-15:

Date: 22.3.15

GPS (UTM 47): 76185.963 m N 373089.111 m E

Outcrop Location: 200 m upstream of Nias013-15, turning point

Lithology: Sand-Siltstone, Claystone

Stratigraphy: Lelematua Formation

Description:

This waypoint simply marks the turning point of our trail along the river. Lithologically and stratigraphically this point is identically to Nias013-15 and Nias012-15. In figure 43 the thick red arrow marks the turning point of our march along the river and the thin red arrow resembles the flow direction.

Figure 43: Google Earth image of the outcrop locations Nias010-15 to Nias014-15 in addition to Nias004-15 (From Google Earth)

Nias015-15:

Date: 23.2.15

GPS (UTM 47): 84570.665 m N 373838.47 m E

Outcrop Location: 1-2 km NW of Hiliobolata

Lithology: Limestone

Stratigraphy: Gomo Formation (Late Miocene)

Description:

This outcrop is located near a river further north than Nias010-15 – Nias014-15, but the dip direction and dipping of the sedimentary layers appeared to be uniform compared to previously described accessible outcrops further to the south (Figure 44). The terrain was difficult and slightly dangerous to walk-on. Therefore measurements of the bedding plains could only be estimated in the distance. Figure 45 shows sinter formation through thermal alteration along a fracture.

Figure 44: Sedimentary bedding in the riverbed

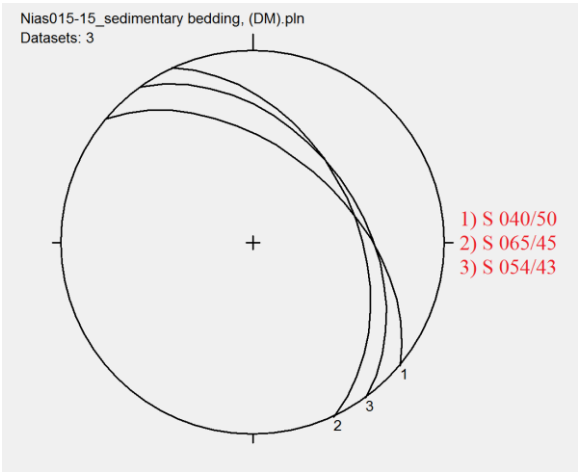

Plot 7: Sedimentary bedding plains

Figure 45: Sinter formation along a fault

Nias016-15:

Date: 23.2.15

GPS (UTM 47): 84462.949 m N 373275.998 m E

Outcrop Location: 1-2 km NW of Hiliobolata, behind house

Lithology: Limestone, Siltstone

Stratigraphy: Gomo Formation (Late Miocene)

Description:

Figure 46 shows a fault plane with a strike slip lineation. No clear shear sense indicators have been observed. The dip direction and dipping of the sedimentary bedding is around 010/30. The lithology is mostly limestone with sporadic silt layers.

Figure 46: Fault plane with lineation but no shear sense

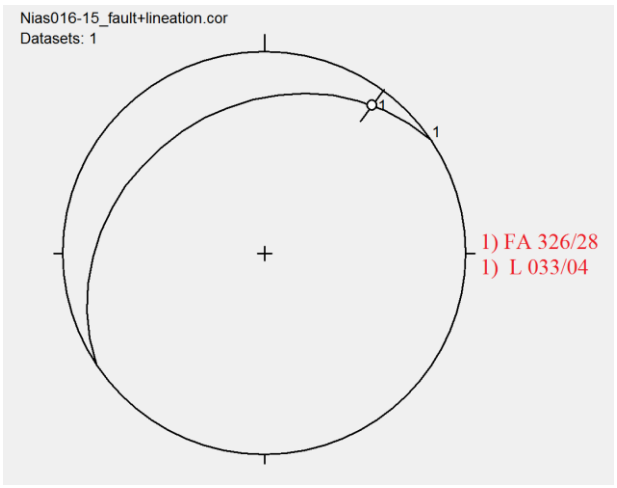

Plot 8: Plotted fault plane with lineation towards NE

Nias017-15:

Date: 23.2.15

GPS (UTM 47): 86853.69 m N 371862.205 m E

Outcrop Location: 1-2 km NW of Hiliobolata, behind house

Lithology: Sand-Siltstone, Claystone

Stratigraphy: Lelematua Formation

Description:

Figure 47 shows unconsolidated sandstones, approximately 1-2 meter thick interbedded with clay- and siltstone layers with about 0.2-1 meter in thickness. The dip direction and dipping of the layers is subvertical and strikes NW – SE.
Figure 49 shows a SC-fabric indicating a reverse fault meaning that northern block was moving upwards.
On some sandstone layers we found ichnofazies which indicate bioturbation. Figure 48 possibly shows a Thalassinoides ichnofacies.
Sinter formations are common and indicate active precipitation of flowstones.

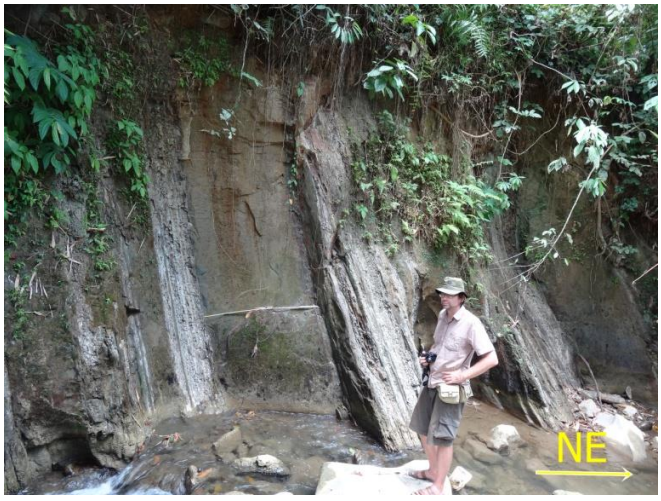

Figure 47: Sandstone layers interbedded with clay- and siltstone

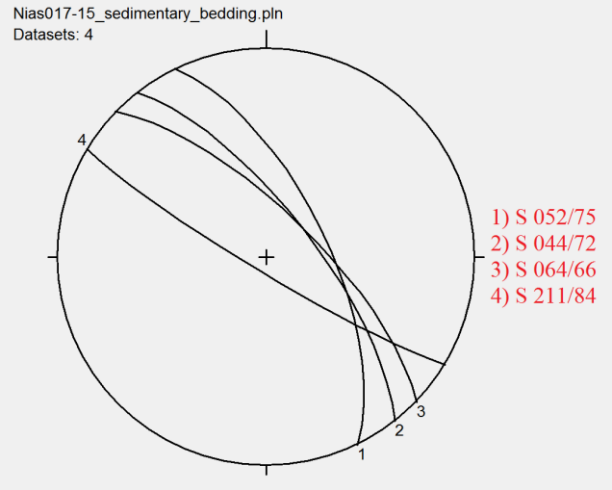

Plot 9: Sedimentary bedding

Figure 48: Bioturbation in sandstone

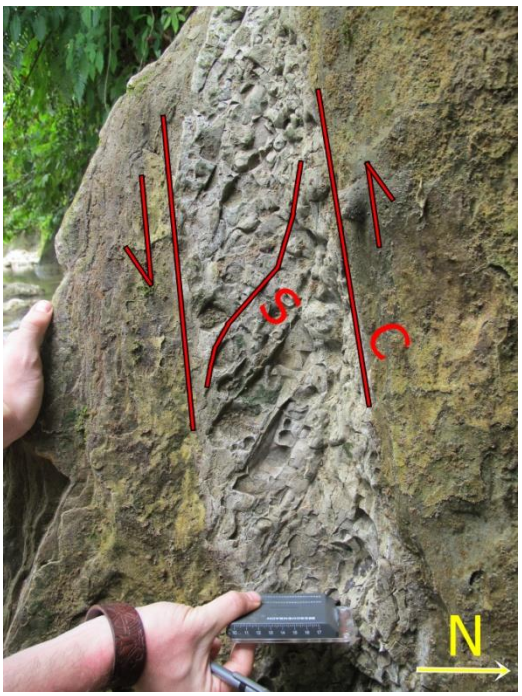

Figure 49: SC- fabric in soft sediment

Figure 50: Sinter formation, wooden stick for scale equals 1m

Nias018-15:

Date: 23.2.15

GPS (UTM 47): 93138.06 m N 375914.421 m E

Outcrop Location: 15 km N of Hiliobolata

Lithology: Claystone

Stratigraphy: Alluvial & Reef

Description:

The dark grey claystone featured many fossilized plant and shell fragments. (Figure 51) On the sedimentary bedding plane we found two different lineations, without shear sense. (Plot 10) Due to the bad conditions of the road, advancing in west direction was not possible.

Figure 51: Dark grey claystone with black fossilized plant remnants *Figure 52: Bad conditions of the road*

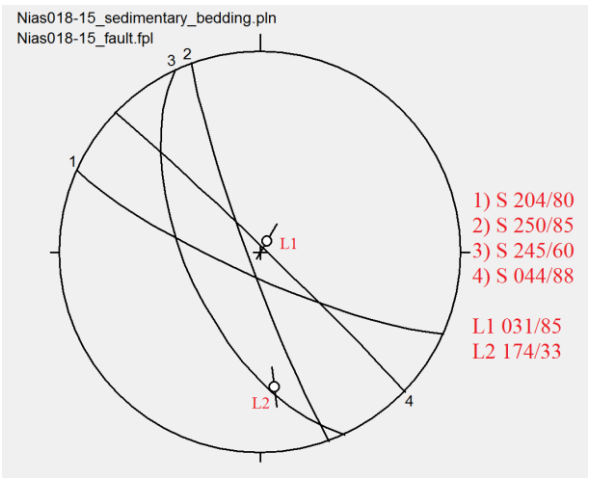

Figure 53: Desiccation cracks on the surface of the clay *Plot 10: Sedimentary bedding with two different lineations*

Nias019-15:

Date: 23.2.15

GPS (UTM 47): 93921.797 m N 375290.634 m E

Outcrop Location: 1 km distance to outcrop Nias018-15

Lithology: Claystone

Stratigraphy: Alluvial & Reef

Description:

Further west from Nias018-15 no meaningful geological outcrops have been observed at least in by foot reachable distances and therefore we did not advance further land inwards.

Figure 54: Turning point of the journey further inland

Figure 55: Google Earth image of the outcrop locations Nias018-15 to Nias019-15 (From Google Earth)

Nias020-15:

Date: 24.2.15

GPS (UTM 47): 67618.680 m N 363413.310 m E

Outcrop Location: Landslide 1km south of Bawomataluo (Monolithic village)

Lithology: Clay-/Siltstone

Stratigraphy: Ophiolithic Melange

Description:

South east of the Bawomataluo village, well known for its monolith culture, numerous landslide events have been observed. Duo to the strong vegetation in the jungle the detailed relative chronological order of events is difficult to discriminate. However, many fallen young and old trees are scattered on the jungle floor suggesting a series of recent historical landslide and/or earthquake events (Figure 57). The only part of the landslides which are clearly to distinguish in the forests are the tear-off edges of the mass movements. These can have heights up to 2 m (Figure 58).

Figure 56: Tear-off edge of a landslide, sliding direction SW

Figure 57: Fallen trees caused by the mass movement

Figure 58: Fault scarp (tear-off edge) 2 m height

Nias021-15:

Date: 24.2.15

GPS (UTM 47): 67214.848 m N 363675.024 m E

Outcrop Location: 1km distance SE to Nias020-15, small riverbed in forest

Lithology: Sandstone

Stratigraphy: Ophiolithic Melange

Description:

In the dense jungle small river beds were the only source of information about the lithological composition of the regional geology.

Figure 59: Sandstone in small riverbed

Nias022-15:

Date: 24.2.15

GPS (UTM 47): 676618.680 m N 363413.310 m E

Outcrop Location: 200m distance SE of Nias021-15, big riverbed

Lithology: Basalt embedded in clay-siltstone

Stratigraphy: Ophiolithic Melange

Description:

Seen at figure 61-63 are spherical structures up to a size of 1 m embedded in a subhorizontal sedimentary layering. They are interpreted as pillow basalts also known as pillow lava which develop through the subaquatic extrusion of basaltic melt. They are considered to be part of the Ophiolithic Melange Zone in this area.

Figure 60: Panorama of the outcrop, river flows from NE to SW

Figure 61-63: Pillow lava

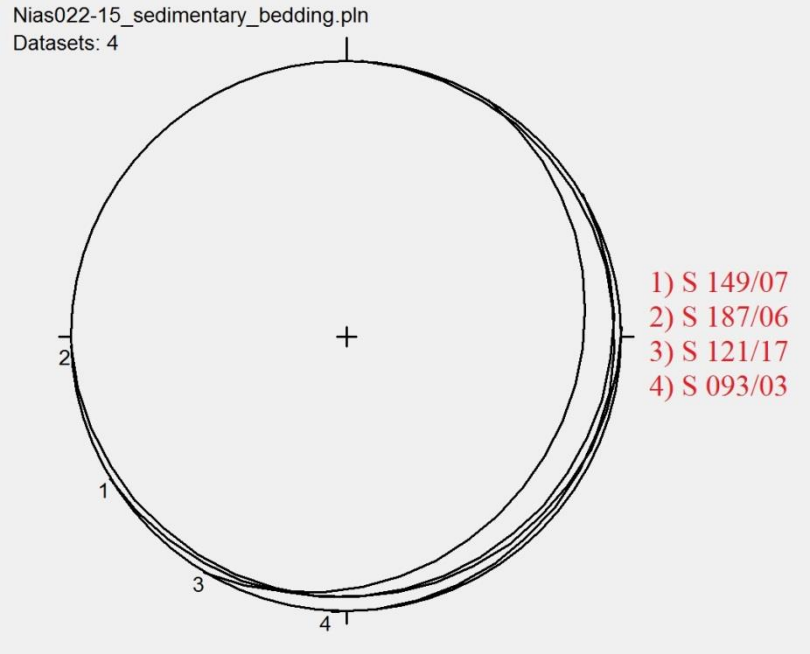

Plot 11: Sedimentary bedding

Nias023-15:

Date: 24.2.15

GPS (UTM 47): 66953.079 m N 364099.591 m E

Outcrop Location: Huge landslide 500m SE of Nias022-15, "Desa Bawomataluo"

Lithology: Limestone with corals, Conglomerate of sandstone-pebbles in clay matrix moderately sorted

Stratigraphy: Potential border between Lelematua Furmation and Ophiolithic Melange

Description:

This huge landslide appeared approximately 1 km SE from the village Bawomataluo. The tear-off edge is about 50 m long (Figure 65). Lithologically, the rocks consist of limestone with coral fragments and conglomerates with sandstone pebbles in a clay matrix, which is moderately sorted. Most of the rock fragments are scattered on the uppermost portion of the landslide. Sliding direction is SW.

Figure 64 Sliding direction of the landslide SW

Figure 65: Fault scarp with about 50 m in diameter

Figure 66: Coral fragments

Nias024-15:

Date: 24.2.15

GPS (UTM 47): 66415.883 m N 364120.698 m E

Outcrop Location: 1 km south of the huge landslide (Nias023-15), riverbed

Lithology: Limestone

Stratigraphy: Ophiolithic Melange

Description:

Within the limestone many karst structures appear along and close to the river. The waterfall on the right of figure 67 formed a pool or basin like structure in the central portion of the figure, which according to the locals is about 12 m deep and several children died due to the dangerous currents in the pool.
Figure 68 and 69 show cave-like structures along the trail.

Figure 67: Panorama view of the western side of the outcrop

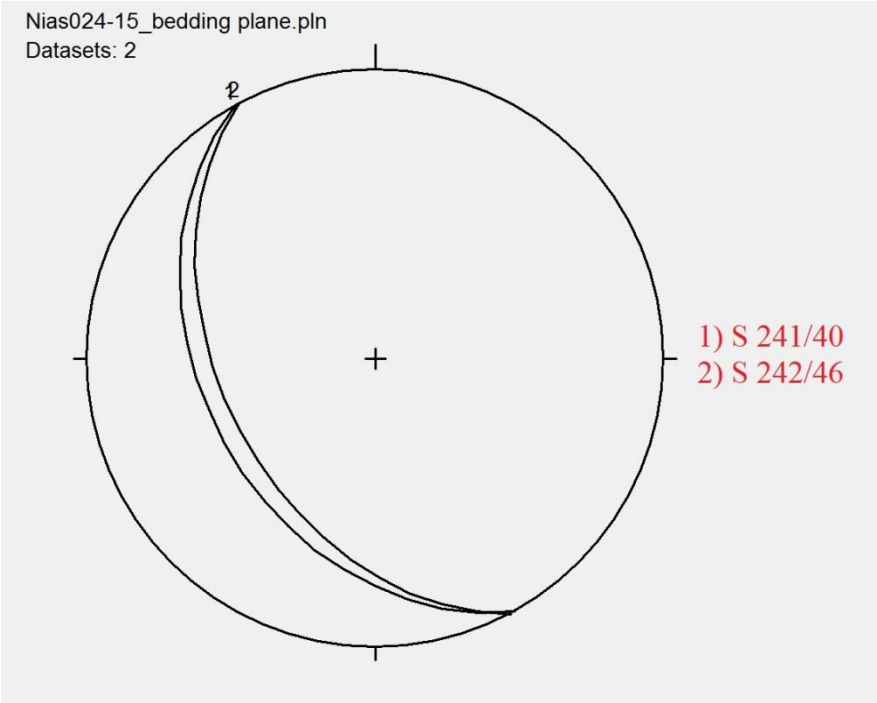

Plot 12: Sedimentary bedding

Figure 68-69: 100 m distance to Nias024-15, underground cave system

Nias025-15:

Date: 25.2.15

GPS (UTM 47): 94203.646 m N 371693.280 m E

Outcrop Location: 10 km NNW of Hilibolata, "Air Dingin" → cold spring (north side of the river), "Desa Mehage"

Lithology: Reef limestone

Stratigraphy: Gomo Formation (Late Miocene)

Description:

On the northern side of the river some cold springs occur at the base of a rock wall. They are most likely associated with karst formations, frequently observed in this region. In figure 70 the red arrows mark the spot of the water pouring out of the rock wall.

Figure 70: Cold spring, arrows mark the spot where the water pours out of the rock wall

Nias026-15:

Date: 25.2.15

GPS (UTM 47): 94130.068 m N 371660.323 m E

Outcrop Location: Pathway along the northern side of the river, 100m distance SW to Nias025-15, looking at the southern side of the river, flow direction of the river W-E

Lithology: Reef limestone

Stratigraphy: Gomo Formation (Late Miocene)

Description:

The dipping direction and dip angle of the sedimentary bedding is around 080/30 and could only be estimated from distance. The surrounding bedrock is covered with dense vegetation.

Figure 71: Panorama view of the southern side of the river

Nias027-15:

Date: 25.2.15

GPS (UTM 47): 94001.618 m N 371543.167 m E

Outcrop Location: 200m distance SW to Nias026-15 → cold spring (northern side of the river)

Lithology: Reef limestone

Stratigraphy: Gomo Formation (Late Miocene)

Description:

As seen in plot 12 the sediments dip towards ENE, but the rock wall was not reachable by foot, therefore we estimated sedimentary bedding from distance, as we did in Nias026-15. We detected another cold spring on the northern river side (Figure 72).

Figure 72: Cold spring

Figure 73: Consistent dipping direction of the sediments

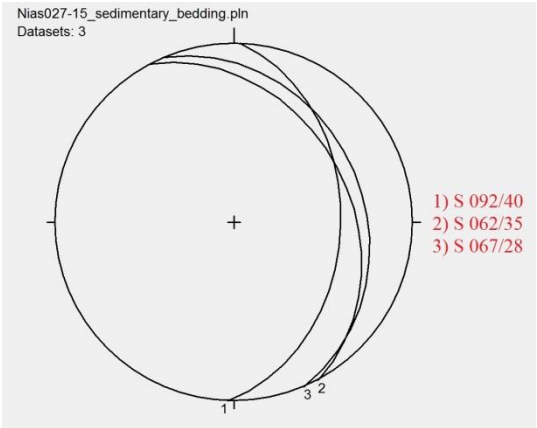

Plot 13: Plot of the general dipping directions of the sedimentary layers, measured from approximately 30m distance

Nias028-15:

Date: 25.2.15

GPS (UTM 47): 94026.384 m N 371234.095 m E

Outcrop Location: 300m distance W to Nias027-15 →cold springs

Lithology: Boundary between sandstone (hanging wall) and limestone (footwall)

Stratigraphy: Gomo Formation (Late Miocene)

Description:

In figure 74 you see a lithological change from limestone in the footwall and sandstone in the hanging wall. This could represent the lithological border between the Gomo Formation in the central East and the Lelematua Formation in the central West of Nias.
A set of fractures enable water to pour out from a cold water spring. This karst wells could be linked to the lithological boundary in this area and therefore could be used as a marker for the lithological contact.

Figure 74: Subvertical fractures

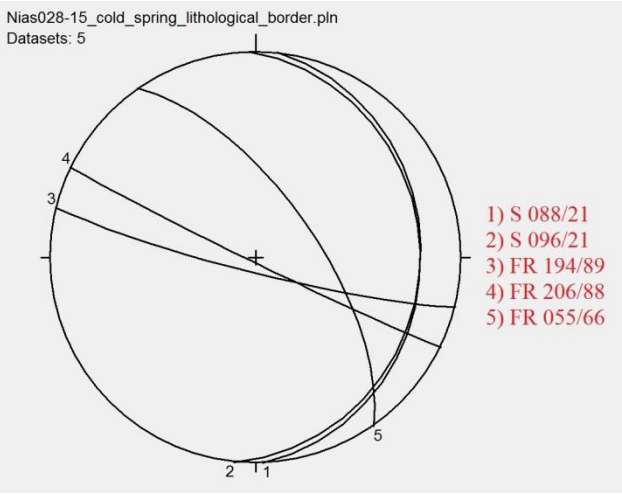

Plot 14: Sedimentary bedding, set of fractures

Figure 75-76: Karst spring along a potential lithological border

Nias029-15:

Date: 25.2.15

GPS (UTM 47): 93777.888 m N 371329.295 m E

Outcrop Location: 300m distance SSE to Nias028-15, cave in the jungle, "Togi Helua"

Lithology: Limestone

Stratigraphy: Gomo Formation (Late Miocene)

Description:

Through the help of some assisting locals, we found "Togi Helua", a cave of large dimensions half an hour walking distance from the nearest village Desa Mehaga.
Karst formation is associated with the limestones of the Late Miocene Gomo Formation. This outcrop is a text book example for tropical karst. Figure 77 shows flowstone formations. In figure 78 stalactites are growing from the roof of the cave. In general karst structures in a cave develop after CO_2 saturated water caused by vegetation leaks on a rock wall, from the first or rather the ceiling of the cave for a certain period of time. Due to the fact that the CO_2 partial pressure in the cave is lower than outside the calcite precipitates along the rock wall and forms this type of structures.
The seismic activity in this region is very high that is the reason why many caves commonly have collapsed (Figure 79). Due to the tropical environment, the high amount of biomass and the osmotic potential of the waters in these latitudes, cave formation needs less time than in colder areas of the earth.

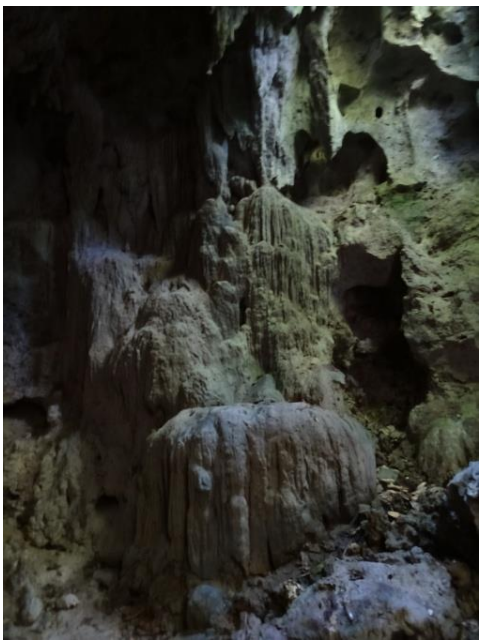

Figure 77: Flowstone formation

Figure 78: Stalactites

Figure 79: Partly collapsed cave with broken flowstones and stalactites

Figure 80: Cave formation in limestone

Nias030-15:

Date: 26.2.15

GPS (UTM 47): 62099.614 m N 367566.947 m E

Outcrop Location: 5km distance E to Telukdalam, quarry around military area

Lithology: Limestone (Grainstone) interbedded with clay layers, Sandstone fossil-rich

Stratigraphy: Gunungsitoli Formation (late Pliocene)

Description:

Outcrop Nias030-15 is the most southern part of this huge quarry, which is in some parts still active. The size of the quarry is about 0.5 km². The sedimentary layers generally dip with moderate angles toward ENE (see plot 15).

After the classification of Dunham the sediments consist of grainstone, a carbonatic rock or rather limestone that is grain supported. At some locations the grayish sandstone layers bore millimeter to several decimeter sized concretions (Figure 84).

The sedimentary bedding plane in figure 83 bears two different generations of faults only visible on this plane.

Figure 81: Macroscopic image of the outcrop

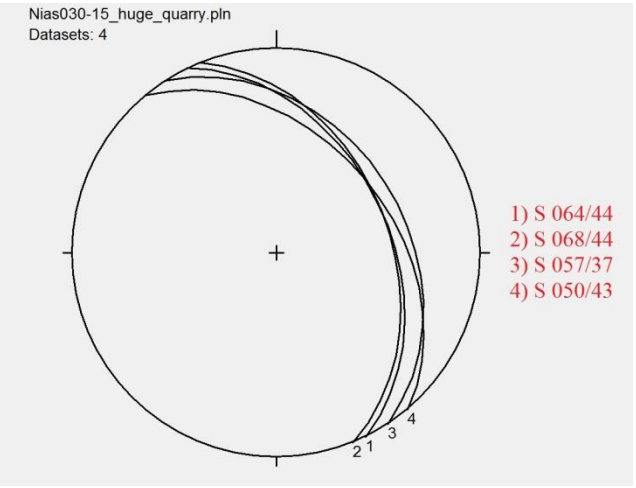

Plot 15: Sedimentary bedding

Figure 82: Grayish sandstone to the left

Figure 83: Two different generations of conjugate faults

Figure 84: Concretion in sandstone

Nias031-15:

Date: 26.2.15

GPS (UTM 47): 62317.573 m N 367745.286 m E

Outcrop Location: Quarry around military area, 400m distance NE to Nias030-15

Lithology: Limestone (Grainstone) interbedded with clay layers

Stratigraphy: Gunungsitoli Formation (late Pliocene)

Description:

From distance it is obvious that the sediments underwent a folding event (Figure 85). After plotting the dipping directions and dip of the sediments from several spots at the outcrop, it is clearly to see that there are two different folding directions. One compressional direction is about NNW-SSE, leading to the anticlinal folding (Figure 85). The striking from plot 17 to plot 19 is changing from ENE-WSW to WNW-ESE indicating that there is a change of the orientation of the original fold curving around the east. At the most southern part of this huge quarry (Nias030-15) the sediments strike NNW-SSE and approximately 300m further NE (Nias031-15) they strikes E-W, leading to the assumption that there is a not disclosed, underground syncline between Nias030-15 and Nias031-15, which is curving around the west. The central section of the anticline in figure 85 records a dense network of extensional fractures (Figure 86), which can be used to derive the orientation of the local fold axis (Plot 20). Moreover there are sinter formations along some boulders around the quarry, which suggest the existence of eroded caves in this area. (Figure 87 and 88)

Figure 85: Anticline of outcrop Nias031-15, with marked spots of measurements

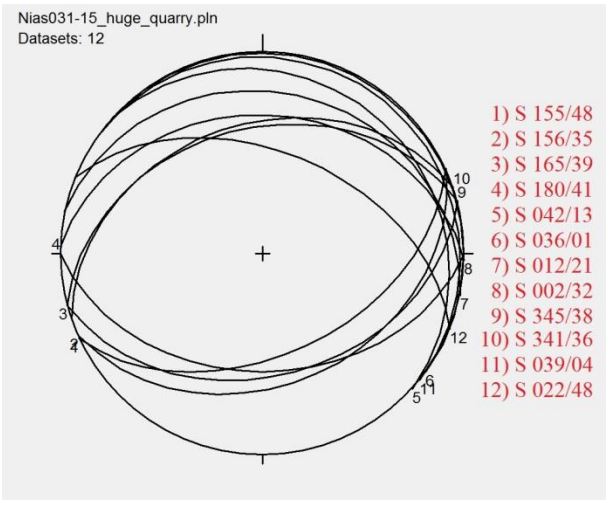

Plot 16: Folded sedimentary bedding

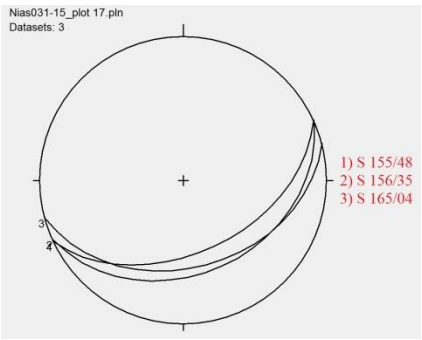

Plot 17:

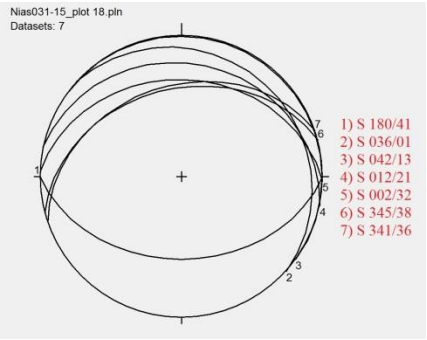

Plot 18:

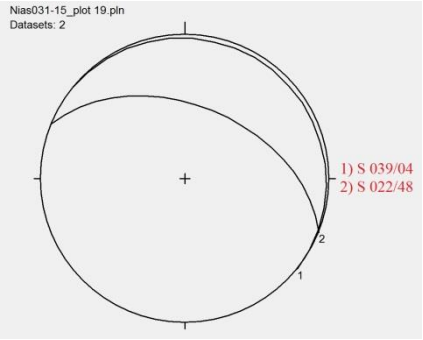

Plot 19:

Figure 86: Extensional fractures at anticline

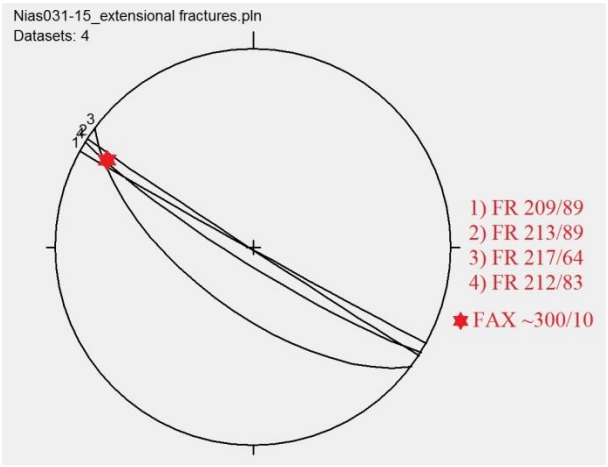

Plot 20: Extensional fractures with fold axis ~300/10

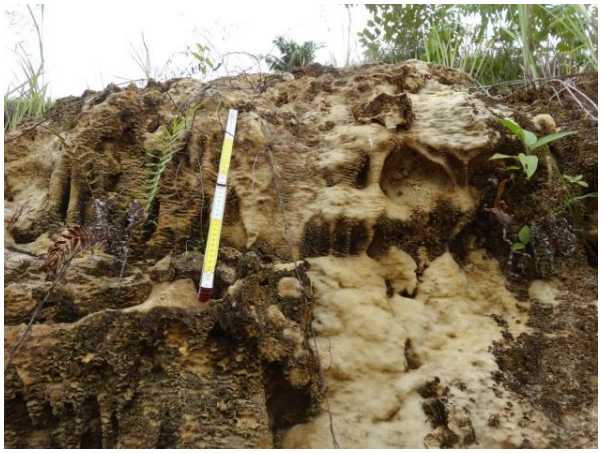

Figure 87-88: Sinter formations on boulders scattered around the quarry

Figure 89: Oriented organic material

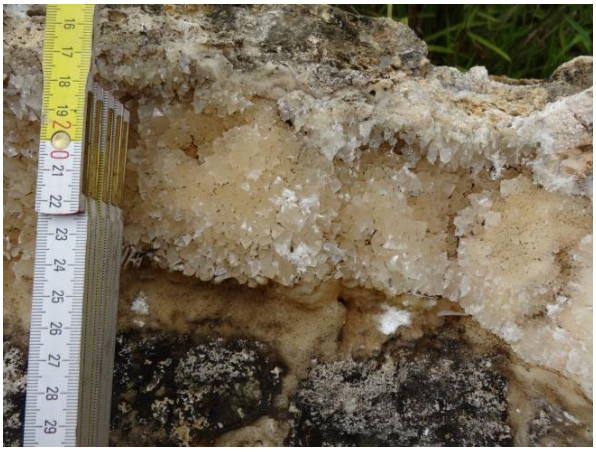

Figure 90: Calcite crystals

Nias032-15:

Date: 26.2.15

GPS (UTM 47): 63102.072 m N 367011.553 m E

Outcrop Location: Quarry around military area, 1km distance NW to Nias031-15

Lithology: Limestone (Grainstone) interbedded with clay layers

Stratigraphy: Gunungsitoli Formation (late Pliocene)

Description:

This outcrop is only 200m further East of Nias003-15. The sedimentary layers are slightly and uniformly tilted NNW. Sinter formations are found all around this area. It is very likely that the whole area was pervaded by one or several cave systems in the past and the sinter formations and calcite structures are remnants.

Figure 91: Sedimentary layers tilted towards north

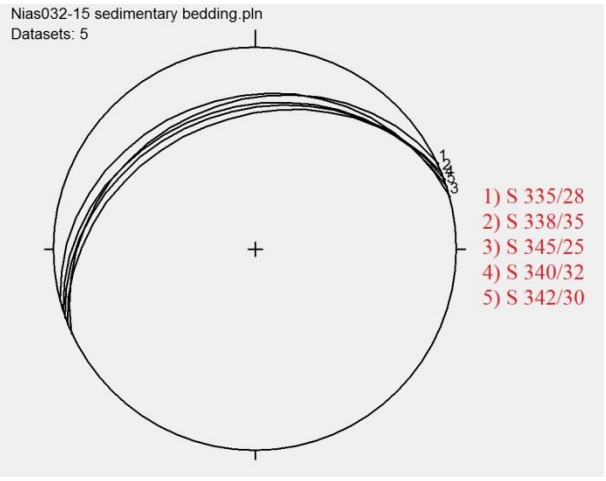

Plot 21: Sedimentary bedding

Figure 92: Sinter formation on bolder

Nias033-15:

Date: 27.2.15

GPS (UTM 47): 62456.032 m N 367727.974 m E

Outcrop Location: Quarry around military area, 200 distance N to Nias031-15

Lithology: Limestone (Grainstone) interbedded with clay layers, Sandstone

Stratigraphy: Gunungsitoli Formation (late Pliocene)

Description:

This outcrop is only about 100 m away from Nias031-15 and it is the third of three closely located outcrops that potentially took part in the same folding events suggested in outcrop Nias030-15 and Nias031-15.

Plot 24 shows the dipping directions of sedimentary layers from outcrop Nias030-15, Nias031-15 and Nias033-15 to get a better understanding of the folding events in this area. Between Nias030-15 and Nias031-15 is a synclinal fold and Nias031-15 shows an anticlinal fold, as folding event number one. The synform seems to bend around the west and the antiform further north around the east.

Additionally a fault zone cuts the sedimentary layers with sinistral shear sense (Figure 94).

Figure 93 Sedimentary layers dip towards north

Figure 94 Fault zone with sinistral slickensides

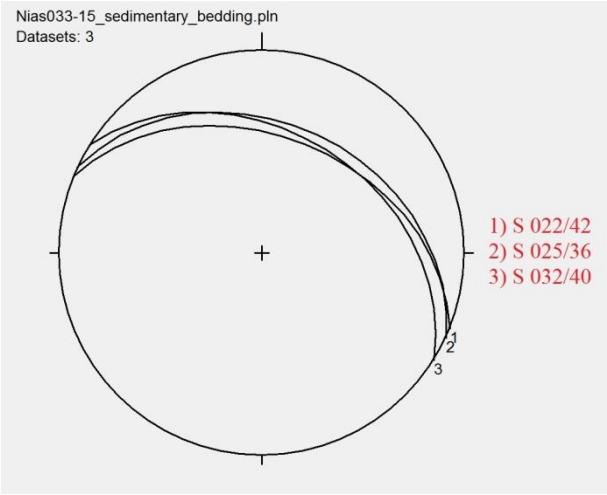

Plot 22: Dip direction and dip angle of sediments

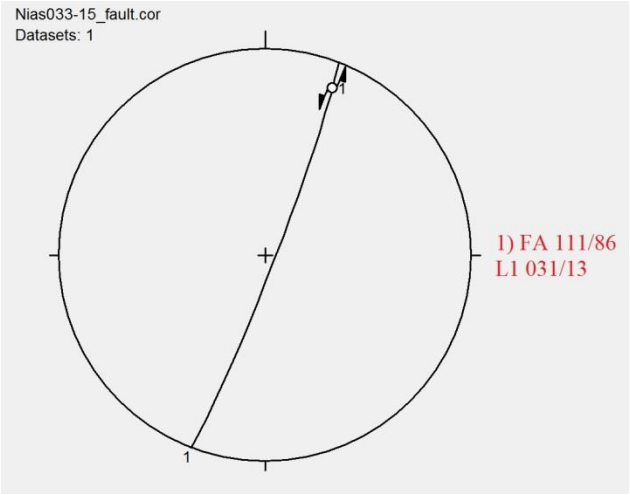

Plot 23: Fault zone with sinistral shear sense

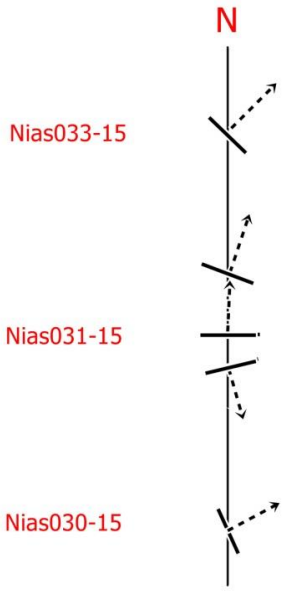

Plot 24: Dip directions of three closely located outcrops

Nias034-15:

Date: 27.2.15

GPS (UTM 47): 69487.858 m N 359545.198 m E

Outcrop Location: Road subsidence, 6km distance NNW to Telukdalam

Lithology: Clay with clasts of basalt, Serpentinite (Melange Zone)

Stratigraphy: Lelematua Formation

Description:

Especially in the west coast of Nias occurred many mass movements and landslide events at various scales. In figure 95 parts of the road and the stone wall are creeping downslope towards WNW 280°.The displacement distance measured in terms of offset of the road wall is about half a meter. The soft and weak clay of the Lelematua Formation triggers slope movements and landslides in accord with seismic activity. The shear strength of the clay layers seems to be highly anisotropic since not all clay layers act as weak horizons. At some spots the clay has clasts of serpentinite and basalts in it probably associated with the formation of the Melange Zone.

Figure 95: Road subsidence

Figure 96: Very weak clay sediments in the underground

Nias035-15:

Date: 28.2.15

GPS (UTM 47): 68253.651 m N 357973.915 m E

Outcrop Location: Road subsidence, 2 km distance SW of Nias034-15

Lithology: Clay with clasts of serpentinite (Melange Zone)

Stratigraphy: Lelematua Formation

Description:

This road creeps downslope and has been tilted towards W similar to the location Nias034-15, although the road is less damaged (Figure 97). The displacement of the roadside is approximately 40 cm. Lithologically, the rocks consists of clay layers with serpentinite clasts belonging to the Melange Zone (Figure 99-100).

Figure 97: Road subsidence

Figure 98: Approximately 40 cm offset

Figure 99-100: Clay layers including clasts of serpentinite

Nias036-15:

Date: 28.2.15

GPS (UTM 47): 71358.451 m N 359496.335 m E

Outcrop Location: Small valley on the north-western side of the road, looking at the opposite side of the valley, outcrop size 15x10m, distance to the road 10m, not reachable by foot

Lithology: Clay

Stratigraphy: Lelematua Formation

Description:

Due to the fact that the outcrop was not reachable by foot, we tried to investigate the lithology in approximately 5m distance. We assumed that the outcrop belongs to the Lelematua Zone.

Figure 101: Different intensities of clay weathering

Nias037-15:

Date: 28.2.15

GPS (UTM 47): 73853.576 m N 359293.029 m E

Outcrop Location: 3 km distance N to Nias036-15

Lithology: Clay

Stratigraphy: Lelematua Formation

Description:

In the western parts of Nias good outcrops are rare. We restricted our standards and just looked at the lithologies whenever possible just to find the stratigraphic Melange Zone. Figure 102 is a panorama of the outcrop with clay as lithology.

Figure 102: Panorama view of outcrop

Nias038-15:

Date: 28.2.15

GPS (UTM 47): 74594.698 m N 358132.945 m E

Outcrop Location: 1 km NW to Nias037-15

Lithology: Serpentinite

Stratigraphy: Melange Zone

Description:

This outcrop consists of serpentinite, which is found as part of the Melange Zone. We found a fault system with few clear recognizable shear sense indicators (Figure 104-105; Plot 25), which could be a sign of a NW-SE extensional direction. Figure 106 shows two normal faults associated with fault drag.

Figure 103: Panorama of the outcrop

Figure 104-105: Slickenside with no clear sense of shearing

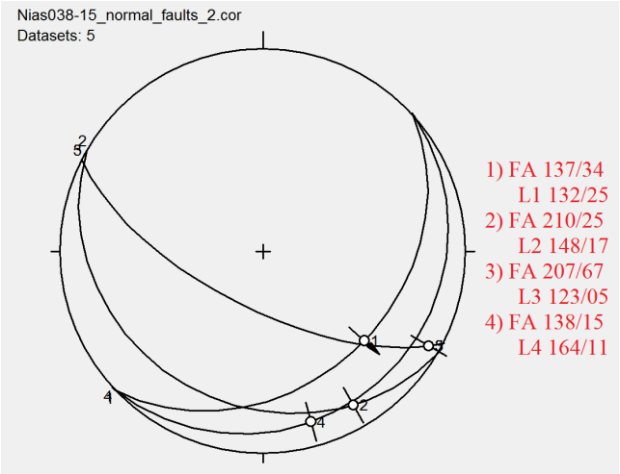

Plot 25: Fault system with potential NW-SE extensional direction

Figure 106: Fault drag associated with two normal faults

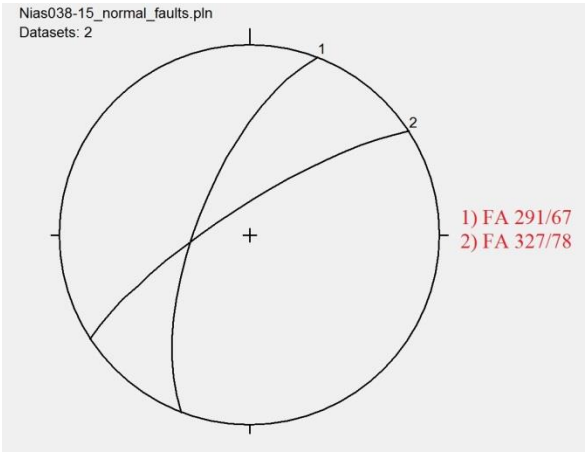

Plot 26: Two normal faults

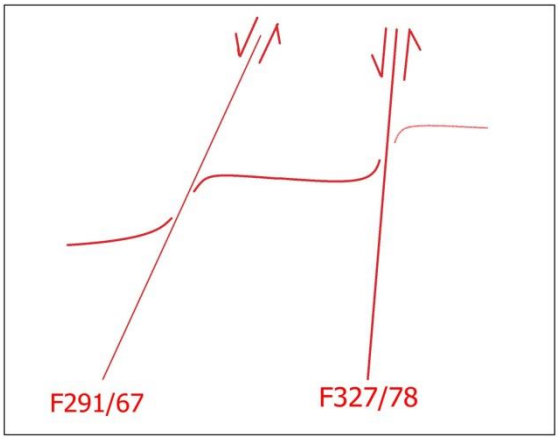

Sketch of figure 106

Nias039-15:

Date: 1.3.15

GPS (UTM 47): 111972.301 m N 361557.054 m E

Outcrop Location: Village near "Air Panas", original location of the hot spring, near the public bath

Lithology: Limestone

Stratigraphy: Gomo Formation (Late Miocene)

Description:

This is the original location of the hot spring prior to the earthquake in 2005. Exhalation of sulfur rich vapor is still evident. In the pools and around the small stream whitish and black bacteria and sinter deposits can be recognized (Figure 108), which are relicts of the time when the hot spring was originally active at this spot.

Figure 107: Original location of the hot spring before 2005

Figure 108: Whitish and black deposits

Figure 109: The local bath at Air Panas, which is no more filled by the hot spring as it was prior to the earthquake in 2005.

Nias040-15:

Date: 1.3.15

GPS (UTM 47): 112165.945 m N 361317.246 m E

Outcrop Location: Following the river in which the hot spring is located upstream to the W, distance 500m

Lithology: Limestone interbedded with silt-/clay layers

Stratigraphy: Gomo Formation (Late Miocene)

Description:

The fault system visible in plot 26 indicates an extensional direction oriented N-S similar to a number of boudinage structures in this area (Figure 111). The potential Riedel structure in figure 110 reveals a dextral strike slip movement.
A big boulder in the riverbed consisting of coral fragments has been strongly altered by hydrothermal activities in the area.

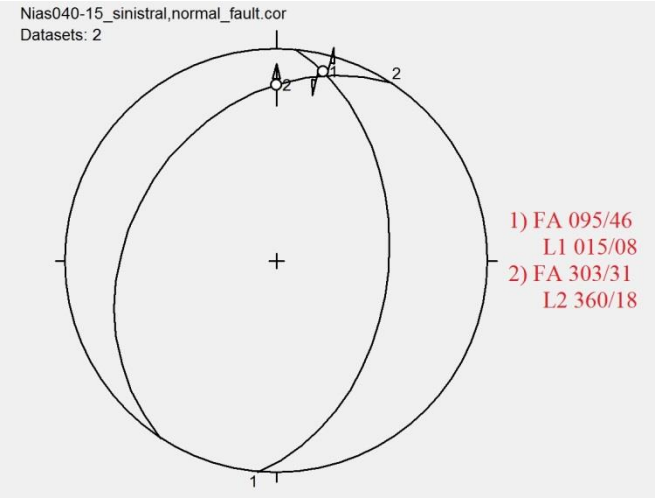

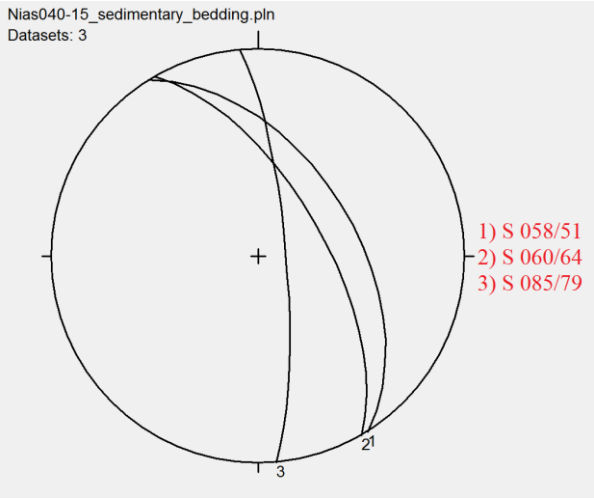

Plot 26: Fault system extensional direction N-S

Plot 27: General dipping of the sedimentary layers

Figure 110: Riedel structure

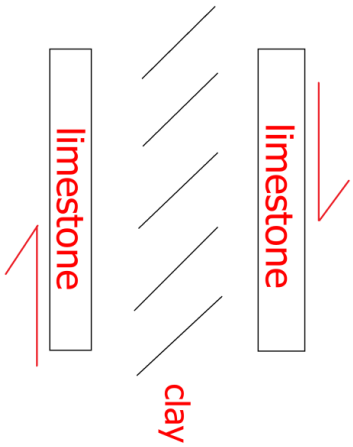

Sketch of Figure 88

Figure 111: Linear arrangement of concretions resembling Boudinage structure

Figure 112: Hard linked fault segments indicating dextral shear sense

Figure 113: Hydrothermally altered corals

Nias041-15:

Date: 2.3.15

GPS (UTM 47): 142725.088 m N 343408.099 m E

Outcrop Location: 2 km distance NW to Gunungsitoli

Lithology: Limestone, sandstone, clasts of siltstone

Stratigraphy: Gomo Formation (Late Miocene)

Description:

In this outcrop a set of spectacular nomal faults, which dip to southeast have been observed. They could be part of a pull-apart basin located around the capital of Nias called Gunungsitoli. This pull-apart basin eventually developed as a result of the dextral movement along the potential Mentawai fault zone in this area.
Figure 119 shows a complex zone of deformation outlined by the line drawing. In some parts the sediments are very iron rich and record red-brown weathered colors.

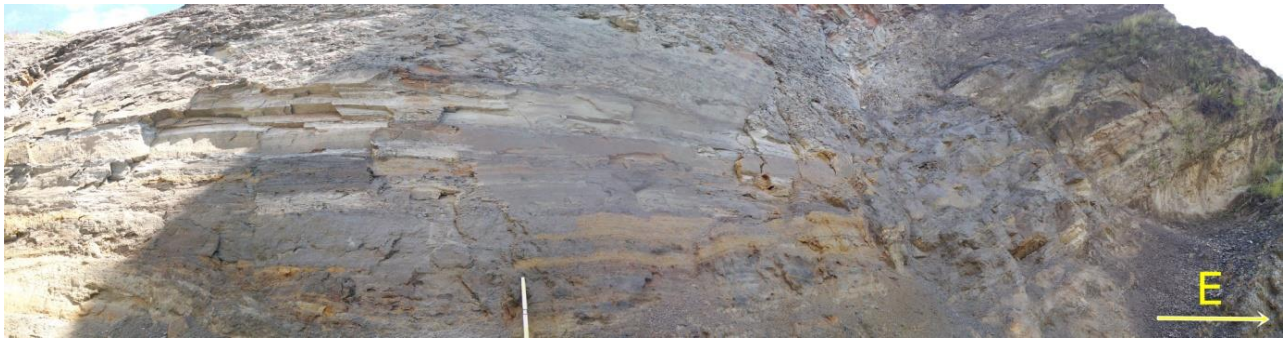

Figure 114: Panorama of the outcrop

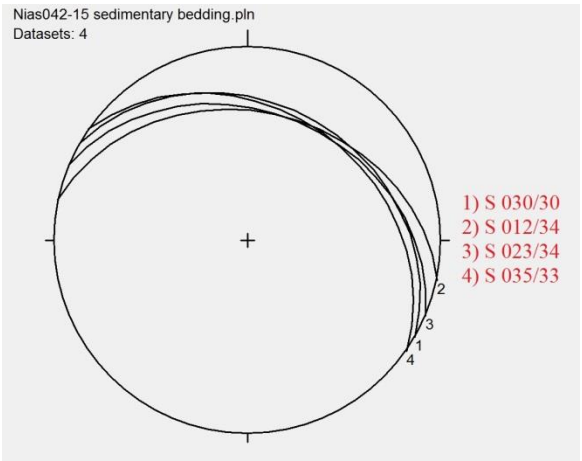

Plot 28: Sedimentary bedding

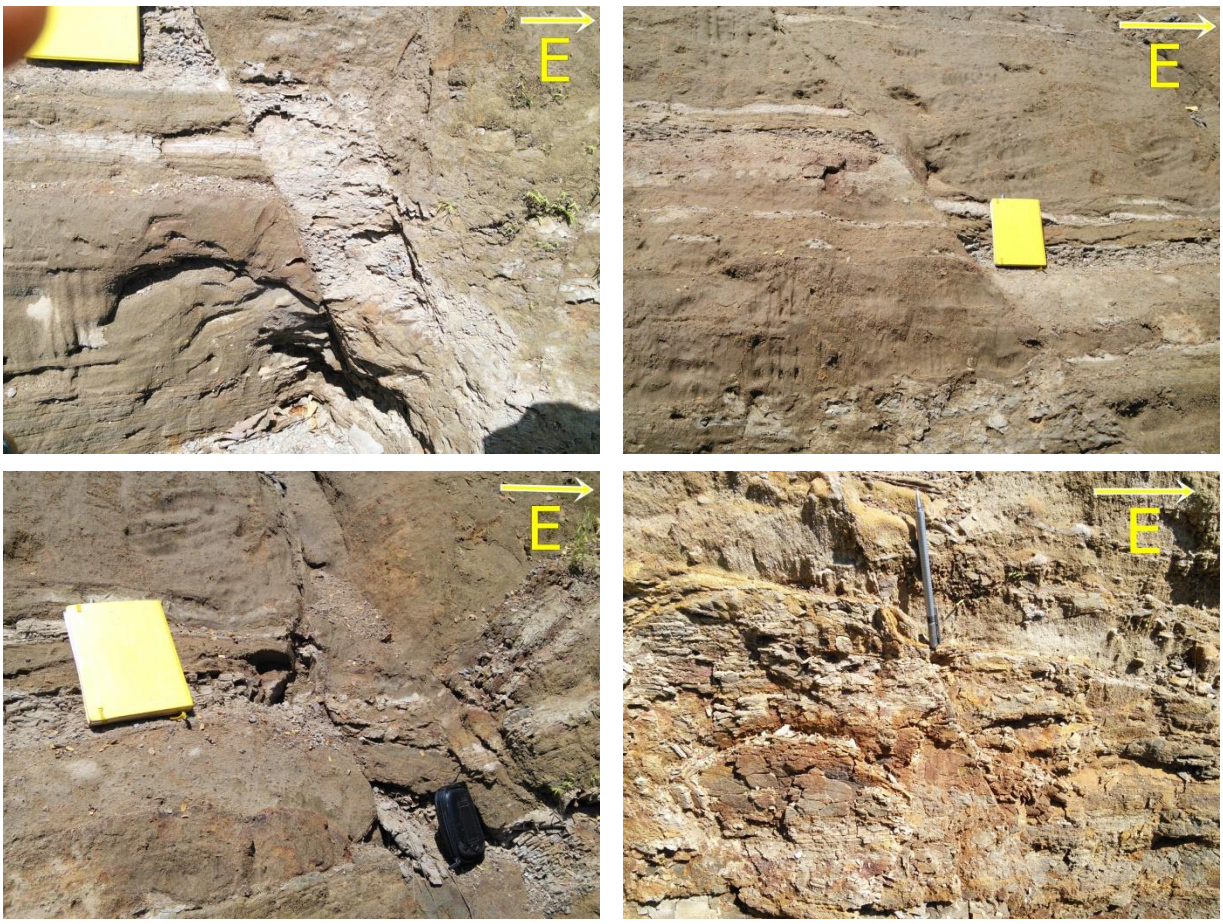

Figure 115-118: Several normal faults

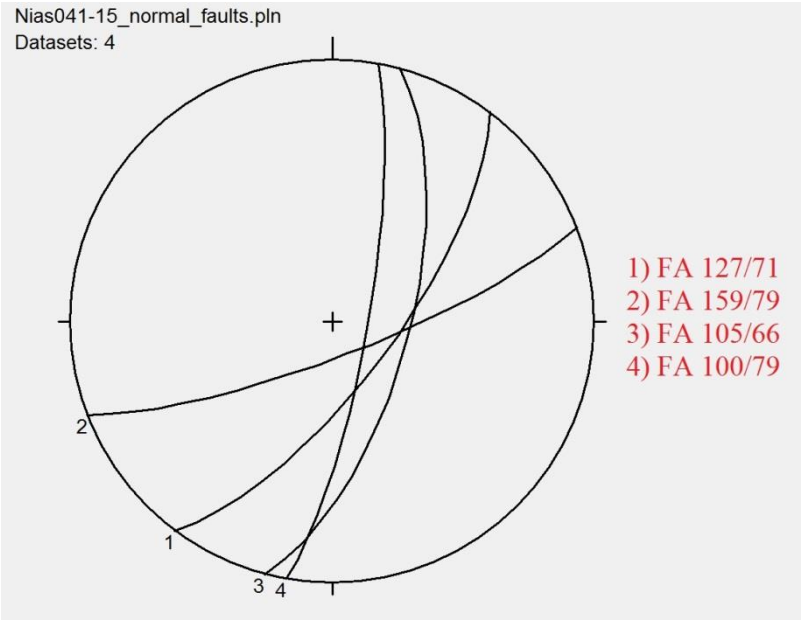

Plot 29: Normal faults dipping to E and SE

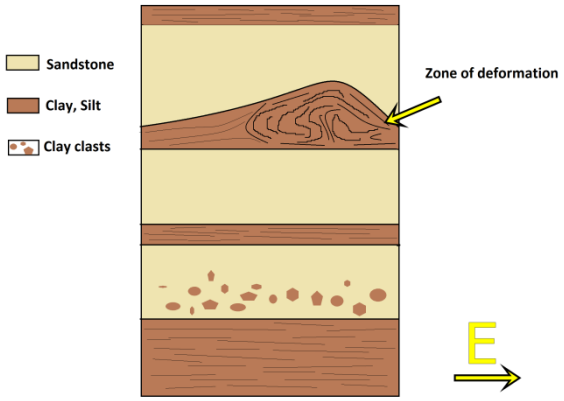

Sketch of the outcrop

Figure 119: Zone of deformation outlined in the sketch above

Figure 120: Iron rich fluid penetrating the sediments

Nias042-15:

Date: 2.3.15

GPS (UTM 47): 143805.988 m N 341729.458 m E

Outcrop Location: 5 km distance NW to Gunungsitoli

Lithology: Limestone, clay

Stratigraphy: Border between Gomo (Late Miocene) and the Gunungsitoli Formation (Late Pliocene)

Description:

This river bed exposes a lithological change from limestone in the footwall to clay in the hanging wall and potentially marks the border between the Gomo and the Gunnungsitoli Formation. In the most western part of the outcrop a huge cave located along a fracture in the limestone formed. Although it was not possible to directly measure the fault plane, which facilitated the cave formation, a value of 045/89 has been estimated.
At the potential lithological border a waterfall formed due to different erodibilities and weathering of limestone and clay (Figure 122). The difference in height is around 10 m.
In figure 124 two fractures which cross cut the clay layers are visible (045/45). The light brown color of the fracture indicates the involvement of an iron rich fluid.
Plot 32 visualizes two different sets of extensional fractures which we could identify on the limestone perpendicular to its bedding plain (Figure 121) and on the topmost layer (Figure 122). The formation of these extensional structures could be connected with the normal fault structures approximately 2 km to the southeast (Nias041-15).
In the weak clay layers a penetrative pattern of small scale folding has been observed (Figure 125).

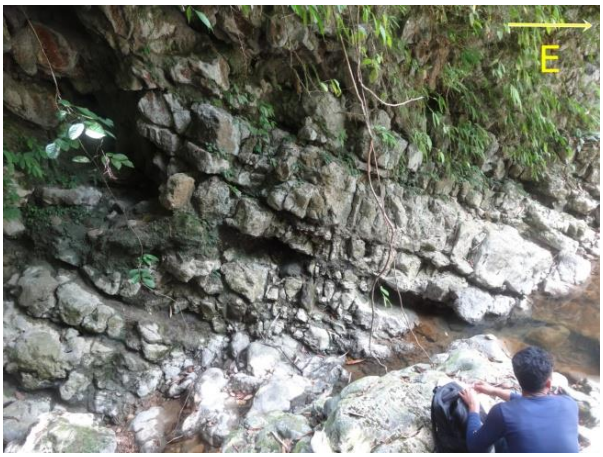

Figure 121: Sedimentary bedding of the limestone

Figure 122: Waterfall at a potential lithological border

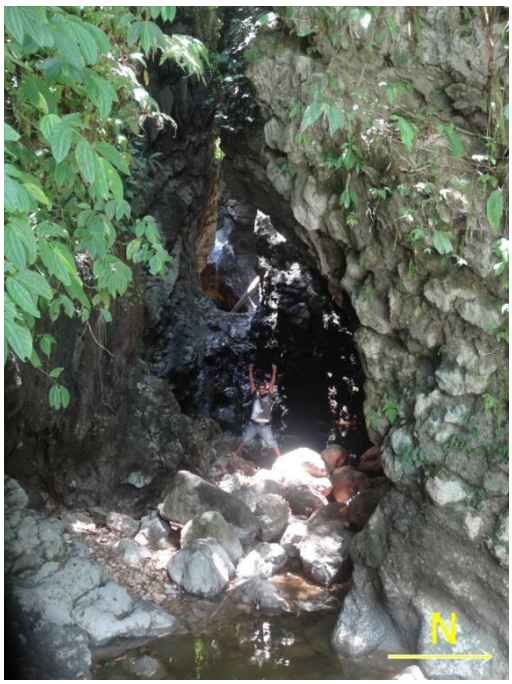

Figure 123: Cave formation along a fracture

Figure 124: Two fractures penetrating the clay layers and filled with iron rich fluids

Figure 103: Intense folding in the clay

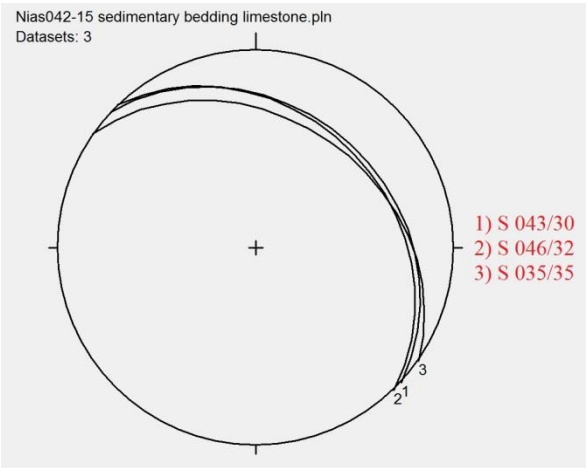

Plot 30: Sedimentary bedding of the limestone

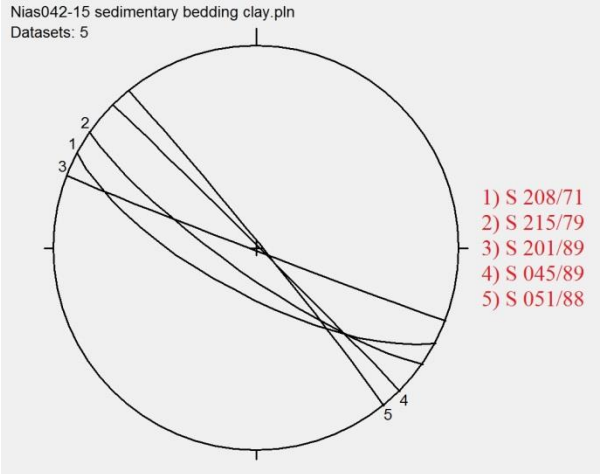

Plot 31: Sedimentary bedding of the clay

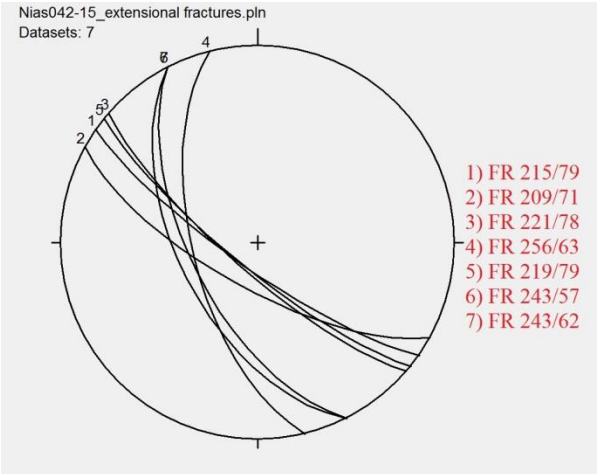

Plot 32: Two sets of extensional fractures

Nias043-15:

Date: 2.3.15

GPS (UTM 47): 141834.007 m N 343613.332 m E

Outcrop Location: 1 km distance to Gunungsitoli

Lithology: Limestone

Stratigraphy: Gomo Formation (Late Miocene)

Description:

Around 1 km south of Nias041-15 another cave has formed in the limestone. Numerous karst-cave structures like stalactites, stalagmites and flowstones developed by carbonate dissolution - precipitation processes. The high frequency of scattered rocks on the floor speaks for a high instability of the caves, mirroring the high seismic activity in the region.

Figure 125: Stalactites hanging from the first in the cave

Figure 126: Flowstone formation

Figure 127: Partly collapsed cave system

Nias044-15:

Date: 3.3.15

GPS (UTM 47): 135265.411 m N 344978.650 m E

Outcrop Location: 6 km distance S to Gunungsitoli

Lithology: Silt-, sandstone with clay layers

Stratigraphy: Gomo Formation (Late Miocene)

Description:

Figure 128 shows anticlinal folding of the sediments which is partly offset by a set of faults. Plot 33 shows the dipping directions and dips of the fold with the fold axis in SSE direction (FAX ~170/45). The folding direction indicates WSW-ENE shortening. Plot 34 visualizes the diffuse pattern of offsets along the fold which are strongly heterogeneous.

Figure 128: Anticlinal folding of the sedimentary layers

Figure 129: Incrusted clay-, silt clasts

Figure 130-131: Offset of clay layers

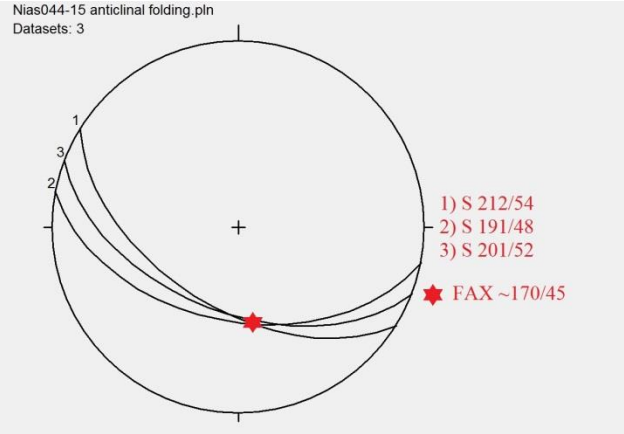

Plot 33: Anticlinal folding of sediments

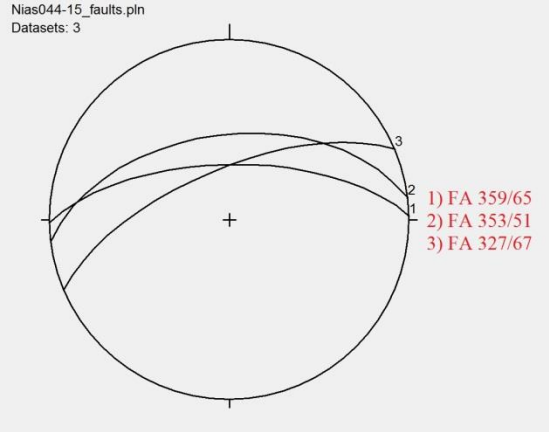

Plot 34: Diffuse offsets of the folded sediments

Nias045-15:

Date: 3.3.15

GPS (UTM 47): 134808.518 m N 344599.624 m E

Outcrop Location: 700 m distance SW to Nias044-15, following the road

Lithology: Silt-/sandstone

Stratigraphy: Gomo Formation (Late Miocene)

Description:

Similar to the outcrop Nias044-15 an anticlinal fold as part of the overall folding in this area southwest of Gunungsitoli has been observed. The fold axial plane of the anticline is estimated at FAP ~030/40 and the fold axis at FAX ~340/30. Figure 133 shows the top of the outcrop with the hinge of the fold nearly observable on top of the rock wall. Plot 35 is a Pi-plot of all the dip directions and dips of the fold limbs and the fold hinge. We tried to estimate the fold axial plane and the fold axis. Some small offsets of the sedimentary bedding plains have been observed in the same way found in Nias044-15.

Figure 132: Panorama of the outcrop

Figure 133 Top of the outcrop, nearly visible is the

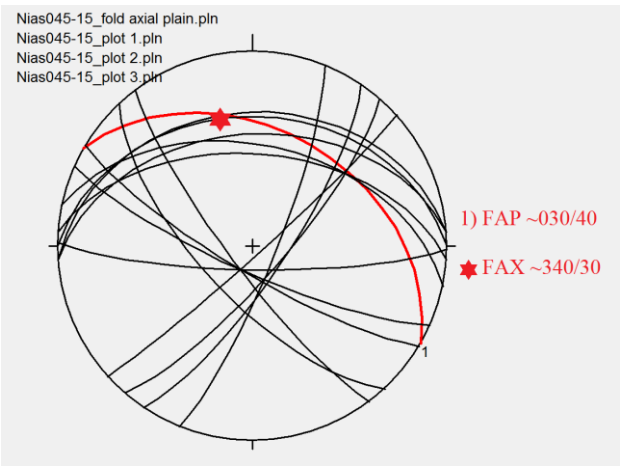

Plot 34: Anticlinal fold with estimated fold axis (FAX)

hinge of the anticline *and the estimated fold axial plane (FAP)*

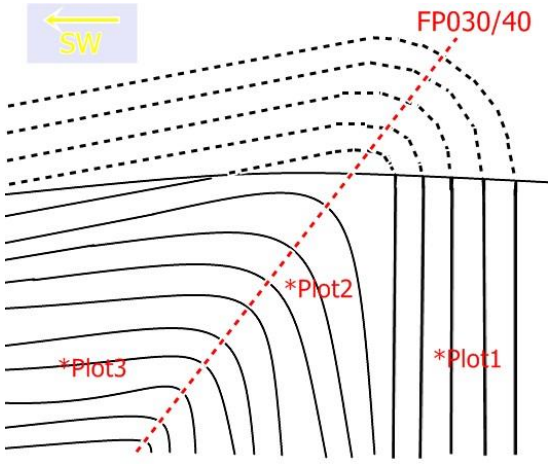

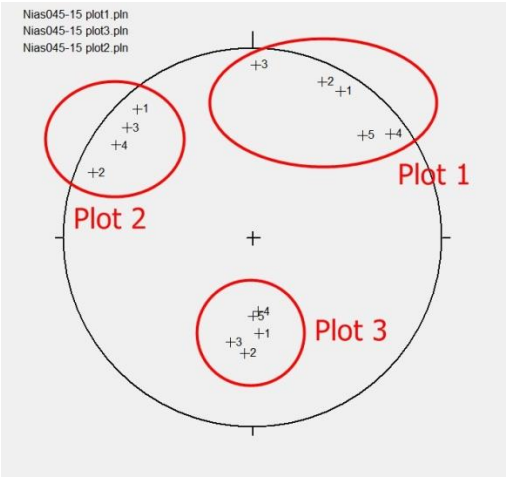

Sketch of the anticlinal folding *Plot 35: Pi-plot of all the data*

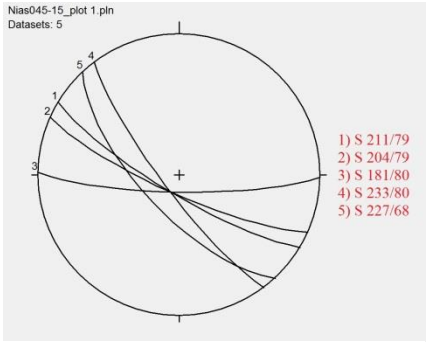

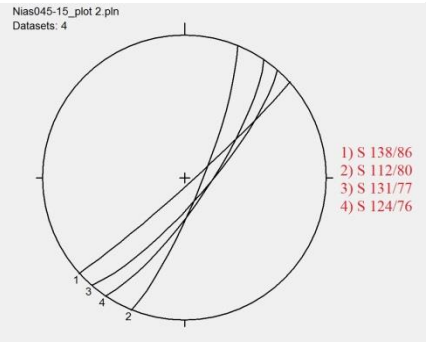

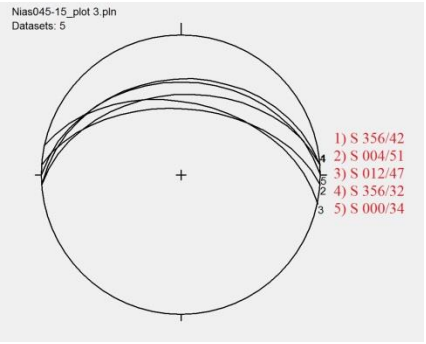

**Plot 1:* **Plot 2:* **Plot 3:*

Nias046-15:

Date: 3.3.15

GPS (UTM 47): 134652.622 m N 344438.561 m E

Outcrop Location: 200 m distance SW to Nias045-15, following the road

Lithology: Silt-/sandstone

Stratigraphy: Gomo Formation (Late Miocene)

Description:

The sedimentary bedding seen in figure 134 is striking NW-SE and it is dipping uniformly to NE. Approximately 10 m to the west, behind a house the striking of the sediments changes to W-E and the dipping gets less steep. Plot 36 shows two domains of primary dipping of the sediments. Measurements 1 – 5 were taken at the location of figure 134, measurements 6 – 8 were taken approximately 10 m further south west behind a house. The strike and dip changes from NE to SW from of the outcrop from NW-SE to W-E striking direction and the dip is decreasing. The change in strike and dip of the sediment and the close proximity to outcrops Nias044-15 and Nias045-15 would indicate a similar anticlinal folding event as seen in the two prior outcrops.

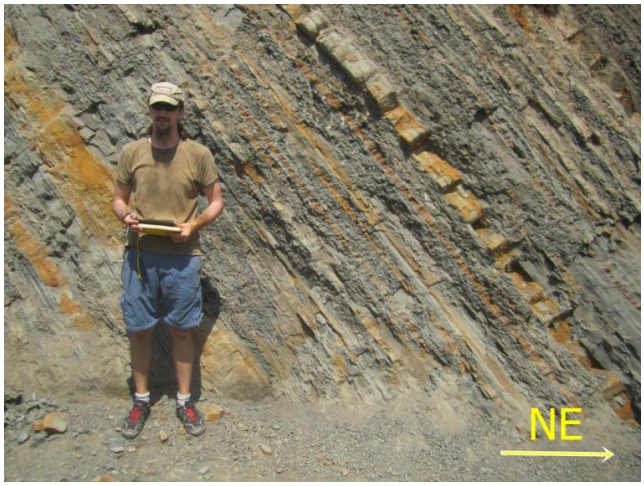

Figure 134: Sedimentary bedding dipping towards NNE

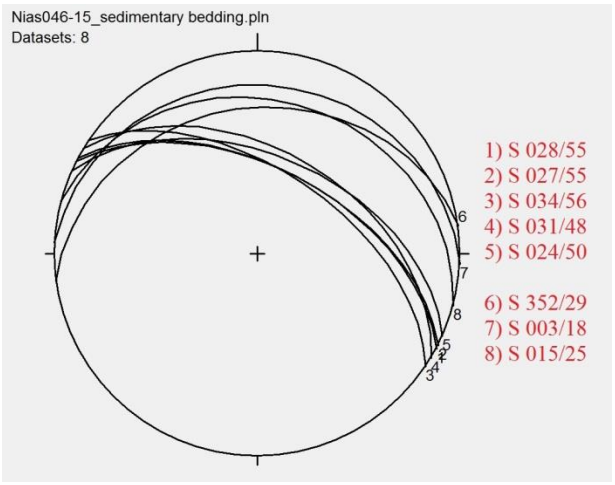

Plot 36: Sedimentary bedding

Nias047-15:

Date: 3.3.15

GPS (UTM 47): 122926.823 m N 342272.478 m E

Outcrop Location: Riverbed SE of the road

Lithology: Limestone, clay, boulders of metamorphic rocks e.g. basalt, serpentinite

Stratigraphy: Ophiolithic Basement/Gomo Foramtion (Late Miocene)

Description:

The in-situ lithology of this outcrop is limestone (Figure 135). However, the big boulders in the river record a suite of various conglomerates and igneous, in addition to metamorphic rocks (mainly basalts and serpentinites). Obviously the river flows partly through the Melange Zone.

Figure 135: Limestone, in-situ rock

Figure 136: Boulder of conglomerate

Figure 137: Hydrothermally overprinted metamorphic rock

Nias048-15:

Date: 4.3.15

GPS (UTM 47): 134593.832 m N 343993.805 m E

Outcrop Location: On the way back from Nias047-15 to Gunungsitoli, 6 km distance S to the city

Lithology: Silt-/sandstone

Stratigraphy: Gomo Formation (Late Miocene)

Description:

From outcrop Nias046-15, which is located about 500m further to the E to this outcrop, the sedimentary layers rotate from subvertical to subhorizontal. A possible interpretation would be that Nias046-15 and Nias048-15 belong to one bigger anticlinal fold with an amplitude of about 500m that is only partly outcropping in the field (Sketch at the bottom).
Outcrop Nias044-15, Nias045-15, Nias046-15, Nias048-15 happen to be in the same stratigraphic unit and seem to be part of one or several overall, anticlinal folding events including several fold trains of anticlines and synclines.

Figure 138: Sedimentary bedding

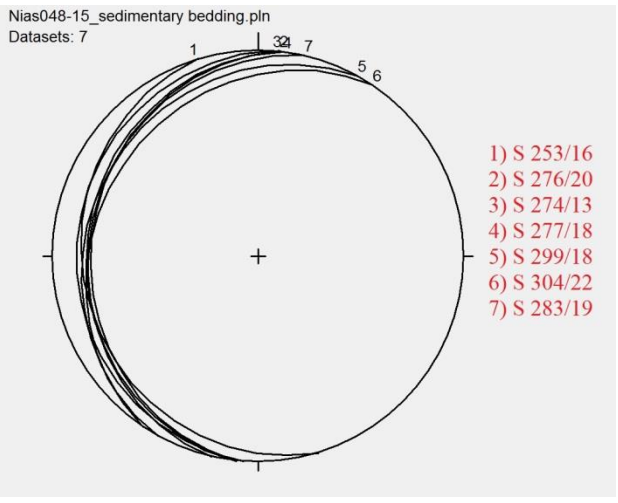

Plot 37: Sedimentary bedding dipping towards W

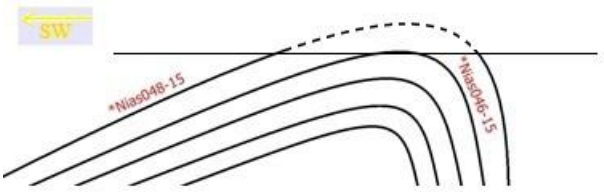

Sketch of the potential overall anticlinal folding

Nias049-15:

Date: 4.3.15

GPS (UTM 47): 132752.937 m N 347680.445 m E

Outcrop Location: 10 km distance SSE to Gunungsitoli

Lithology: Silt-/Sandstone (fine-grained)

Stratigraphy: Gomo Formation (Late Miocene)

Description:

The sedimentary bedding planes dip towards NE and are cut more or less parallel to the striking, increasing the potential risk for landslides. Figure 140 shows a translational mass movement, sliding to the NE. As far as the villagers reported many people have lost their lives in this area by landslides.

Figure 139: Sedimentary bedding planes

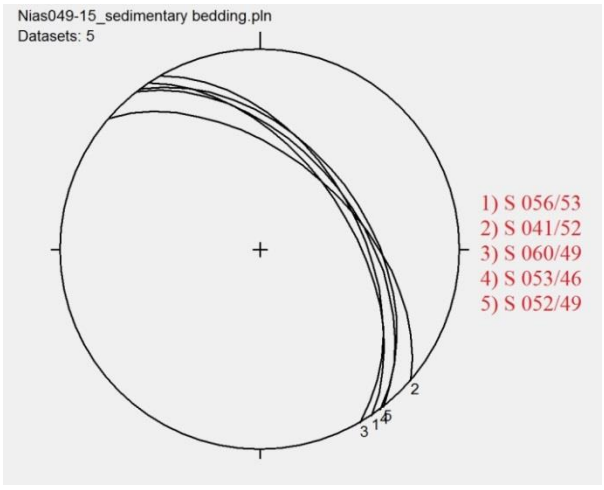

Plot 38: Sedimentary bedding dipping towards NE

Figure 140: Landslide sliding direction NE

3.3. Interpretation

In this chapter I focus on the important data I collected in the field and compare my results with work from other authors mainly published in the 1970s and try to derive a conceptual model for the kinematic evolution of the Mentawai fault.

In outcrop Nias004-15, shown in figure 26 (p.55), we identified several zones of intensive, cataclastic shearing. The tectonic movements clearly reflect shearing along a fault in the brittle regime. The resolving heat due to friction was not high enough to produce pseudotachylites or carbonate pseudotachylite, but the dissipated energy pulverized the material within the shear zone resulting in a cohesionless ultracataclasite or rather a fault gauge indicating a formation depth of 1 – 4 km, according to Reuther (2012), (p. 42 in book) (Figure 141).

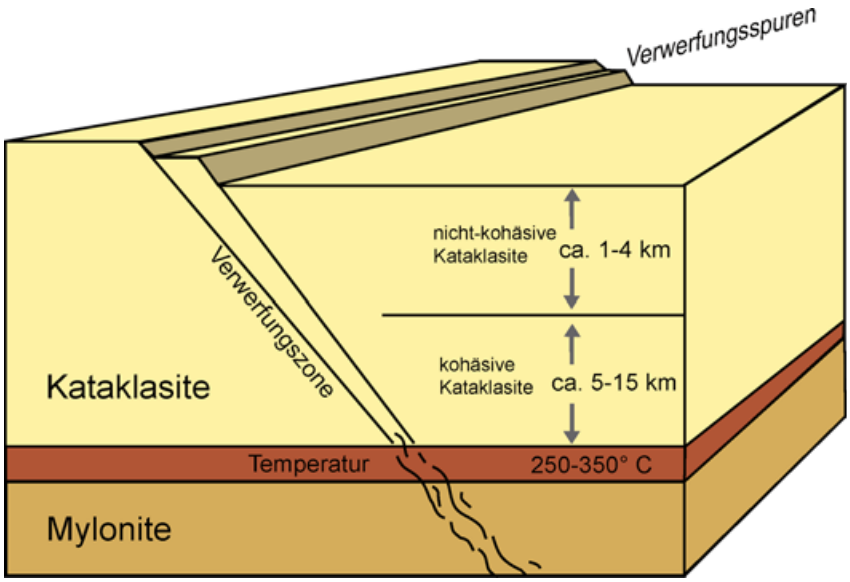

Figure 141: Model for different settings of fault rock formation in respect to depth, respectively heat and confining pressure. Approximately in the first 15 km depth the rock inside the shear zone (germ. Verwerfungszone) experience brittle shearing. Further down starts the ductile deformational regime. In the top 4 km depth heat and pressure are small compared to zones in greater depth, therefore results in cohesionless rock powder or a fault gauge as given (From Claus-Dieter Reuther, 2012).

The outcrop is difficult to access and strongly weathered and therefore shear sense indicators were difficult to identify. The overall impression of dextral shear sense was supported by observations from previous investigation (pers. comm. Bernhard Grasemann) interpreting a pull-apart basin connected with the dextral slip along the Mentawai fault. Geographically the outcrop is approximately located near the potential continuation of the Mentawai fault on Nias, which was already identified by Karig et al. (1980) as a flexure zone. Stratigraphically and lithologically the outcrop shows a clear grading and shallowing upward sequence resembling the Nias Beds characterized by Moore and Karig (1980). The grey clay sediments are on the bottom, overlain by sandstone with reef debris and conglomerate, following limestone.

In outcrop Nias010-15 we identified a sinistral fault (Figure 38, p. 62), which potentially could be a conjugated, sinistral, transcurrent fault or a conjugated, antithetic, Riedel shear fault, resulting from the oblique, transpressional forces acting on the supposed dextral Mentawai fault. The next outcrop Nias011-15 we found a dextral fault (Figure 40, p. 64), which would also match the model of Riedel shearing for the supposed Mentawai fault, because of its orientation. The dextral fault we found

does not show the same strike like the Mentawai fault, but has a sligth clockwise rotation. A potential interpretation therefore is seen in plot 39. For matching purposes I had to slightly rotate the Mentawai fault (Nr.1 in plot 39) clockwise 10 to 20 degrees from the N300° to N310° proposed by Diament et al. (1990) and estimate measurements for fault nr. 3, which I wasn't able to detect in the field. The compressional direction in the conjugated fault system seen in figure 36, p. 62 matches the contractional orientation seen in plot 39. Figure 142 is a model for the development of those hypothesiced Riedel shear structures following Reuther, 2012 (p. 66 in book).

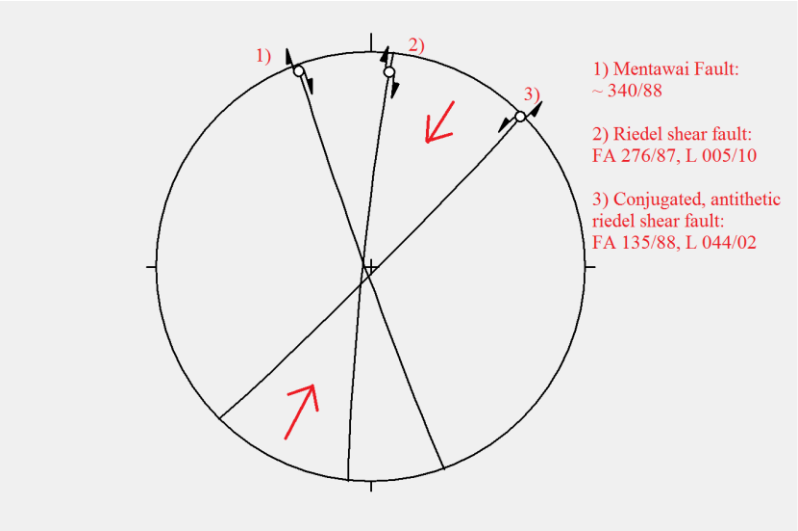

Plot 39: Synthetic and antithetic Riedel shear faults

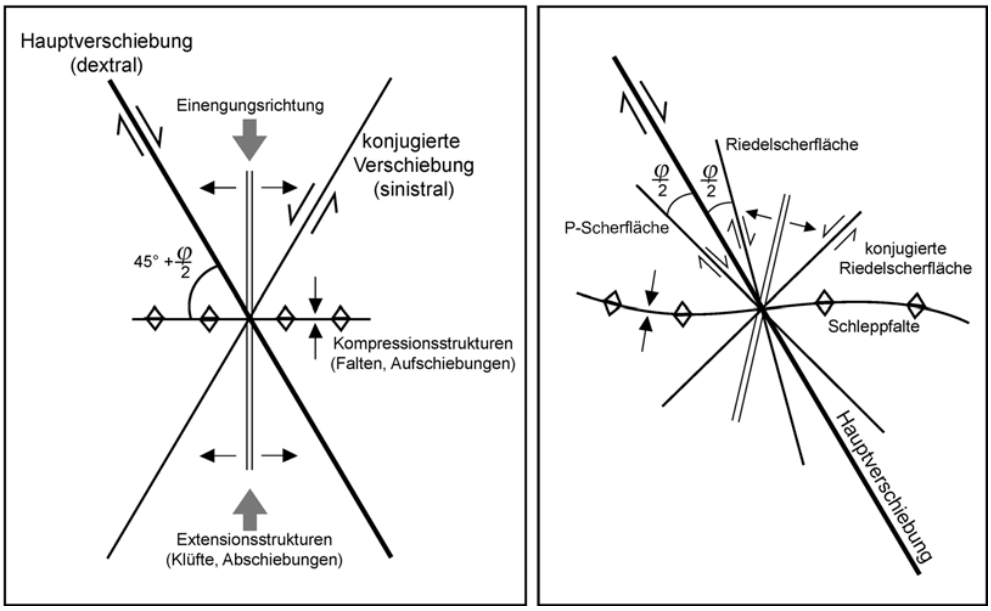

Figure 142: Schematic model for certain structures resulting from a transcurrent fault and its causing forces *(From Claus-Dieter Reuther, 2012).*

According to the interpretation of the field data the Mentawai fault is a dextral strike-slip fault in a transpressional regime, which continues up north-northwest to Nias along the outer-arc ridge. If the

fault is recently reactive in a transcurrent kinematic regime is subject of further investigations. The identified faults were found in the Lelematua Formation which would mean that the faults are not older than early to middle Miocene.

In outcrop Nias001-15 (p. 51) we documented the lateral movement of a hot spring along a proposed fault line prior and after the massive 2005 Nias-Simeulue megathrust rupture along a strike of around approximately N310°. That is the same estimate for the strike of the Mentawai fault according to Diament et al. (1992). Obviously the movement of the hot spring from SSW around 200m further NNW has been triggered by the intense seismic activity. This movement is very likely to occur along a pre-existing fault and could indicate the recent activity of the Mentawai fault in the Nias area.

Figure 143: The movement of a hot spring prior to and after the Nias-Simeulue earthquake along a potential fault from SSW to NNE (From google earth)

Nevertheless, the N-S striking Riedel shear fault I marked in plot 39, identified in outcrop Nias011-15 would also fit in the model of extension of the forearc microplate. Samuel and Harbury (1996) identified many arc-crossing strike-slip faults with a strike more or less N-S and W-E. The dextral fault could be one of this N-S striking faults responsible for arc-parallel extension. The normal faults found in outcrop 038-15 (p. 101) also fit the model of Samuel and Harbury (1996), who state that normal faults further accommodate the NNW-SSE extension of the forearc microplate, in addition to the arc-crossing strike-slip faults. Matson and Moore (1992) as well interpreted these structures as indicators for necking and extension resembling the present Sunda Strait. In figure 6, p. 22 Natawidjaja and Sieh (2000) proposed a potential model for the history of deformation along the Sunda Arc. They state that the area of Nias once resembled the Sunda Strait region, due the experienced stretching and extension, resulting from the change of frontal to oblique convergence 4

Ma prior to present, when the continental margin south of the equator still experienced frontal, normal convergence and only the continental margin to the north of the equator oblique convergence. They claim that the continental margin of Sumatra was rotated over the past 4 Ma piece by piece. At first only the part north of the equator was rotated, therefore we had similar conditions in the Nias area resembling those of nowadays Sunda Strait.

In outcrops Nias030-15, Nias031-15 and Nias033-15 we identified a zone of big scale folding with a synform and an antiform in a huge quarry. More folding was found in outcrops Nias044-15, Nias045-15, Nias046-15 and Nias048-15 as a big scale antiform stretching over several outcrops. Samuel and Harbury (1996) as well identified these in the field. They interpret these folding events in central Nias (to the west of Gunnungsitoli) and the southeastern part of Nias resulting from the cessation of convergence, according to Schlüter et al. (2002) correlated with the frontal collision of India with Eurasia, which affected the big scale, global plate dynamics and the later reset of plate convergence.

4. Perspectives

In my opinion, further work could be done in adding to the reconstruction of the evolution of the Indonesian continental margin and its incorporated former subduction zones, island arcs etc. in general, which due to its complexity still has many aspects of speculation. Moreover I find the context of the Sumatran continental margin in respect to global scale tectonics fascinating and therefore would find it very pleasant to further analyse Sumatran tectonics in context of the Indo-Australian plate and its subduction of extinct middle-ocean ridges, like the Investigator or the Wharton Ridge or other topographic relicts and its influence on seismicity, coupling or deformation in connection with subduction.

While my research and summary of pre-existing papers I was missing research about seismicity triggered movement of phenomena like hot springs. When we got aware of the movement of the one hot spring we found on Nias, this was pretty fascinating and definitely worth of further research. Maybe there is a connection with the mud volcanoes we could not find in the field and triggering seismicity due to several earthquakes which activate and deactivate such phenomena. Further research in these fields could potentially lead to interesting results.

Last but not least, studying hazardous phenomena like earthquakes especially in densely populated areas like Indonesia to better handle the resulting consequences, like devastation of cities or countries and its impact on the affected population, as well as understanding the development of tsunamis and other dangerous consequences of earthquakes are definitely worth putting scientific effort into. Although it seems to be a long or endless road, in the future mankind could be able to forecast certain seismic events due to the detailed knowledge about earthquake phenomena. Therefore, in my opinion every little step in the right direction is worth taking.

5. Conclusion

The basis for this master thesis was the fieldwork from 20.2.15 to 5.3.15 on Nias Island, to the west of Sumatra. The overall interest of the project is animal perception of seismic phenomena (Straka, 2013 - 2019). My contribution to the project and the main focus of my master thesis was the geological mapping of the island with a main focus on the northwestern continuation of the Mentawai fault which was identified to the south-east of Nias by Diament et al. (1990) next to the Mentawai archipelago, hence the name. They proposed a dextral sense of shearing, due to its appearance as a positive flower structure in the seismic profiles for the newly discovered fault, but in the following years until now, many authors speculate about the nature of this fault in terms of activeness; its potential uptake of oblique, converging motion of the tectonic plates close to Sumatra; its origin; sense of shearing and its context in respect to the Sumatran fault. In this work we identified a nearly vertical fault zone potentially resembling the northwestern continuation of the Mentawai fault on Nias Island. It is a cataclastic shear zone or localized fault in the brittle regime of the crust, which in the upper 1-4 km depth produces a non-cohesive cataclasite, resulting in our case in a fine, rock powder produced by locals for concrete production. This area is likely to be a part of a pull-apart basin within the kinematic frame of a dextral transpressional strike-slip fault. Due to its stratigraphic location in the Gomo Formation the fault zone should not be older than middle Miocene. This could mean the fault was active around 10 Ma and probably represents also an active fault. Additionally, several measurements of faults found most frequently in the riverbeds of Nias could match Riedel shear structures with a slight adjustment and correction of some values, also indicating a dextral sense of shearing. That is why I would interpret the data I collected in the field as indicating a fault zone with dextral sense of shearing on Nias Island, which probably resembles the northwestern continuation of the Mentawai fault. Although many authors at least question the recent state of activeness for the fault, the movement of a hot spring on Nias in accord with seismic activity or rather the earthquake in 2004 would in my opinion suggest at least a small amount of present activity along a potential fault in-line with the Mentawai fault further southeast.

6. Acknowledgement

I want to thank Univ.-Prof. Mag. Dr. Bernhard Grasemann, giving me the opportunity to participate in this project and supervising me doing field work in Indonesia. I also want to thank project leader Dr. Wolfgang Straka who supported me in working out the methodology of data collection. Moreover I would like to thank Red Bull Media House GmbH for funding the project. Additional thanks go to my friends MSc. I Putu Krishna Wijaya for accompanying me in the field, Matthias and Santana Bachmann who provided me a solid work opportunity while writing my master thesis, Mag. Klaus Steinbauer who gave me precious advice for my thesis, and to my girlfriend Eva Lahnsteiner for mental support, patience, motivation and sharing my enthusiasm for natural science.

7. References

- Straka W.01.07.2013 – 31.03.2019. Animal Perception of Seismic and Non-Seismic Earthquake Phenomena, Part 2. Funded by Red Bull Media House GmbH.
- Abercrombie R. E., Antolik M., Ekstrom G. 2003. The June 2000 M-w 7.9 earthquakes south of Sumatra: Deformation in the India-Australia Plate. Journal of Geophysical Research-Solid Earth 108, art. no.-2018.
- Allen C., Gillespie A., Yuan H., Sieh K., Buchun Z., Chengnan Z. 1984. Red River and associated faults, Yunnan Province, China: Quaternary geology, slip rate and seismic hazard. Geol. Soc. Am. Bull., 95, 686-700.
- Baadsgaard P. H. 1960. Barbados, W. I.: Exploration results, 1950-58. Int. geol. Congr. Rep. Twenty-first Session, 18, 21.
- Barber A. J., Tjokrosapoetro S., Charlton T. R. 1986. Mud volcanoes, shale diapirs, wrench faults and melanges in accretionary complexes, eastern Indonesia. Amer. Assoc. Petrol. Ceol. Bull., 70, 1729-1741.
- Barber A. J., Crow M. J., Milsom J. S. 2006. Sumatra: Geology, Resources & Tectonic Evolution. Geological Society of Londen, London.
- Beaudry D., Moore G. F. 1985. Seismic stratigraphy and Cenozoic evolution of west Sumatra forearc basin. American Association of Petroleum Geologists Bull., 69, 742-759.
- Beck R. H., Lehner P. 1974. Oceans, new frontier in exploration. Am. Assoc. Petroleum Geologists Bull., v. 58, p. 376-395.
- Beck M. E. 1983. On the mechanism of tectonic transport in zones of oblique subduction. Tectonophysics 93, 1–11.
- Bock Y., Prawirodirdjo L., Genrich J. F., Stevens C. W., McCaffrey R., et al. 2003. Crustal motion in Indonesia from Global Positioning System measurements. J. Geophys. Res., 108, 2367–88.
- Briggs R. W., Sieh K., Meltzner A., Natawidjaja D., Galetzka J., et al. 2006. Deformation and slip along the Sunda megathrust in the great 2005 Nias-Simeulue earthquake. Science, 311, 1897–901.
- Briggs R. W., Sieh K., Amidon W. H., Galetzka J., Prayudi D., et al. 2008. Persistent elastic behavior above a megathrust rupture patch: Nias island, West Sumatra. J. Geophys. Res., 113, B12406.
- Bürgmann R., Kogan M. G., Steblov G. M., Hilley G., Levin V. E., et al. 2005. Interseismic coupling and asperity distribution along the Kamchatka subduction zone. Journal of Geophysical Research-Solid Earth 110.
- Cameron N. R., Bennett J. D., Bridge D. McC., Clarke M. G. C., Djunuddin A., et al. 1983. The Geology of the Takengon Quadrangle (0520), Sumatra, Scale 1:250 000. Geological Research and Development Centre, Bandung.
- Chen C. W., Zebker H. A. 2002. Phase unwrapping for large SAR interferograms: statistical segmentation and generalized network models. IEEE Transactions on Geoscience and Remote Sensing, 40, 1709-1719.
- Chesner C. A., Rose W. I., Deino A., Drake R., Westgate J. A. 1991. Eruptive history of Earth's largest Quaternary caldera (Toba, Indonesia) clarified. Geology, 19, 200-203.
- Curray J. R., Shor G. G., Raitt R. W., Henry M. 1977. Seismic refraction and reflection studies of crustal structure of the eastern Sunda and western Banda Arcs. Jour. Geophys. Research, v. 82, p. 2479-2489.
- Curray J. R., Moore D. G., Lawver L. A., Emmel F. J., Raitt R. W., et al. 1979. Tectonics of the Andaman Sea and Burma. In: Watkins J.S., Montadert L., Dickerson P.W. (eds) Geological and Geophysical Investigations of Continental Margins. American Association of Petroleum Geologists, Memoirs, 29, 189-198.
- Curray J. R., Emmel F. J., Moore G. E., Kieckhefer R. M. 1981. Sediment budget and accretionary prism volume variations around the Sunda Arc. Proc. Symp. on Convergence and Subduction, College Station TX, Apr. 1981 (abst).

- Curray J. R. 1989. The Sunda Arc: a model for oblique plate convergence. Netherlands Journal of Sea Research, 24, 131 - 140.
- Curray J.R. 2005. Tectonics and history of the Andaman Sea region. J. Asian Earth Sci. 25, 187–232.
- Daly M. C. 1989. Correlations between Nazca/Farallon plate kinematics and forearc basin evolution in Ecuador. Tectonics, 8, 769-790.
- Daly M. C., Cooper M. A., Wilson I., Smith D. G., Hooper B. G. D. 1991. Cenozoic plate tectonics and basin evolution in Indonesia. Marine and Petroleum Geology, 8, 2-21.
- Davis D., Suppe J., Dahlen F. A. 1983. Mechanics of fold-and-thrust belts and accretionary wedges. J. Geophys. Res. 88, 1153.
- DeMets C., Gordon R. G., Argus D. F., Stein S. 1994. Effect of recent revisions to the geomagnetic reversal time scale on estimates of current plate motions. Geophys. Res. Lett., 21, 2191–94.
- DeShon H. R., Engdahl E. R., Thurber C. H., Brudzinski M. 2005. Constraining the boundary between the Sunda and Andaman subduction systems: Evidence from the 2002 Mw 7.3 Northern Sumatra earthquake and aftershock relocations of the 2004 and 2005 great earthquakes. Geophys. Res. Lett. 32, L24307.
- Diament M., Déplus C., Haijono H., Larue M., Lassai O., et al. 1990. Extension in the Sunda strait (Indonesia): A review of the Krakatau programme. Oceanologica Acta, Special Volume, 10, p. 31-42.
- Diament M., Harjono H., Karta K., Deplus C., Dahrin D., et al. 1992. Mentawai fault zone off Sumatra: a new key to the geodynamics of western Indonesia. Geology, 20, 259–62.
- Dickinson W. R., Seely D. R. 1979. Structure and stratigraphy of forearc regions. Am. Assoc. Petrol. Geol. Bull., v. 63, p. 2-31.
- Douville H. 1912. Les Foraminiferes de l'Ile de Nias. Sammlungen Geol. Reichsmus., v. 8, p. 255-278.
- Fauzi R., McCaffrey R.,Wark D., Sunaryo, Prih-Haryadi P.Y. 1996. Lateral variation in slab orientation beneath Toba caldera, northern Sumatra. Geophys. Res. Lett., 23, 443–46.
- Fisher R. V., Schmincke H. U. 1984. Pyroclastic rocks. Springer Verlag, Berlin, 472pp.
- Fitch T. J., Scholz C. H., 1971. Mechanism of underthrusting in southwest Japan: a model of convergent plate interactions. J. Geophys. Res. 76, 7260.
- Fitch T. J. 1972. Plate convergence, transcurrent faults and internal deformation adjacent to southeast Asia and the western Pacific. J. Geophys. Res., 77, 4432-4462.
- Frisch W., Meschede M. 2011. Platten Tektonik: Kontinentverschiebung und Gebirgsbildung. 4. Edition. WBG.
- Genrich J. F., Bock Y., McCaffrey R., Prawirodirdjo L., Stevens C.W., et al. 2000. Slip distribution at the northern Sumatra Fault System. J. Geophys. Res., 105, 28327–41.
- Glebovsky V. Y., et al. 1995. Mid-oceanic ridges and deep oceanic basins: AMF structure. In: Anomalous Magnetic Field of the World Ocean, edited by A. M. Gorodnitsky, pp. 67 – 144, CRC Press, Boca Raton, Fla.
- Hall R. 1998. The plate tectonics of Cenozoic SE Asia and the distribution of land and sea. In: Biogeography and Geological Evolution of SE Asia, edited by R. Hall and J. D. Holloway, pp. 99 – 131, Backhuys, Leiden, Netherlands.
- Hamilton W. 1973. Tectonics of the Indonesian region. Geol. Soc. Malaysia Bull., v. 6, p. 3-10.
- Hamilton W. 1979. Tectonics of the Indonesian Region. U.S. Geol. Surv. Prof. Pap., 1078, 345.
- Huchon P., LePichon X. 1984. Sunda Strait and central Sumatra fault. Geology, 12, 668-672.
- Ji C., Wald D. J., Helmberger D. V. 2002. Source description of the 1999 Hector Mine, California, earthquake, part I: Wavelet domain inversion theory and resolution analysis. Bull. Seism. Soc. Amer., 92, 1192-1207.
- Kallagher H. J. 1989. The structural and stratigraphic evolution of the Sunda Forearc Basin, North Sumatra

Indonesia. Ph.D. Thesis, University of London.

- Karig D. E. 1974. Tectonic erosion of trenches. Earth Planet. Sci. Lett., 21, 209-212.
- Karig D. E., Sharman G. F. 1975. Subduction and accretion in trenches. Geol. Soc. America Bull., v. 86, p. 377-389.
- Karig D. E., Suparka S., Moore G. F., Hehunassa P.E. 1979. Structure and Cenozoic evolution of the Sunda Arc in the central Sumatra region. ln: Watkins J. S., Montadert L., Dickerson P.W. (eds) Geological and Geophysical Investigations of the Continental Margins. American Association of Petroleum Geologists Memoirs, 29, 223-237.
- Karig D. E. 1980. Material transport within accretionary prisms and the 'knocker' problem. J. Geol., 86, 27-39.
- Karig D. E., Lawrence M. B., Moore G. F., Curray J. R. 1980. Structural framework of the fore-arc basin, NW Sumatra. Journal of the Geological Society, London, 137, 77-91.
- Karig D. E., Sarewitz D. R., Haeck G. D. 1986. Role of strike-slip faulting in the evolution of allochthonous terranes in the Philippines. Geology, 14, 852-855.
- Katili J. A., Hehuwat F. 1967. On the occurrence of large transcurrent faults in Indonesia. Journal of Geosciences, Osaka City University, 10, 5-16.
- Kerr R. A. 2005. Model shows islands muted tsunami after latest Indonesian quake. Science 308, 341.
- Kieckhefer R. M., 1980. Geophysical studies of oblique subduction zone in Sumatra. Unpubl. Ph.D. Thesis, Scripps Inst. of Ocean., UCSD, 1-119.
- Konca O. et al. 2008. Partial rupture of a locked patch of the Sumatra megathrust during the 2007 earthquake sequence. Nature, 456, 631–635.
- Lassal O., Huchon P., Haijono H. 1989. Extension crustale dans le détroit de la Sonde (Indonésie). Données de la sismique reflexion (campagne Krakatoa): Paris. Académie des Sciences, Comptes Rendus, v. 309, p. 205-212.
- Lay T., Kanamori H., Ruff L. 1982. The Asperity Model and the Nature of Large Subduction Zone Earthquakes. Earthquake Prediction Research 1, 3-71.
- Le Pichon X., Sibuet J. C. 1981. Passive margins: A model of formation. J. Geophys. Res., 86, 3708-3720.
- Longley I. M. 1997. The tectonostratigraphic evolution of SE Asia. in Petroleum Geology of Southeast Asia, edited by Fraser A. J., Matthews S. J., Murphy R. W., Geol. Soc. Spec. Publ., 126, 311 – 339.
- Malod J. A., Kemal B. M., Beslier M. O., Deplus C., Diament M. et al. 1993. Deformations du bassin d'avant-arc au nord-ouest de Sumatra. Une response à la subduction oblique. Comptes Rendus de l'Acaddmie des Sciences de Paris, 316, Serie II, 791-797.
- Malod J. A., Kemal B. M. 1996. The Sumatra margin: oblique subduction and lateral displacement of the accretionary prism. In: Hall, R., Blundell, D. (Eds.), Tectonic Evolution of Southeast Asia, vol. 106, Geological Society Special Publication, London, pp. 19e28.
- Masturyono, McCaffrey R., Wark D. A., Roecker S. W., Fauzi G., et al. 2001. Distribution of magma beneath Toba Caldera, North Sumatra, Indonesia, constrained by 3-dimensional P-wave velocities, seismicity, and gravity data. Geochem. Geophys. Geosyst., 2, 2000GC0096.
- Matson R. G., Moore G. 1992. Structural influences on Neogene subsidence in the central Sumatra forearc basin. In: WATKINS, J.S., ZHIQU1ANG, F. ET AL. (eds) Geology and Geophysics of Continental Margins. American Association of Petroleum Geologists Memoirs, 53, 157-181.
- McCaffrey R. 1991. Slip vectors and stretching of the Sumatran fore arc. Geology, 19, 881–84.
- McCaffrey R. 1992. Oblique plate convergence, slip vectors, and forearc deformation. J. Geophys. Res., 97, 8905–15.
- McCaffrey R., Zwick P., Bock Y., Prawirodirdjo L., Genrich J., et al. 2000. Strain partitioning during oblique plate

convergence in northern Sumatra: geodetic and seismologic constraints and numerical modeling. J. Geophys. Res., 105, 28363–76.

- McCaffrey R. 2009. The Tectonic Framework of the Sumatran Subduction Zone. Annu. Rev. Earth Planet. Sci., 2009. 37, 345–66.
- McCarthy A. J., Elders C. F. 1997. Cenozoic deformation in Sumatra: Oblique subduction and the development of the Sumatran Fault System. In: Petroleum Geology of Southeast Asia, edited by Fraser A. J., Matthews S. J., Murphy R. W., Geol. Soc. Spec. Publ., 126, 355 – 363.
- McCloskey J., Nalbant S. S. 2005. Earthquake risk from co-seismic stress. Nature, v. 434.
- Meltzner A. J., Sieh K., Abrams M., Agnew D. C., Hudnut K. W. et al. 2006. J. Geophys. Res. 111, B02407.
- Moore G. F. 1979. Petrology of subduction zone sandstones from Nias Island, Indonesia. Jour. Sed. Petrology, v. 49, p. 71-84.
- Moore G. F., Karig D. E. 1976. Development of sedimentary basins on the lower trench slope. Geology, v. 4, p. 693-697.
- Moore G. F., Karig D. E. 1980. Structural geology of Nias Island, Indonesia: implications for subduction zone tectonics. American Journal of Science, 280, 193-223.
- Moore G. F., Wheeler R. L. 1978. Structural fabric of a mélange, Kodiak Islands, Alaska. Am. Jour. Sci., v. 278, p. 739-765.
- Natawidjaja D., Sieh K., Ward S. N., Cheng H., Edwards R. L., et al. 2004. Paleogeodetic records of seismic and aseismic subduction from central Sumatran microatolls, Indonesia. Journal of Geophysical Research 109, doi:10.1029/2003JB0002398.
- Natawidjaja D. H., Sieh K., Galetzka J., Suwargadi B. W., Cheng H. 2007. Interseismic deformation above the Sunda Megathrust recorded in coral microatolls of the Mentawai islands, West Sumatra. J. Geophys. Res. 112.
- Newcomb K. R., McCann W. R. 1987. Seismic history and seismotectonics of the Sunda arc. Journal of Geophysical Research, 92, 421-439.
- Nishimura S., Nishida J., Yokoyama T., Hehuwat F. 1986. Neo-tectonics of the Strait of Sunda, Indonesia. J. Asian Earth Sci., 1, 81 – 91.
- Pacheco J.F., Sykes L.R. Scholz C.H. 1993. Nature of seismic coupling along simple plate boundaries of the subduction type. Journal of Geophysical Research 98: doi: 10.1029/93JB00349. issn: 0148-0227.
- Perfettini H., Ampuero J. P. 2008. Dynamics of a velocity strengthening fault region: Implications for slow earthquakes and postseismic slip. Journal of Geophysical Research.
- Plafker G., Savage J. C. 1970. Mechanism of the Chilean earthquakes of May 21 and 22, 1960. Geol. Soc. Am. Bull. 81, 1001.
- Platt J. P. 1993. Mechanics of oblique convergence. Journal of Geophysical Research: Solid Earth, v. 98.
- Prawirodirdjo L., et al. 1997. Geodetic observations of interseismic strain segmentation at the Sumatra subduction zone. Geophys. Res. Lett., 24, 2601-2604.
- Rampino M. R., Ambrose S. H. 2000. Volcanic winter in the Garden of Eden: the Toba supereruption and the late Pleistocene human population crash. Geol. Soc. Am. Spec. Pap., 345, 71–82.
- Reuther C. D. 2012. Grundlagen der Tektonik: Kräften und Spannungen der Erde auf der Spur. Springer-Verlag Berlin Heidelberg 2012.
- Rosen P. A., Henley S., Peltzer G., Simons M. 2004. Update repeat orbit interferometry package released. Eos Trans. AGU, 85, 47.
- Ruff L., Kanamori H. 1983. The rupture process and asperity distribution of three great earthquakes from long-

period diffracted P-waves. Phys. Earth. Planet. Inter., 31, 202—230.

- Rundle J. B., Kanamori H. 1987. Application of an Inhomogeneous Stress (Patch) Model to Complex Subduction Zone Earthquakes - a Discrete Interaction Matrix Approach. Journal of Geophysical Research-Solid Earth and Planets 92, 2606-2616.
- Samuel M. A., Harbury N. A., Jones M. E., Matthews S. J. 1995. Inversion of an outer-arc ridge: The Sumatran Forearc, Indonesia. In: Buchanan J. H., Buchanan P. G. (eds) Basin Inversion. Geological Society of London Special Publication, 88, 473-492.
- Samuel M. A., Harbury N. A. 1996. The Mentawai fault zone and deformation of the Sumatra forearc in the Nias area. In: Hall R., Blundell D.J. (eds) Tectonic Evolution of Southeast Asia. Geological Society, London, Special Publications, 106, 337-352.
- Samuel M. A., Harbury N. A., Bakri A., Banner F.T., Hartono L. 1997. A new stratigraphy for the islands of the Sumatran Forearc, Indonesia. Journal of Southeast Asian Earth Sciences, 15, 339-380.
- Schlüter H. U., Gaedicke C., Roeser H. A., Schreckenberger B., Meyer H., et al. 2002. Tectonic features of the southern Sumatra - western Java forearc of Indonesia. Tectonics, 21, 1047.
- Seely D. R., Vail P. R., Walton G. G. 1974. Trench slope model, In: Burk C. A., Drake C. L., eds., Geology of continental Margins. New York, Springer-Verlag, p. 249-260.
- Sieh K., Book Y., Rais J. 1991. Neotectonic and paleoseismisc studies in west and north Sumatra, Eos Trans. AGU 72(44), Fall Meet. Suppl., 460.
- Sieh K., Ward S. N., Natawidjaja D., Suwargadi B. 1999. Geophys. Res. Lett. 26, 314.
- Sieh K., Natawidjaja D. 2000. Neotectonics of the Sumatran fault, Indonesia. J. Geophys. Res., 105, 28295–28326.
- Subarya C., Chlieh M., Prawirodirdjo L., Avouac J.P., Bock Y., et al. 2006. Plate-boundary deformation associated with the great Sumatra–Andaman earthquake. Nature, volume 440, pages 46–51.
- Thatcher W. 1990. Order and diversity in the modes of Circum-Pacific earthquake recurrence. J. Geophys. Res. 95, 2609-2623.
- Tjia H. D., Boentaran T. 1969. A morpho-structural study of Nias: Bandung, Indonesia. Natl. Inst. Geology Mining Bull., v. 2, p. 21-28.
- Underhill J. R., Gayer R. A., Woodcock N. H., Donnelly R., Jolley E. J. et al. 1988. The Dent Fault System, northern England - reinterpreted as a major oblique-slip fault zone. Journal of the Geological Society, Landon, 145, 303- 316.
- Zachariasen J., Sieh K., Taylor F. W., Hantoro W. S. 2000. Modern Vertical Deformation above the Sumatran Subduction Zone: Paleogeodetic Insights from Coral Microatolls. Bull. Seismol. Soc. Am. 90, 897.
- Zen M. T. 1983. Krakatau and the tectonic importance of Sunda Strait. Bull. Jurusan Geol., 12, 9 – 22.